**M-PM-WS2-1**

INCREASED EXPRESSION OF HEAT SHOCK GENES IN CELLS EXPOSED TO EM FIELDS. ((R. Goodman[1], A. Henderson[2] and M. Blank[3])) Columbia University Health Sciences, Departments of Pathology[1], Physiology and Cellular Biophysics[2], New York, NY 10032, and Hunter College-CUNY[3], Biological Sciences, New York, NY 10021

Specific transcripts are increased when cells are exposed to 15-120Hz EM fields (8$\mu$T-80$\mu$T). Experiments have used dipteran salivary gland cells, yeast and human HL-60 cells. Increased transcript levels were found for some oncogenes, as well as genes involved in metabolic activity, development and cell division. Recent data on protein synthetic patterns showed elevated levels of "heat shock" proteins in samples exposed to either EM fields or elevated temperature. Based on these observations, we have retested RNA from exposed and control samples, and measured increased transcript levels for the heat shock gene hsp70 in HL-60 cells and dipteran salivary gland cells, and the homologous gene SSA1 in yeast. In light of the over-expression of some heat shock genes, in the absence of elevated temperature, we conclude that EM fields appear to stimulate a natural pathway that is similar to the one used by cells in response to heat shock and other physical stresses. The response to EM fields occurs at a much lower energy density. (Supported by EPRI, DOE, ONR, and NIEHS).

**M-PM-WS2-2**

SPATIAL AND TEMPORAL COHERENCE AFFECTS THE RESPONSE OF BIOLOGICAL SYSTEMS TO ELECTROMAGNETIC FIELDS. ((Theodore A. Litovitz)) Physics Department, Catholic University of America, Washington, DC, 20064.

The association of biological effects with exposure to weak ELF electromagnetic fields (EMF's) remains controversial. Skepticism is due in large measure to theoretical arguments based upon signal-to-noise considerations. The signal-to-noise dilemna arises because cells, respond to exogenous EMF's 1000 times smaller than the local thermally generated noise EM fields. We propose that cells discriminate against local EM noise fields because they are *spatially incoherent*; a significant number of cell membrane receptors must be simultaneously and coherently activated to produce a bioeffect. We have already demonstrated that *temporal coherence* is necessary if bio-effects are to be observed (Litovitz, Mullins and Krause, 1991). We have hypothesized that if a spatially coherent but temporally incoherent random EM noise field were superimposed upon a coherent signal, then at some signal/noise value the observed EM induced bio-effects would be suppressed. This suppression has been observed in a number of models including, chick embryos, E. coli, human leukemia (HL60) cells, human lymphoma (Daudi) cells and breast cancer (MCF-7) cells.

**M-PM-WS2-3**

$CA^{2+}$ TRANSIENTS AS A TRANSDUCTION SIGNAL FOR EXTREMELY LOW FREQUENCY ELECTRIC FIELDS

K.J. McLeod and H.J. Donahue
Musculo-Skeletal Research Laboratory, Department of Orthopaedics
State University of New York at Stony Brook, 11794-8181.

The search for a transduction signal for low level electromagnetic fields in the extremely low frequency range has concentrated on cellular calcium fluxes and the dynamics of intracellular calcium levels. This has occurred as the energy level of these fields are so low it appears they would only be capable of perturbing a metastable system. Outside of the nervous system, tonic or phasic patterns of calcium transients are a conspicuous characteristic of many cell systems. We will review recent research addressing the sensitivity of calcium signalling to ELF fields and report on work we have undertaken on the spontaneous calcium transient activity in ensembles of growing rat osteosarcoma cells (ROS 17/2.8) during exposure to both ELF electric fields. In these cells, calcium transients lasting approximately five seconds and reaching concentration levels of 10-100 times basal (1-10 $\mu$M) can readily be recorded. Electric field exposure at 30 Hz, 500 $\mu$V/cm results in a significant decrease in transient activity occurring within 15 minutes. Full recovery of the cells occurs within 90 minutes following field removal.

This work is supported by the Electric Power Research Institute Grant #2965-21, and grant #ES06287 from the National Institute of Environmental Health Sciences, NIH.

**M-PM-WS2-4**

Na,K-ATPASE FUNCTION IN 60Hz ELECTROMAGNETIC FIELDS. ((M. Blank)) Department of Physiology and Cellular Biophysics, Columbia University, New York, NY 10032

The Na,K-ATPase is a model membrane protein for studying interactions with electromagnetic fields. These studies have also elucidated active transport mechanisms. Decreased ATP-splitting by low frequency electric fields appears due to increased binding of activating ions on the Na,K-ATPase surface (Blank, FASEB J 6:2434-2438, 1992). Activation by ions also accounts for the frequency dependence (Blank, J Electrochem Soc 134:1112-1117, 1987), as well as the difference between optimal frequencies for ion influx and efflux observed by Tsong et al (Bioelectrochem Bioenerg 21:319-331, 1989). Using an Electric Research & Management (Pittsburg) exposure system, we measured effects of low frequency magnetic fields between 0-300Hz and 0-300mG, and found increases in enzyme activity of 5 to 15%, with optima around 50mG and 60Hz. Inhibition by electric fields and stimulation by magnetic fields probably arise from different charge movements in the enzyme. Electric fields increase ion binding at the surface, and magnetic fields increase charge movements within the protein that coordinate the surfaces. The frequency dependence of electric (Blank & Soo, Bioelectromag 13:329-333, 1992) and magnetic field effects is similar, suggesting that the two charge movements are part of a closely coupled rate limiting process. (We thank EPRI for their support.)

## IMMUNE FUNCTION

**M-Pos1**

THE INFLUENCE OF A FREE THIOL IN THE CDR REGION ON THE ASSEMBLY AND STABILITY OF HUMANIZED IgG4 ANTIBODIES.

((Cynthia Gwynne Long, Elizabeth Craig Lombardi, Leonard J. Super, Danlin Xu, Robert A. Zivin, Daniel J. Kroon, and Lewis S. Hanna)) The R. W. Johnson Pharmaceutical Research Institute, P.O. Box 300, Route 202, Raritan, NJ 08869.

The assembly of an immunoglobulin G (IgG) molecule requires the proper formation of both intrachain and interchain disulfide bonds. In the case of IgG4 antibodies, it has been observed that the formation of inter-heavy chain disulfide bonds is incomplete, resulting in a heterogeneous population of whole ($H_2L_2$) and half (HL) antibody molecules. The CDR regions of the murine antibodies OKT®3 and OKT®4a have been used to generate humanized antibodies of the G1 and G4 isotype. The amino acid sequence of OKT®3 shows that there is a cysteine residue in the third loop of the heavy chain CDR region. Based on the structure of known antibodies, this cysteine is expected to exist as a free thiol in the native molecule. In this study, we present the biophysical characterization and comparison of a number of related humanized OKT®3 molecules containing mutations of the cysteine in the CDR loop, as well as residues in the hinge region and the CH2 domain. Quantitation of the disulfide bonds and free thiol groups indicates that in the native state, the free thiol is not solvent exposed, and the remaining cysteine residues are involved in disulfide bonds. The antibodies migrate as a single peak on gel filtration HPLC, and have comparable stabilities to guanidine denaturation. However, on non-reducing SDS polyacrylamide gels, these antibodies show HL populations ranging from 0 to 50%. The implications of these results on the assembly of antibody molecules will be discussed.

**M-Pos2**

A KNOWLEDGE-BASED APPROACH TO MODELING THREE-DIMENSIONAL STRUCTURES OF IMMUNOGLOBULIN FRAGMENTS.

((D. S. Linthicum, C. Mandal and S. Subramaniam)) Dept. Biochem. & Biophys., Texas A&M Univ., College Station, TX 77845 and Beckman Institute, Dept. Physiol. & Biophys. Univ. Illinois, Urbana, IL 61801.

Immunoglobulin (Ig) amino acid sequences are highly conserved and often have sequence homology ranging from 70-95%. Antigen binding fragments (Fab) of more than 25 antibodies have been crystallized and display a high degree of structural similarity. Based on this observation, several homology modeling approaches have been recently developed for the prediction of Fab structures prior to their experimental determination. We have extracted features from existing Ig sequences and known structures to build an automated AntiBody structure GENeration (ABGEN) method for obtaining structural models of antibody fragments. The features we have used include invariant and strictly conserved residues, structural motifs of known Fab, canonical features of hypervariable loops, torsional constraints for residue replacements and key intra-residue interactions. In addition, molecular mechanics and dynamics methods have been used to further refine the ABGEN structures. We have explored the validity of our approach using a five-fold cross validation using the existing Ig fragment structures. Using ABGEN we generated the Fab structure of an anti-sweetener antibody prior to crystallographic refinement and the model structure has an RMSD of less than 2 Å when compared with the crystal structure. Supported by NIH/NIGMS GM46535.

**M-Pos3**

ELONGATED STRUCTURE OF THE HUMAN MUCIN MUC-1 TANDEM REPEAT DOMAIN, ((J. D. Fontenot[1], S. V. Santhana Mariappan[1], P. Catasti[1], N. Domenech[2], O. J. Finn[2], and G. Gupta[1])) [1]Los Alamos National Lab, T-10, MS-K710 Los Alamos, NM 87545: [2]University of Pittsburgh, Pittsburgh PA, 15216 (Sponsored by Micah Dembo)

The human breast and pancreatic tumor antigen encoded by the mucin muc-1 gene contains from 40 to 150 tandem repeats of the highly (Ser/Thr) o-glycosylated sequence PDTRPAPGSTAPPAHGVTSA. In tumor cells, aberrant glycosylation results in the exposure of the tandem repeat protein core throughout the cell surface. The protein core was thought to be random coil and to derive its structure from the addition of carbohydrates to threonine and serine residues. However, many mucin specific, tumor reactive antibodies and CTL clones have been identified in cancer patients. Hence, the following questions arise: Are the antibody and T-cell receptors recognizing an existing well defined structure or is structure induced by the antibody / T-cell receptor binding? Secondly, how does the addition of tandemly repeated sequences influence the development of protein structure?

We prepared synthetic peptides corresponding to one, two, and three tandem repeats of the muc-1 repetitive domain. Using multi-dimensional $^1$H-NMR techniques (TOCSY, ROESY, and NOESY) the proton resonances of the 1 and 3-tandem repeat peptides (20 and 60 amino acids) were assigned. A method combining MC simulated annealing and full matrix NOESY simulations was used to arrive at a set of structures in agreement with the NMR data.

This novel structure consists of each 20 amino acid segment forming an elongated but ARC shaped segment or disk with the first 12 amino acids in consecutive turns, and residues 13-20 in an extended conformation. The NMR data of the 20 and 60 mers indicates different dynamics in the two molecules and that structure is induced by the addition of tandem repeats. These results seem to explain the immunodominance of the APDTR sequence in the tumor state, as this sequence forms protruding knobs which obscures accessibility to the rest of the molecule by antibody and T cell receptors on the surface of lymphocytes. The role of glycosylation on the alteration of this structure and masking of the immunodominant epitope in normal cells will be discussed.

**M-Pos4**

NOESY MODELING AND HETERONUCLEAR COUPLING TO DETERMINE THE CONFORMATION OF THE ANTIGENIC EPITOPE OF A STREPTOCOCCAL POLYSACCHARIDE.
((Rossitza Gitti, S. Mohan, Qiuwei Xu and C. Allen. Bush.))
Department of Chemistry & Biochemistry, U. Maryland Baltimore Co., Baltimore, MD 21228

The interpretation of molecular modeling and $^1$H NOESY data have indicated that certain complex oligosaccharides may adopt conformations considerably more rigid than those of small peptides. In order to test this hypothesis, we have attempted to measure 3-bond $^1$H-$^{13}$C coupling constants in complex polysaccharides to supplemement the NOE data. We have prepared a cell wall polysaccharide from *Streptococcus mitis* strain J22 with uniform $^{13}$C enrichment to facilitate these measurements. In spite of linewidths of 10 to 20 Hz, it has been possible to measure $^3J_{CH}$ as small as 1 Hz with a precision of $\pm$ 0.5 Hz using a recently described E-COSY method. Glycosidic dihedral angles are derived from interresidue $^3J_{CH}$ using published correlation formulas. NOESY spectra for the same polymer are reported and interpreted by a full matrix spin simulation method. The data from the two experiments are reconciled with molecular modeling calculations including molecular dynamics simulations.

Research supported by NIH Grant GM-31449

**M-Pos5**

PRODUCTION OF ANTI-PEPTIDE ANTIBODIES IN RABBITS AND CHICKENS: A COMPARATIVE STUDY
((M. Jarnot, M.A. Vander Klok, and A.M. Corbett)) Department of Physiology & Biophysics, Wright State University, Dayton, OH 45435

Polyclonal antibodies against synthetic peptides are valuable tools in the study of membrane channel and receptor subtypes. Two methods for the production of these antibodies were compared in this study. 3 synthetic peptides (17 amino acids; ~33% sequence similarity) corresponding to sequences from rat brain sodium channel subtypes were synthesized, and peptide 3 coupled via a terminal cysteine to keyhole limpet hemocyanin. Peptide-carrier complexes were emulsified in Freund's adjuvant and 1.5 ml or 2 ml injected intramuscularly into rabbits or laying hens, respectively at monthly intervals. IgG from serum collected from rabbits 1 week after each boost was compared to IgY (avian IgG) isolated from the yolks of eggs collected daily from hens. IgG and IgY were quantitated by ELISA antibody sandwich assays. Specific antibody production was first detected approximately 40 days postinjection; peak total rabbit IgG levels were reached at day 120 and declined thereafter. An initial chicken IgY peak at approximately day 45 was followed by a brief decline, and then by an increase from day 100 onward. Maximal specific IgG in rabbits at day 99 was 13.2% of total IgG, or 1.44 mg/ml. Maximal specific IgY in chickens, calculated from a single time point from the same period, was 14% of total IgY, or 0.52 mg/ml. This corresponds to a monthly specific volume of 10 mg IgG and 90 mg IgY. Chicken IgY showed no crossreactivity to peptides 1 and 2 at dilutions above 1:1000; rabbits showed no crossreactivity to peptide 1 above 1:1000, but significant crossreactivity to peptide 2 at dilutions up to 1:500,000. Preincubation of IgY with 1 nM peptide 3 blocked antibody binding 70% at day 37 and 100% subsequently. 1 nM peptide 3 blocked rabbit IgG binding by approximately 50% on days 99 and 238; greater than 90% block was achieved with peptide concentrations of >0.5 $\mu$M for both time points. The quantity of antibody produced and ease of isolation make hens a viable option for antipeptide antibody production. Supported by NIH Grant NS28377.

**M-Pos6**

POTENTIAL-DEPENDENT REGULATION OF CYTOKINE RELEASE IN THP-1 CELLS. ((D.S. Krafte and L. Hamel)) Vascular and Biochemical Pharmacology, Sterling Winthrop Inc., Collegeville, PA 19425.

THP-1 cells are monocytic cells which release cytokines (IL-1$\beta$ and TNF$\alpha$) in response to stimulation. We have investigated the role of membrane potential in regulating such cytokine release by increasing $[K^+]_o$ concentrations to depolarize cells during stimulation. Patch-clamp experiments indicate that THP-1 cells have a K conductance which contributes to membrane potential. Cells ($10^6$/ml) were stimulated with 0.01% IgGsorb (16 hrs) in 1, 5, 10, 30, 100, and 140 mM $[K^+]_o$. Supernatants were collected and cytokine concentrations determined by solid-phase ELISA. Percent inhibition was calculated based upon values obtained in 5 mM $[K^+]_o$. Increasing $[K^+]_o$ inhibited release of both IL-1$\beta$ and TNF$\alpha$ in a dose-dependent manner with $IC_{50}$ values of 20 mM and 37 mM, respectively. In these experiments, $[Na^+]_o$ was reduced to maintain osmolarity. Parallel experiments demonstrated that decreasing $[Na^+]_o$ had a stimulatory effect upon cytokine release. The true $IC_{50}$ values for $K^+$ may, therefore, be lower. Cell viability, as assessed by calcein and ethidium homodimer fluorescence, was not significantly affected in these experiments for $[K^+]_o \leq 100$ mM. Charybdotoxin, $\alpha$-dendrotoxin and iberiotoxin, polypeptide toxins known to block potassium channels, did not inhibit cytokine release (test conc. 100 nM). These data suggest negative membrane potentials may be necessary for cytokine release in THP-1 cells and that depolarization of these cells can inhibit release. As such, specific blockers of monocytic $K^+$ channels may be useful inhibitors of cytokine release.

**M-Pos7**

**CORRELATION BETWEEN THE EARLY EXPRESSION OF ANTIGEN TO VESICULAR STOMATITIS VIRUS AND THE APPEARANCE OF CYTOKINES, AS DETECTED BY IN SITU HYBRIDIZATION.** **((Yatian Zhang, M.D., Ph.D.)) Department of Biology , New York University, New York, NY 10003**

**Vesicular stomatitis virus (VSV) infection requires specific attachment of the virus to receptors, propagation of the virus within a cell, and transmission of the progeny to new susceptible cells. Pathology that accompanies viral infection can be caused by three distinct mechanisms: viral-induced cell damage; tissue response to viral infection (production of cytokines); or immunologic attack on infected and neighboring cells. We have begun studies on changes in the expression of the cytokine gene in brains of infected mice to determine if cytokines are involved in the pathogenesis. Preliminary in situ hybridization studies on 2 day infections showed that the inflammatory and neurotoxic cytokines IL-1, IL-6, and TNF-$\alpha$ were rapidly upregulated in the area of infection, while IL-4 was not expressed at this time. In addition, TGF-$\beta$, which antagonized TNF-$\alpha$ activity, was also upregulated. Data on the appearance and disappearance of eight cytokines during the infection, in conjunction with Nissl histochemical staining and VSV-immunoreactivity, indicate that at least some cytokines are associated with the process of VSV infection. In particular, IL-1 cytokine both overlays the VSV infection area and extends beyond to the mirtral cell layer. This suggests that IL-1 may sensitize cells to attack by the advancing VSV.**

**M-Pos8**

ANTIPHOSPHOLIPID ANTIBODY BINDING TO BILAYER MEMBRANES: ROLE OF LIPID HEADGROUP AND CHARGE DENSITY
((A.R. Obringer, N.S. Rote, A. Walter)) Depts. Physiol. & Biophys. and Micro. & Immunol., Wright State University, Dayton, OH 45435. (Spon. by R.W. Putnam)

Thrombosis, recurrent fetal loss and thrombocytopenia are associated with antibodies (Abs) that recognize negatively charged phospholipids in ELISA. Neither the ability of these Abs to bind to bilayer phospholipids nor the composition dependence of binding is known. Here, we establish a reliable method for testing Ab binding to lipid bilayer membranes, compare binding in this system with that in ELISA, and determine the requirements for binding. Three IgMs were tested which on ELISA have different specificities for cardiolipin (CL) and phosphatidylserine (PS) representing the three patterns of reactivity in patients with aPL Abs: BA3B5C4 (CL+/PS+), 3SB9b (CL-/PS+), and D11A4 (CL+/PS). We investigated the immunoreactivity of these mouse monoclonal IgMs against bilayers composed of 0-100% PS or CL in egg phosphatidylcholine in physiological saline and as a function of ionic strength and pH. Bilayers were formed on the surface of 1.6 $\mu$m diameter glass microspheres; the percent that bound Ab and the Ab that bound per bilayer was detected using flow cytometry. All three mAbs bound to CL-containing bilayers; BA3B5C4 and 3SB9b bound to PS-containing bilayers. aPS Abs bound to bilayers that contained as little as 10-20% PS. BA3B5C4 and 3SB9b saturate CL-containing bilayers when 25% CL is present. D11A4 bound to, but never saturated CL-containing bilayers at equal IgM concentration. The ionic strength and pH dependence of the binding suggests that the intermolecular attractive forces between aPS Abs and PS-containing bilayers are multiple weak electrostatic bonds. Since, two of the mAbs tested can react with the low levels of PS presented in the plasma membranes of activated platelets, apoptotic lymphocytes and senescent red blood cells, these surfaces are plausible candidates for the site of pathologically relevant antibody interaction. This method may be useful for evaluating other membrane-protein interactions.

**M-Pos9**

SPECTROFLUORIMETRIC ANALYSIS OF THE COMPLEXATION REACTION BETWEEN MONOCLONAL ANTI-FLUORESCEIN ANTIBODIES AND FLUORESCEIN ((T. K. Nanavaty, M. Krishna Sastry and D. S. Linthicum)) Dept. Biochem. & Biophys., Texas A&M Univ., College Station, TX 77845

Intermolecular interactions between monoclonal anti-fluorescein antibodies and the ligand, sodium fluorescein, have been examined by following fluorescence quenching. We produced a panel of mouse monoclonal antibodies against fluorescein coupled to the protein carrier via the 4'-position. Antibody producing hybridoma clones were isolated by positive reactivity in an enzymeimmunoassay. Monoclonal antibody clones F43.1 and F55.3 showed 100% ligand-associated fluorescence quenching upon complexation with the ligand. For F43.1 the intrinsic association constant was calculated to be $2.63 \times 10^9\ M^{-1}$ at 30°C. To obtain a comparable analysis with ligand fluorescence quenching, the intrinsic antibody tryptophan fluorescence was examined during antibody-ligand complexation. For both antibodies examined, tryptophan fluorescence was quenched upon complexation with the ligand. Thermodynamic data was obtained from the temperature dependent association constants. These data suggest that antibody binding site tryptophan residues may participate in ligand recognition and complexation. Supported by NIH/NIGMS GM46535.

**M-Pos10**

THE 2-D NMR CHARACTERIZATION OF A 39 RESIDUE IMMUNOGENIC CHIMERIC PEPTIDE DERIVED FROM $HIV_{MN}$. ((D. Myers, M.A. Moody, B.F. Haynes, and L.D. Spicer)) Departments of Biochemistry, Radiology, Immunology and Medicine, and the Duke Center for AIDS Research, Duke University, Durham, NC 27710.

$HIV_{MN}$ is a common HIV strain that accounts for approximately 50% of HIV isolates in the USA. T1SP10MN(A) is a chimeric synthetic peptide derived from the principal B cell neutralizing determinant [SP10MN(A)] and a T cell helper determinant [T1] of the gp120 envelope protein of $HIV_{MN}$. This peptide has a structure that by circular dichroism criteria is mostly random coil; however, NOESY connectivities that can best be interpreted as transient or nascent structures are observed. T1SP10MN(A) has an unusual NOE pattern in the putative GPGR β turn (from the V3 loop region) that leads us to suggest that the turn has either been shifted or expanded to include an adjacent alanine. The possibility that peptides containing the principal neutralizing determinant of $HIV_{MN}$ may be in equilibrium between a tight turn form and an expanded form is considered.

**M-Pos11**

SYSDOC PREDICTION OF LIGAND BINDING TO FKBP12: COMPARISON WITH SPECTROSCOPIC EXPERIMENTS. ((Norberto Silva, Jr., Yuan-Ping Pang*, Alan Kozikowsk* and Frank Prendergast)) Mayo Clinic, Guggenheim 14, 200 First St. SW, Rochester, MN 55905; *Neurochemistry Research, Mayo Foundation for Medical Education and Research, 4500 San Pablo Rd., Jacksonville, FL 32224. (Spon. by J. Blinks)

The immunosuppresant drug tacrolimus (FK506) binds to a protein called FK506 binding protein (FKBP12) and this complex inhibits calcineurin phosphatase activity which in turn arrests signal transduction connected with transcriptional control in T lymphocytes.The search for more effective drugs to bind to FKBP12 would clearly involvethe use of complex computer simulations which docks a drug (host) to aprotein (guest). One such computer program, SYSDOC, has been applied to FKBP12 with encouraging success. In particular, SYSDOC has been able to reproduce the FK506-FKBP12 crystal complex with 0.56 Å RMS deviation given: a) each crystal conformation of FKBP12 and FK506, separately, from the FK506-FKBP12 complex and b) a region enclosing the aromatic binding pocket of FKBP12 in which the guest is systematically rotated and translated to achieve energetically favorable docking. In addition, SYSDOC predicts that a chromophore such as 1-anilinonaphthalene-8-sulphonate, ANS, can bind to FKBP12. The binding of ANS involves the interaction of its aromatic groups with other aromatic residues of FKBP12's binding pocket. This offers the unique opportunity of spectroscopically testing the SYSDOC prediction since FKBP12 has a single Trp residue (W59) at the center of the binding site. The test relies on performing fluorescence energy transfer experiments between W59 and bound ANS (as predicted by SYSDOC). We accomplish this by measuring the steady state and time-resolved fluorescence of FKBP12 with and without ANS. The experimental results are discussed in light of theoretical predictions. (Supported by Mayo Foundation and GM34847.)

## G PROTEINS

**M-Pos12**

HEXAMETHYLENE BISACETAMIDE INDUCES THE DISSOCIATION OF G PROTEINS AND PROTEIN KINASE C FROM THE PLASMA MEMBRANE ((P.V. Escriba, M. Sastre and J.A. García-Sevilla)). University of the Balearic Islands, E07071 Palma de Mallorca, Spain.

Hexamethylene bisacetamide (HMBA) is an inducer of differentiation of murine erythroleukemia cells (MELC)[1]. Although no direct binding of HMBA to proteins or DNA has been found, the activity of proteins involved in signal transduction, such as protein kinase C (PKC) is altered in cells cultured in the presence of this drug[2]. We have observed that preincubation of rat brain membranes with HMBA at concentrations used in cancer chemotherapy and tissue culture of MELC (5 mM, 30 min, 4°C) induced the dissociation from the plasma membrane to, approximately, a 50% of the control values of G protein subunits and PKC (measured by immunoblot analysis with specific antisera, as previously described[3]). Since it has not been demonstrated a direct interaction between HMBA and these proteins, a possible alteration in the structure of the lipid component of the plasma membrane was studied. Differential Scanning Calorimetry studies on liposomes of 1-palmitoyl-2-oleoyl phosphatidylethanolamine (POPE) showed that HMBA caused a concentration-dependent decrease in the the lamellar to hexagonal ($H_{II}$) phase transition enthalpy of POPE: ΔH changed from 0.53 kcal/mol to 0.05 kcal/mol in the absence or presence of 10 mM HMBA, respectively. Hexagonal phases, which are the more abundant non-lamellar lipid structures in biological membranes, are required for the association of peripheral proteins (such as G proteins and PKC) with the plasma membrane[4]. The observed effect of HMBA on the dissociation of these proteins from the plasma membrane could be mediated by the alteration caused by this drug on the lipid structure. G proteins and PKC are peripheral membrane proteins involved in the signal transduction of multiple membrane receptors. The observed alterations in the protein:membrane interactions caused by HMBA could, thus, account for the alterations in the signalling pathways leading to differentiation of MELC. References: [1]. Marks, P; Breslow, R.; Rifkind, RA.; Ngo, L and Singh R (1989) Proc. Natl. Acad. Sci. USA 86, 6358. [2]. Melloni, E; Pontremoli, S; Sparatore, B; Patrone, M; Grossi, F; Marks, PA and Rifkind, RA (1989) J. Biol. Chem. 264, 18414. [3]. Escriba, PV; Sastre, M and García-Sevilla, JA (1994). Arch. Gen. Psychiat. in press. [4]. Seddon, JM (1990) Biochim. Biophys. Acta 1031,1.

**M-Pos13**

KINETIC MECHANISM OF THE RELEASE OF GDP FROM rap1B AND rhoA CATALYSED BY GDS. ((J.P. Browne and J.F. Eccleston)) National Institute for Medical Research, Mill Hill, London NW7 1AA, U.K.

The mechanism of the GDS catalysed release of GDP from rap1B has been investigated using a combination of kinetic, fluorescence intensity and anisotropy techniques. The fluorescent analogue of GDP, 2'(3')-O-N-methylanthraniloyl GDP (mantGDP) has been synthesised and shown to bind to rap1B (expressed in and purified from baculovirus infected Sf9 cells) with a three fold enhancement of its fluorescence. Following addition of a large excess of GDP to a stoichiometric rap1B.mantGDP complex, the rate of dissociation of mantGDP could be followed by monitoring the decrease in fluorescence intensity and anisotropy, which occurred with a rate constant of $6.8 \times 10^{-5} s^{-1}$. In the presence of excess GDS over rap1B.mantGDP this rate constant was $8 \times 10^{-3} s^{-1}$, an acceleration of ~120 fold. In the absence of GDP, titration of rap1B.mantGDP with GDS showed tight (<0.1 μM) stoichiometric binding of GDS to rap1B.mantGDP. However, even addition of excess GDS in the absence of GDP did not cause all of the mantGDP to be released from rap1B as shown by the fact that the fluorescence anisotropy after this additon was significantly above that of the free mantGDP. In contrast, with rhoA.mantGDP, the presence of both GDS and GDP were required for any release of mantGDP. The results are discussed in terms of the substituted enzyme mechanism proposed for the release of GDP from elongation factor Tu catalysed by EF-Ts and the sequential mechanism proposed for the interaction of initiation factor 2 with its exchange factor (J.N. Dholakia and A.J. Wabba, *J. Biol. Chem.*, (1989), **264**, 546-550).
Supported by the Medical Research Council (UK) and Human Frontier Science Program.

M-Pos14

**ACTIVATION OF $P_i$ RELEASE FROM p21ras BY GAP MEASURED BY A NOVEL FLUORESCENCE PROBE FOR $P_i$**

((Andrew E. Nixon, Martin Brune, John E.T. Corrie and Martin R. Webb)) National Institute for Medical Research, Mill Hill, London. NW7 1AA, U.K.

A new probe has been developed for $P_i$, based on the phosphate binding protein (PBP) of *E. coli*. A single point cysteine mutant was labeled with a new coumarin fluorophore and the purified, labeled protein gives a 5-fold increase in fluorescence on binding $P_i$. The binding is rapid and the $K_d$ is $< 1\mu M$.

This probe was used to measure the rate of $P_i$ release from p21ras, due to GAP-activated GTP hydrolysis, in order to investigate the mechanism of the transformation from GTP-bound to GDP-bound states. The described experiments use the catalytic domains of p120-GAP and neurofibromin. For measurements in real time of a single turnover of GAP.p21.mantGTP (where mant = 2',3'-methylanthraniloyl), $P_i$ release was measured in a stopped-flow apparatus. This gives $k_{cat} = 15s^{-1}$ and $K_D = 25\mu M$.

The $P_i$ release reaction was also measured in the steady state using the absorbance change on coupling the ras reaction to the reaction of 2-amino-6-mercapto-7-methylpurine ribonucleoside with purine nucleoside phosphorylase. With p21N-ras.mantGTP as substrate and conditions where each GAP catalyzes many turnovers of p21.mantGTP, this gave $k_{cat} = 5s^{-1}$, $K_M = 24\mu M$ at 30°C, low ionic strength. The results will be compared with other kinetic measurements of the GAP-ras mechanism.

(Supported by M.R.C., U.K. and by the European Community)

M-Pos15

**3-DIMENSIONAL NMR AND MODELING STUDIES OF THE Cdc42Hs PROTEIN.**

((J.L. Feltham[1], M.J. Sutcliffe[2], D. Manor[1], R.A. Cerione[1], and R.E. Oswald[1])) [1]Dept. Pharmacology, Cornell University, Ithaca, NY 14853 USA; [2]Biological NMR Centre, University of Leicester, Leicester, UK

Cdc42 is a member of the rho subgroup of the ras superfamily of low molecular weight GTP-binding proteins. Although substantial structural information is available for certain members of this family (i.e. ras and EF-Tu), no direct structural studies have been done on any member of the rho subfamily. We have modeled Cdc42 based on several different crystal structures of H-ras. Models based on the GDP-bound structures of both wild-type H-ras and its G12V mutant suggest two possible conformations for a 13-residue insertion which occurs in Cdc42 with respect to ras. The first is a relatively compact helix-turn-helix motif and the other a more extended double-stranded anti-parallel β sheet structure which forms a "flap" over the GDP binding site. Interestingly, in models of Cdc42 built on GMPPCP-bound H-ras and the GTP-bound G12V H-ras mutant, only the extended motif is observed, which suggests that a major conformational change may occur within the Cdc42 protein upon exchange and hydrolysis of bound nucleotide. This result also suggests a possible mechanism by which the dbl oncogene product could enhance the nucleotide exchange rate of Cdc42Hs but not ras. Based on these intriguing possibilities, we have undertaken multidimensional NMR experiments aimed at solving the tertiary structure of Cdc42Hs. Although this is a fairly large protein for NMR, the spectral resolution attainable in preliminary one- and two-dimensional spectra suggest that Cdc42 is particularly amenable for such studies. Three-dimensional experiments with a homogeneously $^{15}N$-labelled sample have begun and sequential assignments of backbone resonances are presented.

M-Pos16

**ACTIVATION OF MUSCARINIC $K^+$ CHANNEL BY $G_K$* AND BRAIN $G_{\beta\gamma}$ THROUGH THE SAME MECHANISM.**

((M. Yamada. A. Jahangir, Y. Hosoya, A. Inanobe, T. Katada and Y. Kurachi)) Division of Cardiovascular Diseases, Mayo Clinic, Rochester, MN 55905

A pertussis toxin-sensitive G protein ($G_K$) links muscarinic cholinergic and $A_1$-purinergic receptors with an inwardly rectifying $K^+$ ($K_{ACh}$) channel in cardiac atrial cell membranes. Although the βγ subunits of pertussis toxin-sensitive G proteins ($G_{\beta\gamma}$) have been reported to fully activate this channel, it is not known whether exogenously-applied $G_{\beta\gamma}$ interacts with the $K_{ACh}$ channel through the same mechanism as the active subunit of endogenous $G_K$ ($G_K$*). We examined in inside-out patches the relationship between the concentration of GTP and $K_{ACh}$ channel activity with or without preactivation of the channels by either GTPγS or $G_{\beta\gamma}$ purified from bovine brain. In the control, $K_{ACh}$ channels were activated by intracellular GTP (with acetylcholine in the pipette) in a positive cooperative manner (the Hill coefficient ~ 2.5). As the channels were preactivated by GTPγS to progressively higher levels, the GTP-channel activity relationship shifted more to the left, but the Hill coefficients of the curves remained the same. The same changes were observed when $K_{ACh}$ channels were preactivated with brain $G_{\beta\gamma}$. These results indicate that endogenous $G_K$* and exogenous $G_{\beta\gamma}$ share a common molecular mechanism to activate the $K_{ACh}$ channel.

M-Pos17

**GTP ENHANCEMENT OF ATP MEDIATED ACIDIFICATION IMPLICATES A G-PROTEIN MEDIATED NETWORK.**

((D.M. Rimmer, J.D. Altazan, E.M. Besser, J.A. Watkins, and J. Glass)) Hematology-Oncology Section, Center for Excellence in Cancer Research, Treatment, and Education, LSUMC-S, Shreveport, LA, 71130.

Acidification of endosomes is a kinetically important event in the processing of diferric transferrin (Tf) and iron absorbtion via endocytosis by reticulocytes. Isolated reticulocyte endosomes are reasonably well characterized and provide a good model for studying processes involved in intravesicular acidification. The GTP dependent enhancement of ATP mediated acidification was examined in an effort to determine if GTP effects are due to cooperative phenomena involving the vacuolar $H^+$-ATPase or effects arising from a G-protein mediated network. Acidification was monitored using fluorescein labeled Tf contained in the isolated vesicles. Simultaneous and sequential addtions of 1 mM GTP and/or 1 mM ATP indicated that GTP enhances the rate of acidification and decreases the apparent rate of ΔpH dissipation. However, when ATP was added first, the effect of GTP was less than when GTP was added first or by itself. As measured by acidification rates, the apparent $K_M$ and $V_{max}$ for GTP and ATP were similar at 130±50 μM and 2.4±0.2 x $10^{-2}$ $s^{-1}$ respectively. Less than 50 μM GTP increased the $V_{max}$ for ATP to 3.8±0.2 x $10^{-2}$ $s^{-1}$ and decreased the rate of ΔpH dissipation from 1.2±0.1 x $10^{-5}$ $s^{-1}$ to 0.3±0.1 x $10^{-5}$ $s^{-1}$. Based on models of endosomal acidifcation and coupling to $Na^+$ and $Cl^-$ transporters, a new model of ionic fluxes can be suggested. It is proposed that the effect of GTP is due to a G-protein (rab4 and/or rab5) mediated phosphorylation network which modifies the $Na^+/H^+$ antiport and/or $H^+$-ATPase. It is postulated that the G-protein mediated network is a controlling factor of endosomal acidification. Supported by NIH DK-37866.

## KINASES

M-Pos18

**KINETIC EVIDENCE FOR A 3-PHOSPHOGLYCERATE INDUCED CONFORMATIONAL CHANGE OF PHOSPHOGLYCERATE KINASE (PGK)**

((P.P. Schmidt, F. Travers and T. Barman)) INSERM U128, CNRS, BP 5051, 34033 Montpellier Cedex, France. (Spon. by D. Mornet)

PGK is a key enzyme on the glycolytic cycle : ADP + 1,3-diphosphoglycerate (diPG) ⇔ ATP + 3-phosphoglycerate (PG). Much is know of its structure but little on its reaction pathway, in particular, whether or not the PG induced fit process is rate limiting. We have studied PGK in the direction of diPG production. Reaction mixtures (PGK +PG + [γ $^{32}$P]ATP at pH 7.4 and 4°C) 4-300ms old were quenched in acid (decomposing any diPG to [$^{32}$P]Pi + PG) and the [$^{32}$P]Pi determined. At 5mM PG and 0.1mM ATP the progress curves were identical, whether or not the PGK was preincubated with PG : rapid rises of 0.3 mol diPG / mol PGK, steady states of $28s^{-1}$ and then the approach to equilibrium at times about 25ms ($K_{eq} = 10^{-4}$) . The initial kinetics were too fast to measure and to slow them down the buffer was made 40% in ethylene glycol. After preincubation with PG, there was a rapid rise of kinetics $100s^{-1}$ and amplitude of 0.3 mol diPG / mol PGK and steady state 4.5 $s^{-1}$. This suggests that the products release steps are rate limiting. When the bare enzyme was mixed with PG + [γ $^{32}$P]ATP, the initial burst was reduced greatly, suggesting that here the *PG induced fit process is rate limiting.*

P.P. S was supported by an INSERM fellowship.

M-Pos19

**REGULATION OF THE PROTEIN KINASE C:PHOSPHATIDYLSERINE INTERACTION BY PHORBOL ESTERS AND DIACYLGLYCEROL**

((Marian Mosior and Alexandra C. Newton)) Department of Chemistry, Indiana University, Bloomington, IN 47405

The binding of protein kinase C to phosphatidylserine is regulated by the second messenger diacylglycerol. This molecule increases the affinity of protein kinase C for phosphatidylserine-containing membranes by over two orders of magnitude. Here we show that phorbol esters have an even greater effect on the interaction of protein kinase with phosphatidylserine, increasing the apparent binding constant by 4 orders of magnitude. In addition to the greater effect on the affinity for membranes, the effects of phorbol esters differ from those of diacylglycerol in one other aspect: phorbol esters cause a slow, time-dependent increase in the binding of protein kinase C to membranes. The high-affinity binding to phosphatidylserine-containing membranes promoted by either diacylglycerol or phorbol esters is sensitive to ionic strength: increasing the ionic strength from 100 to 300 mM KCl decreases the apparent binding constants approximately 10-fold. However, because the apparent binding constants are 2 - 4 orders of magnitude higher in the presence of either diacylglycerol or phorbol esters, physiological ionic strength would have little observable effect on the amount of protein kinase C bound to cellular membranes while inhibiting the binding in the absence of these ligands. Our data suggest that diacylglycerol and phorbol esters mediate the "translocation" of protein kinase C to the plasma membrane by increasing the affinity of the enzyme for phosphatidylserine-containing membranes by 2 - 4 orders of magnitude.

**M-Pos20**

AUTOINHIBITION AND REGULATION OF SMOOTH MUSCLE MYOSIN LIGHT CHAIN KINASE. ((J.K. Krueger, P.J. Gallagher, J.T. Stull)) Physiology Dept., UT-Southwestern, Dallas, TX 75235-9040.

A current hypothesis for the $Ca^{2+}$/calmodulin (CaM)-dependent regulation of myosin light chain kinase (MLCK) is that an inhibitory sequence, referred to as a "pseudo-substrate", binds to the catalytic core utilizing identical binding sites as those of the regulatory light chain (RLC) substrate. However, recent studies have identified several important acidic residues within the catalytic core which when mutated dramatically lowered the $K_{cam}$ value without affecting the $K_m$ or $V_{max}$ values for the RLC substrate. It was proposed that a lowered $K_{cam}$ value reflected a weakened binding of the inhibitory region to the catalytic core. Only two catalytic core mutations, located within the substrate binding pocket, were found to increase the $K_m$ for RLC as well as lower the $K_{cam}$ value. Those results suggested that the inhibitory sequence was not acting simply as a "pseudo-substrate". We used selected-site mutagenisis to create charge reversal mutations within the catalytic core, the autoinhibitory domain and the connecting region. From these studies, mutation of several basic residues which lie further N-terminal than the originally identified basic residues comprising the "pseudo-substrate" were found to lower the $K_{cam}$ value, thereby, extending the auto-inhibitory sequence. In addition, mutation of two or three acidic residues within the catalytic core increased the $K_m$ value for RLC, but did not effect the $K_{cam}$ value. We predict that there is a distinct electrostatic binding surface for the RLC and for the inhibitory sequence.

**M-Pos21**

MODULATION OF THE ACTIVITY OF SMOOTH MUSCLE MYOSIN LIGHT CHAIN KINASE BY AUTOPHOSPHORYLATION.
((T. Tokui and M. Ikebe)) Department of Physiology and Biophysics, Case Western Reserve University, School of Medicine, Cleveland, OH 44106

Smooth muscle myosin light chain kinase(MLCK) is a $Ca^{2+}$/Calmodulin(CaM) dependent enzyme which catalyzes the phosphorylation of the 20,000-dalton light chain of myosin which is thought to be an integral component of the regulatory mechanism of the smooth muscle contractile apparatus. It has been known that MLCK can be phosphorylated by several protein kinases such as cAMP-dependent protein kinase, C-kinase and CaM-dependent protein kinase II which results in the inactivation of the kinase due to change in the affinity for CaM. It has been suggested that MLCK can phosphorylate itself but the effect of autophosphorylation on the MLCK function as well as the identification of the sites have not yet been elucidated. We report here that MLCK autophosphorylates itself at two distinct sites, i. e., Thr-803 and Ser-814. The serine site was completely blocked in the presence of $Ca^{2+}$/CaM, while the threonine site was not. The MLCK concentration dependence on autophosphorylation suggested that autophosphorylation of the threonine site is an intramolecular event while that of the serine site is an intermolecular process. The phosphorylation at Ser-814 which is located in close proximity to the CaM anchoring residue, Leu-813, decreased the affinity of MLCK for CaM. The most striking finding was, however, that the phosphorylation at Thr-803 activated the MLCK activity in the presence of $Ca^{2+}$/CaM, i. e., produced a partially active kinase. That autophosphorylation produces a constitutively active enzyme has been known for CaM-dependent protein kinase II and present results show that MLCK, another CaM-dependent protein kinase, may have similar molecular mechanism for its regulation.
(Supported by NIH and AHA)

**M-Pos22**

CLONING, EXPRESSION AND CHARACTERIZATION OF RECOMBINANT SMOOTH MUSCLE γ- AND δ-CAM KINASE II ISOFORMS.
((Z-H.L. Zhou and M. Ikebe)) Department of Physiology and Biophysics, Case Western Reserve University, Cleveland, OH 44106

Previously we purified CaM kinase II isoform from chicken gizzard smooth muscle. We demonstrated that γ-isoform was the dominant CaM kinase II isoform in chicken smooth muscle. It is different from brain γ in that it contained a unique insertion at the end of the calmodulin-binding domain. It is distinct from brain α and β−isoforms biochemically in major autophospborylation site and holoenzyme structure. We reported before that two novel γ-CaM kinase II isoforms (γ-b, γ-c) were found in aorta smooth muscle. Another two novel δ−variants were also identified. The difference in the nucleotide sequence of these variants was centered at the variable region at the end of the calmodulin-binding domain. So far little biochemical characterization has been done with brain γ- and δ−CaM kinase II. To compare major smooth muscle isoforms with their brain counterparts in biochemical properties, we expressed two smooth muscle γ-variants(γ-b, γ-c) and brain γ−variant(γ-a) in this study using pET-E.coli expression system. About 60% of the expressed kinase was recovered in supernatant fraction, and the enzyme was further purified using a calmodulin affinity column. Both γ-b and γ-c showed $Ca^{2+}$/calmodulin-dependent kinase activity and were autophosphorylated in a $Ca^{2+}$/calmodulin-dependent manner. Gel filtration analysis showed that both smooth muscle γ-variants(γ-b, γ-c) formed a multimeric structure, but with fewer subunits than γ-a. An estimated molecular weight of γ-a, γ-b, and γ-c were 487 kDa (8-9mer), 258 kDa (4-5mer), and 407 kDa (7-8mer), respectively. These results suggest that the difference in the structure of the variable region at the end of the calmodulin-binding domain of the kinase is responsible for the difference in holoenzyme structure. We are currently expressing δ−isoform variants, identifying major autophsophorylation sites of recombinant CaM kinase II and characterizing autophosphorylation kinetics of various CaM kinase II isoforms expressed in smooth muscle(supported by NIH and AHA).

**M-Pos23**

ACTIVATION OF PROTEIN PHOSPHATASE INHIBITOR-1 BY cGMP-DEPENDENT PROTEIN KINASE.
((T. Tokui, S. Ando* and M. Ikebe)) Department of Physiology and Biophysics, Case Western Reserve University, School of Medicine, Cleveland, OH 44106 and *Biophysics Unit and Experimental Radiology, Aichi Cancer Center Research Institute, Chikusa-ku, Nagoya 464, Japan

Reversible protein phosphorylation is a major mechanism for the control of many intracellular events. The level of protein phosphorylation depends on the relative activities of protein kinases and protein phosphatases. Protein phosphatase inhibitor-1(PPI-1) is a small heat- and acid-stable protein, which specifically inhibits protein phosphatase 1 activity. It has been known that PPI-1 is activated only when it is phosphorylated by cAMP-dependent protein kinase. We now report that PPI-1 can be phosphorylated by cGMP-dependent protein kinase and the phosphorylation significantly enhances the PPI-1 activity. The phosphorylation is catalyzed by cGMP-dependent protein kinase but not other possible contaminated kinases such as cAMP-dependent protein kinase because : 1, the phosphorylation was dependent on cGMP; 2, the phosphorylation was not inhibited by a synthetic peptide inhibitor specific to cAMP-dependent protein kinase. The major phosphorylation sites were identified as threonine residues which is consistent with the site responsible for the activation of PPI-1. The identification of the phosphorylation sites ( whether or not the sites are identical to those by cAMP-dependent protein kinase ) is progressing.
(Supported by NIH and AHA)

**M-Pos24**

PSEUDOSUBSTRATE SEQUENCE IS NOT REQUIRED FOR THE INHIBITION OF MYOSIN LIGHT CHAIN KINASE.
((M. Tanaka, K. Yano, M. Matsuura, R. Ikebe and M. Ikebe)) Department of Physiology and Biophysics, Case Western Reserve University, School of Medicine, Cleveland, OH44106

Smooth muscle myosin light chain kinase (MLCK) is a $Ca^{2+}$/calmodulin (CaM) dependent enzyme which plays a key role in the $Ca^{2+}$ dependent regulation of smooth muscle contraction. Molecular mechanism of the regulation of MLCK has been studied and it has been shown that the intramolecular inhibitory region exists at the N-terminal side of the CaM binding site. The mechanism by which the autoinhibitory region inactivates the enzyme is still obscure, however, because of the sequence similarity between the myosin light chain (substrate) and the autoinhibitory region in terms of their basic amino acid residues: Kemp and Coworkers have proposed the pseudosubstrate inhibitor hypothesis in which the pseudosubstrate sequence of MLCK competes with the substrate thus inhibiting the kinase activity. To elucidate the mechanism of autoinhibition, we produced various truncated mutants of MLCK and characterized their enzymatic properties. Seven truncated mutants were produced i. e., MT799, MT796, MT795, MT793, MT791, MT787 and MT783, which contain amino acid residues 1-799, 1-796 and so on. Both MT799 and MT796 were completely inhibited in their kinase activity but full activity was recovered after limited tryptic proteolysis (activated 50- 100 times). In contrast, MT793, MT791, MT787, MT783 showed full kinase activity without showing any $Ca^{2+}$/CaM sensitivity. MT795 was partially inhibited and tryptic proteolysis further activated it approximately 3 times. The results clearly showed that a cluster of basic residues, Arg 797- Arg 798- Lys 799, which are essential components of the pseudosubstrate sequence is not essential for the autoinhibitor activity. Furthermore, the results show that the residues Tyr 794- Met 795- Ala 796 are essential for the inhibition of the kinase. It should be emphasized that no basic residues are involved in this sequence suggesting that hydrophobic interaction but not ionic interaction is essential for the autoinhibition of the kinase. (Supported by NIH and AHA)

**M-Pos25**

**NON-EQUIVALENCE IN DIACYLGLYCEROL AND PHORBOL ESTER ACTIVATION OF PROTEIN KINASE C.** ((S.J. Slater, Mary Beth Kelly, F.J. Taddeo and C.D. Stubbs)) Department of Pathology and Cell Biology, Thomas Jefferson University, Philadelphia, PA 19107.

The stimulation of protein kinase C (PKC) activity, normally achieved *in vivo* by diacylglycerol (DAG), can also be obtained with phorbol esters, and an involvement of PKC in a cellular process is frequently inferred when it is modulated by these agents. Recent studies suggest disparities between PKC activation by DAG and phorbol esters, however, an explanation for the observed differences remains elusive. In the present study, PKC activation by DAG *together* with the phorbol ester TPA, both at saturating concentrations, was found to be in excess of that attained for either activator alone, indicating that PKC contains minimally two non-equivalent activator binding sites. Support for this comes from the observation that n-butanol inhibited DAG activated PKC, while not affecting TPA stimulation. PKC activated by both TPA and DAG *together* was unaffected by n-butanol, suggesting that the DAG site may be allosterically modified by the TPA interaction. However, curves obtained for the TPA concentration dependence of PKC activity, with and without DAG, indicated that the presence of DAG did not affect the cooperativity of TPA activation, indicating minimal allostery between the two purported activator binding sites. Thus n-butanol inhibition of DAG activation may occur by interaction at a distinct site on the enzyme, itself susceptible to allosteric modulation by TPA interaction with the enzyme. Other experiments showed that PKC activated by DAG, was further stimulated by PE, while phorbol ester induced PKC activation was not potentiated. Also the DAG stimulated PKC activity was inhibited by $Ca^{2+}$ chelation, whereas activation by TPA was only partially inactivated. The conclusion of this study was that DAG and phorbol esters interact at different sites on the enzyme, with differing affinities, and mediate distinct activating conformational changes in the enzyme.

**M-Pos26**

N-ETHYLMALEIMIDE TREATMENT OF LOW K SHEEP RED BLOOD CELLS AT DIFFERENT TEMPERATURES REVEALS ROLE OF THIOLS AND Mg FOR ACTIVATION AND INACTIVATION OF K-Cl COTRANSPORT. P. K. Lauf, R. Moezzi and N. C. Adragna. WRIGHT STATE UNIVERSITY SCHOOL OF MEDICINE, Dayton, OH. 45435.

Exposure of low K sheep red blood cells to low concentrations (<1 mM, 5% hematocrit) of N-ethylmaleimide (NEM), activates K-Cl cotransport whereas high NEM concentrations (>2 mM) reverse this effect. At least two types of thiol groups differing in their apparent $pK_a$ values have been identified. We now report that these two thiols may be further distinguished by NEM treatment at 0°C and 37°C, respectively, followed by analysis of the NEM effect on KCl efflux measured at 37°C in controls and in cells with $Mg_i$ reduced by A23187 and EDTA. Results: 1. At 0°C, NEM up to 20 mM solely activated K efflux in Cl, with saturation at <2 min and 1 mM NEM using dithiothreitol to remove NEM. 2. At 37°C, 5 mM NEM reversed KCl flux stimulation to base values, however, with a tenfold larger time constant. 3. Both KCl flux activation and reversal were approximately equal in control and in low $Mg_i$ cells. Hence $Mg_i$ per se does not affect thiol alkylation. 4. Similarly, KCl flux, stimulated in low $Mg_i$ cells in the absence of NEM, was inhibited by 6 mM NEM. Thus both K-Cl cotransport states,one activated by reduction of $Mg_i$, and the other by thiol alkylation, which affects regulation by $Mg_i$, are similar based on their NEM-inhibition through low affinity thiols. Since ATP is required for both NEM activation and swelling-induced $Mg_i$ inhibition of K-Cl cotransport, and $Mg_i$ fails to inhibit NEM-stimulated KCl flux, MgATP may effect the thiol-catalyzed reversal of K-Cl cotransport stimulated by NEM, $Mg_i$ reduction, and cell swelling, the three principal interventions causing K-Cl cotransport activation. (Supported by NIH 37.160).

**M-Pos27**

QUININE AND QUINIDINE INHIBIT K-Cl COTRANSPORT IN LOW K SHEEP ERYTHROCYTES. N. C. Adragna and P. K. Lauf, WRIGHT STATE UNIVERSITY SCHOOL OF MEDICINE, Ohio, 45401-0927.

Low K (LK) sheep red blood cells (SRBCs) are used as a model to study K-Cl cotransport which plays an important role in cellular dehydration in human erythrocytes homozygous for hemoglobin S. Cinchona bark derivatives such as quinine (Q) and quinidine (QD) are effectively used in the treatment of malaria. In the present study we investigated the effect of Q and QD on K-Cl cotransport in LK SRBCs. Cells with K-Cl cotransport activated by either swelling in hyposmotic media, or by thiol alkylation with N-ethylmaleimide, or by cellular Mg removal through A23187 in the presence of external chelators were exposed to various concentrations of Q and QD and the rate constants of K efflux were determined in Cl and $NO_3$. K-Cl cotransport was defined as the Cl-dependent (Cl minus $NO_3$) K efflux. K-Cl cotransport stimulated by all three interventions was inhibited by both Q and QD in a dose-dependent manner. Full inhibition of K-Cl cotransport occurred at concentrations of Q>2 mM, and of QD of 1 mM. The inhibitory effect of Q was manifested in Cl but not in $NO_3$ whereas QD also reduced slightly K fluxes in $NO_3$. Dixon plots of the 1/K-Cl flux versus the inhibitor concentration revealed curvilinear behavior indicating complex inhibitory kinetics. In contrast to K efflux, Q and QD inhibited KCl influx less effectively in swollen and NEM-treated cells whereas the effect in low Mg cells was more complex. The inhibitory action of these two drugs was reversible and their mechanism of action likely involves diffusion into the cell and inhibition from the cytoplasmic aspect of the membrane. This is the first report of an inhibition by antimalarial drugs of K-Cl cotransport activated by three independent manipulations. (Supported by NIH DK RO1-37160).

**M-Pos28**

ALZHEIMER'S DISEASE-INDUCED CHANGES IN HUMAN RED CELL MEMBRANE TRANSPORT PROCESSES ((A. Janoshazi, A. Satlin and A. K. Solomon)) Biophysical Laboratory, and Dept of Psychiatry, McLean Hospital, Harvard Medical School, Boston MA, 02115.

An altered rate of $SO_4^=$ exchange in red cells of patients with Alzheimer's disease (AD) has been reported by Bosman et al (1991). Does this mean that AD red cell band 3 is different from normal? We compared binding kinetics of the fluorescent anion exchange inhibitor, DBDS (4,4'-dibenzamido-2,2'-stilbene disulfonate) in AD red cells with age-matched controls. In normal red cells DBDS binding is saturable, a bimolecular association followed by a monomolecular conformation change which locks bound DBDS to band 3. In four preliminary experiments in AD red cells, the monomolecular conformation change is absent and binding does not saturate in the μmolar concentration range, consistent with an AD-induced conformation change in red cell band 3. Bosman et al also reported one instance of increased binding of the glucose transport inhibitor, cytochalasin B (Cyt B), in AD red cells, suggesting an AD effect on the glucose transport protein (GLUT1). We have previously reported that Cyt B modulates red cell DBDS binding (Janoshazi and Solomon, 1989) indicating that band 3 and GLUT1 are adjacent in the normal cell membrane. Two preliminary experiments show that 2.5 μM Cyt B modulation of DBDS binding kinetics is altered in AD red cells, consistent with an AD-induced conformational change of GLUT1. (Supported by the Council for Tobacco Research and the Alzheimer's Association).

**M-Pos29**

COUPLING OF THE Na FLUX OF THE Na-$PO_4$ COTRANSPORTER AND THE Na PUMP. EVIDENCE FOR A MEMBRANE POOL OF $Na^+$. ((R. B. Gunn and L. Tadayon)) Department of Physiology, Emory University School of Medicine, Atlanta, GA 30322.

The ouabain- and disulfonic stilbene-insensitive Na-$PO_4$ cotransporter in human red cells provides 25% of the $^{32}P$ influx in a plasma-like medium, but provides 90% of the labeling of the membrane pool of nucleotides (Shoemaker *et al., J. Gen. Physiol.* 92:449-474, 1988) that are preferential substrates for the ouabain-sensitive Na pump. Experiments were performed to test whether the Na cotransported with the phosphate also had a special relationship to the pump as compared to cytoplasmic Na. Human red cells were loaded with $^{22}Na$ by a 60-sec exposure to nigicerin (10 μM) in $MgCl_2$ (110 mM) at 37°C. The ouabain-sensitive $^{22}Na$ efflux was measured in 140 mM NaCl ± 1 mM N-methyl-d-glucamine-$PO_4$. The external $PO_4$ appeared to inhibit the pump 13-30%, but when pump function was assayed by $^{86}Rb$ influx external $PO_4$ had no effect. One explanation is that the influx of nonradioactive $Na^+$ on the Na-$PO_4$ cotransporter was diluting the specific activity of the pump's substrate pool of $Na^+$ and decreasing the tracer efflux but not pump turnover or stoichiometry. One predicted consequence of this membrane $Na^+$ pool is that if the pump is blocked the tracer influx through the Na-$PO_4$ cotransporter should increase since $^{22}Na$ in the pool could no longer be recycled out through the pump. We observed that the influx of $^{22}Na$ into red cells (dinitrostilbene-disulfonate-treated to block anion exchange on band 3) in the presence of 1 mM $PO_{4\text{-out}}$ was increased by ouabain. The coupling of fluxes whereby the product of one enzyme/transporter is not released but used as substrate for another enzyme/transporter is documented in metabolism and the mitochondrial membrane. This relationship for transporters in the plasma membrane of eukaryotes has not been previously described. Supported by USPHS-NIH-HL 28674.

**M-Pos30**

PHOSPHOLIPID STRUCTURAL SPECIFICITY OF A HUMAN ERYTHROCYTE PHOSPHATIDYLSERINE-STIMULATED $Mg^{2+}$-ATPASE. ((M. L. Zimmerman, E. Nemergut, and D. L. Daleke)) Department of Chemistry, Indiana University, Bloomington, IN 47405.

A candidate aminophospholipid flippase, a lipid-dependent, vanadate-sensitive $Mg^{2+}$-ATPase, has been purified from human erythrocytes. The detergent solubilized enzyme is not active in the absence of added lipid and shows a high degree of specificity for its lipid activator. *sn*-1-2-Diacylphosphatidyl-L-serine (PS) stimulates the enzyme maximally, anionic phospholipids afford partial activation and zwitterionic or neutral lipids do not activate the ATPase. Lipid structural elements required for activation were studied using synthetic PS analogs which were modified in the headgroup, phosphate and glycerol backbone. Activation was reduced by removing the carboxyl group (PE, 28% of PS) or the amine moiety (phosphatidylhydroxypropionate, 28% of PS), or by methyl esterification of the carboxyl group (21% of PS). Phosphatidyl-homoserine produce 25% less activity than PS, indicating that the enzyme senses headgroup size. Replacement of the phosphate group with an isosteric, uncharged sulfonate abolished activation of the ATPase, indicating that the phosphate group is another recognition element. ATPase activity was dependent on the stereochemistry of the glycerol backbone, but not the serine headgroup: the D-serine analog of *sn*-1,2-PS was equivalent to the natural L-serine derivative in supporting ATPase activity. However, *sn*-2,3-dilauroyl-phosphatidyl-L-serine and *sn*-2,3-dilauroylphosphatidyl-D-serine afforded only 60% and 32% of the activity in the presence of the *sn*-1,2-isomers. Finally, glycerophosphoserine and phosphoserine, but not the choline analogs or serine alone, significantly inhibited ATPase activation in the presence of PS. These data indicate that the ATPase recognizes several PS structural elements and that each are required for full elaboration of activity. This structural specificity is shared by the aminophospholipid flippase, indicating that these proteins may be identical.

**M-Pos31**

SENESCENT ERYTHROCYTE REMOVAL ((L. Kantor and H.M. Mizukami) Wayne State University, Detroit, MI 48202. (Spon. by H.M. Mizukami)

An anion transport protein, Band 3 (90-100kda) is involved in the two proposals regarding the senescent rbc's (red blood cells) removal. One by Low et al (1985) suggests that Band 3 molecules cluster due to the possible crosslinking of their n-termini. Such close proximity of antigenic sites leads to bivalent binding of autologous antibodies resulting in rbc removal. Another by Kay (1985) states that the cleavage of Band 3 takes place, forcing a part of it, to the surface of the membrane. Due to the presence of Band 3 fragment on a cell surface, such cell is recognized as immunologically foreign, resulting in autologous antibody binding and eventual removal by macrophages from the circulation. Which proposal is right? Most likely both are.

Our research will elucidated the reason two hypothesis exist - both researchers were looking at the dependent events but at different time periods. We will demonstrate that the initial step is the clustering of Band 3's n-termini as mentioned above, coinciding with the accumulation of oxygen radicals. The radicals lead to oxidation of the clustered Band 3's cysteine residues thus forming disulfide bonds between the Band 3 monomers. This results in conformational changes in Band 3, exposing proteolytic sites, previously hidden in the membrane. The surfacing immunologically different antigenic sites become recognized by autologous IgG, leading to macrophage attachment and eventual removal out of the circulatory system.

We will show densitometrically that Band 3 undergoes decrease in its intact form, meaning degradation is taking place. Further, immunoblots with an antibody to surface portion of Band 3 will demonstrate that Band 3 exists in aggregated forms in middle aged rbc's, whereas old rbc's in addition to aggregation, exhibit breakdown products. Young rbc's display only the intact (90-100kDa) form of Band 3, thus supporting our hypothesis for senescent rbc's removal.

M-Pos32

**FORMATION OF DENSE CELLS AND IRREVERSIBLE DEFORMED CELLS IN SICKLE CELL DISEASE PATIENTS.** ((Kazumi Horiuchi and Kwaku Ohene-Frempong)) The Children's Hospital of Philadelphia, Department of Pediatrics, Univ. of Pennsylvania School of Med., Philadelphia, PA 19104

Blood from patients with sickle cell disease (SCD) contains dense cells and irreversibly deformed cells (IDC), which have been considered to play important roles in vaso-occlusive complications in this disease. However, the mechanism of formation of those cells *in vivo* is unclear. Two main mechanisms have been proposed so far; (1) sickling-related and (2) sickling-unrelated. If the dense cell formation is unrelated to sickling, fetal hemoglobin (Hb F) would not be important because it is known that Hb F inhibits polymerization of Hb S and therefore cell sickling. In addition, hemoglobin concentration of Hb S or MCHC may not be important if the mechanism is unrelated to sickling because the sickling is also dependent on MCHC. We studied relationships among %Hb F, MCHC (g/dl), and formation of dense cells (d≥1.11) and IDC during about 2 year treatment of 5 SCD patients with hydroxyurea (HU), an agent to activate Hb F production. They achieved Hb F levels higher than 20% although the extent was different among the patients. We found that formation of dense cells and IDC decreased by an increase in Hb F levels during the therapy, but the changes were patient-dependent. Since MCHC values were different among patients but relatively unchanged in individual patients during the therapy, we could estimate the effect of MCHC on the formation of those cells. We estimated the median Hb F level (18.3%) and calculated % dense cells at Hb F = 18.3% for individual patients using linear regression curves between (1) %Hb F vs %dense cells and (2) % Hb F vs degree of deformation estimated by image analysis. We found that % dense cells at Hb F = 18.3% directly related to MCHC values and a difference in MCHC of 1g/dl induces a change in about 10 percentage points of dense cells, although Hb F reduced % dense cells individually.

M-Pos33

ISOLATION AND RECONSTITUTION OF THE RECEPTOR FOR THE HEMOLYTIC TOXIN AEROLYSIN FROM RAT RED BLOOD CELL MEMBRANES. ((H.J. Gruber, H.U. Wilmsen, S. Cowell*, H. Schindler and J.T. Buckley*)) Inst. for Biophysics, University of Linz, Austria and *Dept. for Biochemistry and Microbiology, University of Victoria, Victoria B.C., Canada

Aerolysin is a bacterial hemolysin which forms ion channels in planar lipid bilayers and which lyses red blood cells (RBC), rat cells being 100 times more sensitive than human cells. The presence of integral membrane proteins from native rat RBC membranes (RBCM) in planar lipid bilayers enhances the incorporation and channel formation of aerolysin by more than two orders of magnitude. The effect is highly species-dependent; human RBCM exert a much weaker receptor effect for the toxin than those from rat, thus reflecting the species dependence found *in vivo*. Using planar lipid bilayer measurements as an activity assay the receptor was partially purified from native rat RBCM. The CHAPS-solubilized receptor binds to a WGA column but not to a Con A column and can be reconstituted into lipid vesicles by detergent removal using Bio-Beads. The toxin receptor is likely to be a sialoglycoprotein, as suggested by its sensivity to trypsin, its denaturation at 37° C under argon, and its binding to a WGA-sepharose column. Glycoproteins extracted from rat RBCM with lithium-diiodosalicylate could also exert a strong receptor activity. Gangliosides from rat RBC and human glycophorin A, however, failed to mimic the receptor effect. In order to screen for a specific aerolysin receptor, rat RBCM proteins were separated by SDS-PAGE and blotted onto nitrocellulose. When incubated with aerolysin and exposed to anti-aerolysin antibody a single band could be detected corresponding to a protein of 37 kDa. It is concluded that rat erythrocytes contain a 37 kDa receptor that is not found in human erythrocytes.

M-Pos34

**IDENTIFICATION OF AMINO ACID RESIDUES IN THE ANION TRANSPORT SITE OF THE HUMAN ERYTHROCYTE ANION EXCHANGE PROTEIN (BAND 3).** ((S.M. Blackman, A.H. Beth, & C.E. Cobb)), Mol. Physiol. & Biophysics, Vanderbilt Univ., Nashville, TN 37232.

Band 3 is an integral membrane protein which mediates the exchange of chloride and bicarbonate across the erythrocyte membrane. Chymotrypsin treatment of intact RBCs cleaves band 3 into integral membrane ~58 k and ~38 k Mr fragments. Trypsin treatment of ghost membranes prepared from these RBCs cleaves a cytoplasmic ~41 k Mr fragment from the ~58 k integral membrane domain, leaving a ~17 integral membrane fragment. Many spectroscopic probes, including maleimide and iodoacetamide eosin derivatives, and covalent reacting stilbene disulfonate derivatives such as SL-DADS-maleimide, have been shown to react with the 17 k peptide under mild conditions. In contrast, covalent labeling of the 38 k peptide with reporter molecules such as fluorophores or spin labels has been more difficult to achieve. We now report that cascade blue, which contains 3 sulfonates and has an azide reactive moiety, covalently labels band 3 with high specificity. Cleavage of band 3 with chymotrypsin and trypsin has shown that both the 17 k and 38 k peptides are labeled, with most of the label residing on the 38 k fragment. Extensive digestion of these detergent solubilized peptides with chymotrypsin has allowed us to isolate small peptides via RP-HPLC. These peptides are now being sequenced in order to identify the specific amino acid residues and their location in the primary structure of band 3. This information will help to further identify the portions of band 3 which reside in and near the anion transport site. The possible utility of this probe in fluorescence resonance energy transfer experiments in conjunction with other suitable fluorophores will also be explored. Supported by R01 HL34737.

M-Pos35

**DISTANCE CONSTRAINTS FOR THE STILBENE DISULFONATE SITE AND A MONOMER-MONOMER CONTACT IN ERYTHROCYTE BAND 3** ((D.J. Scothorn and A.H. Beth)) Dept. of Molecular Physiology and Biophysics, Vanderbilt University, Nashville, TN 37232

Band 3, the erythrocyte anion exchange protein, can be readily cross-linked to covalent dimers in the membrane. Using EPR spectroscopy we have determined that the distance between the nitroxide moiety of [$^{15}$N,$^{2}$H]-sI-$H_2$-DADS-maleimide reacted at the stilbene disulfonate site of Band 3 and a site of intermolecular cross-linking by BSSDA (a spin-labeled analog of $BS^3$) is likely greater than 20Å. Intact RBC's were labeled with 50μM [$^{15}$N,$^{2}$H]-sI-$H_2$-DADS-maleimide, followed by intermolecular cross-link formation with 2mM $^{14}$N-BSSDA. Linear EPR measurements carried out on intact RBC's, ghost membranes and stripped ghost membranes solubilized in 1% $C_{12}E_8$ showed no detectable dipolar coupling between the nitroxide moiety of the [$^{15}$N,$^{2}$H]-sI-$H_2$-DADS-maleimide and the nitroxide moiety of $^{14}$N-BSSDA, indicating a separation of greater than 20Å. SDS-PAGE indicated approximately 70% of the Band 3 monomers were cross-linked to dimers by the BSSDA. Spectral subtraction of the $C_{12}E_8$ solubilized ghost spectra was used to deconvolute the composite spectra into three components: [$^{15}$N,$^{2}$H]-sI-$H_2$-DADS-maleimide at the stilbene-disulfonate site, $^{14}$N-BSSDA at an intermolecular cross-link site and $^{14}$N-BSSDA reacted with lipids. Integration of these signals indicated that approximately 4 moles of BSSDA bound to proteins per 1 mole of sI-DADS-maleimide. The expected ratio of BSSDA to sI-DADS-maleimide would be 1:2 if a unique monomer-monomer cross-link site exists; however, at high concentrations BSSDA has substantial non-specific labelling of additional sites. A dansylated analog of BSSDA is currently being synthesized for use in sequencing cross-linked residues and in FRET studies to better determine the distance between the stilbene disulfonate site and the monomer-monomer interface cross-linked by the bis(sulfo-N-succinimidyl) class of reagents. *Supported by: R01HL34737*

M-Pos36

**EFFECTS OF PROTEOLYTIC CLEAVAGE ON HUMAN ERYTHROCYTE ANION EXCHANGE PROTEIN (BAND 3) ROTATIONAL DYNAMICS.** ((C.E. Cobb, E.J. Hustedt, W.E. Wojcicki, & A.H. Beth)), Mol. Physiol. & Biophysics, Vanderbilt Univ., Nashville, TN 37232.

Erythrocyte (RBC) band 3 is an integral membrane protein which mediates the electroneutral exchange of chloride and bicarbonate. Chymotrypsin treatment of intact RBCs cleaves band 3 into integral membrane ~58 k and ~38 k Mr fragments. Band 3 transport activity (chloride / sulfate exchange) is unaffected by this cleavage. Saturation transfer EPR spectra recorded on control and chymotrypsin treated RBC membranes whose band 3 was labeled with spin labeled DADS maleimide are essentially identical, suggesting that cleavage does not disrupt the assembly of the transmembrane segments of band 3 monomers nor its oligomeric structure. Parallel studies employing time-resolved phosphorescence emission anisotropy (TPA) measurements on membranes whose band 3 was labeled with eosin-5-maleimide support the ST-EPR data, although subtle differences in the anisotropy decay components are detectable. Trypsin treatment of the ghost membranes cleaves a cytoplasmic ~41 k Mr fragment (the domain believed to interact directly with cytoskeletal proteins) from the integral membrane domain. Scission of this peptide linkage results in a modest increase in the band 3 integral membrane domain rotational mobility as measured by ST-EPR, which does not directly correlate with the changes observed in TPA decay. The conclusion from these studies is that the flexibility of the linkage between the cytoplamic domain and the intergral membrane domain of band 3 prevents the cytoskeleton from exerting a major constraint on the rotational mobility of band 3. We are currently evaluating uniaxial diffusion models for fitting and interpreting the ST-EPR and TPA data for band 3 rotational motions in the RBC membrane. Supported by R01 HL34737 & T32 DK07186.

**M-Pos37**

PROBING THE ROLE OF PROTEIN-PROTEIN INTERACTIONS IN THE FUNCTION OF *TRP* REPRESSOR: BEHAVIOR OF THE SUPER-REPRESSOR, DN46.
((Ross J. Reedstrom)) Program in Cell & Molecular Biology, University of Wisconsin-Madison, Madison WI 53706. (Sponsored by Catherine A. Royer)

*Trp* repressor (TR) is a small bacterial repressor protein that, in response to tryptophan, regulates multiple operons involved in aromatic amino acid biosynthesis. Each dimer binds two molecules of tryptophan and is then capable of binding tightly ($K_d \approx 0.2$ nM) to its cognate operator DNA. Although the stoichiometry of binding is nominally one TR dimer per operator, higher stoichiometries have been observed, depending on DNA sequence context and solution conditions. A structure of a 2:1 tandem complex has been recently deduced from X-ray crystallographic diffraction data (Lawson & Carey, Nature in press). Some super-repressors, which repress transcription *in vivo* at lower concentrations of tryptophan, have been shown to preferentially populate 2:1 dimer/operator complexes in gel shift experiments (Liu & Matthews, JBC in press). In addition, TR dimers interact in the absence of DNA (Fernando & Royer Biochemistry **1992**, 31, 3429-3441 ). Taken together, these results point to the importance of including protein-protein, in addition to protein-ligand and protein-DNA interactions, in any model of the mechanism of TR function. The various biomolecular interactions of one super-repressor, DN46, were characterized using fluorescence techniques. The results are compared to those obtained from wild type TR and another super-repressor, EK18, and interpreted in terms of the available structural database.

**M-Pos38**

A DOMAIN MODEL FOR RECOGNITION OF PROMOTER DNA BY THE T7 FAMILY OF RNA POLYMERASES.
((Maribeth Maslak, Charlie Schick, Hoi Hung Ho, & Craig T. Martin)) Department of Chemistry and Program in Molecular & Cellular Biology, University of Massachusetts, Amherst 01003. (Sponsored by R. Prigodich)

The DNA dependent RNA polymerases from the T7 family of bacteriophages are highly specific for the initiation of transcription from a small (≈17 bp) promoter sequence. Previous studies have suggested that the enzyme binds to one face of a mostly closed duplex form of the promoter, consistent with recent modeling studies based on the crystal structure of the enzyme. Kinetic studies of modified oligonucleotide promoters provide specific tests of the interactions between polymerase and promoter. Extensive analyses in the differential recognition region of the promoter confirm a previous model for the interaction of amino acids at position 748 in the family of proteins with dinucleotide steps at positions -10 and -11 in the central region of the promoter DNA. A variety of results in this region all support a simple direct read-out of duplex major groove functional groups. Nearer to the start site for transcription, however, a model is developing in which the enzyme interacts only with the template strand of the DNA in apparent contradiction with footprinting results and with simple docking models. Specific interactions with the template strand have been identified in this region, including interactions with a thymine methyl group at position -3. Probes of binding contacts in the intermediate region of the promoter, between the upstream duplex and downstream single stranded regions, provide further insight into the nature of these domains.

**M-Pos39**

MEDIATION OF MOLECULAR RECOGNITION IN PROTEIN–DNA COMPLEXES BY BOUND WATER: A MECHANISM FOR "STAR ACTIVITY" OF RESTRICTION ENDONUCLEASES.
((C.R. Robinson and S.G. Sligar)) Department of Biochemistry, University of Illinois at Urbana-Champaign, Urbana, IL 61801.

For many restriction endonucleases such as *Eco* RI, accurate protein-DNA recognition is disrupted by changes in buffer composition, leading to an unexplained loss of specificity termed "star activity." We have found that the extent of cleavage by *Eco* RI at non-canonical sites is strongly correlated with the osmotic pressure in the reaction. This relationship is unique to osmotic pressure, and is independent of other physical or chemical properties of the osmolyte. An analogous correlation between osmotic pressure and star activity is observed for other restriction enzymes including *Pvu* II and *Bam* HI. Specificity for cleavage at canonical sites is restored by the application of hydrostatic pressure to counteract the effects of osmotic pressure. Elevated osmotic pressures induce a fundamental change in the selectivity of *Eco* RI — at 100 atm osmotic pressure the rate of cleavage at the canonical site actually decreases, whereas the rate of cleavage at "star" sites increases. The alteration of specificity accompanying release of water clearly implicates one or more water molecules in mediating accurate recognition of specific sequences of DNA by the enzyme. The change in selectivity is manifested in both the association and catalytic steps of the reaction. Under standard conditions, water may participate as a general mediator for sequence specific recognition of DNA by restriction enzymes and other DNA-binding proteins.

**M-Pos40**

MOLECULAR DYNAMICS SIMULATION OF A DNA BINDING PROTEIN FREE AND IN COMPLEX WITH DNA
((Mats Eriksson, Torleif Härd and Lennart Nilsson)) Karolinska Institute Center for Structural Biochemistry, NOVUM Research Park, S-141 57 HUDDINGE, Sweden

Molecular dynamics simulations have been performed on the DNA binding domain (DBD) of the glucocorticoid receptor (GR) free in aqueous solution and bound as a dimer to a DNA duplex, also in aqueous solution. The combined information from these simulations provides insights into structural and dynamic consequences for the GR DBD upon binding to the DNA in terms of the specific and non-specific interactions with DNA and also for the protein-protein interacticons at the dimerisation surface. Comparions are made with experimental data, from {$^1$H} -$^{15}$N-NMR, on the backbone dynamics of the DBD monomer free in solution, and with the NMR and X-ray structures of the monomer and complex, respectively. Thermodynamic studies, by free energy perturbation methods, of the binding of the small antiviral agent netropsin to DNA have been successful in reproducing the known preference for this minor groove binder for AT regions of DNA, and will be discussed in the framework of using similar methods to study interactions between GR DBD and different DNA sequences.

**M-Pos41**

**NMR SOLUTION STRUCTURE OF THE NK-2 HOMEODOMAIN AND ITS INTERACTIONS WITH DNA**
((D. H. H. Tsao, J. M. Gruschus, L.-H. Wang, M. Nirenberg, J. A. Ferretti)) NHLBI, N.I.H., Bethesda, MD 20892

Homeodomain proteins are transcription factors that bind to sequence specific DNA, thereby regulating gene expression in eukaryotes. The NK-2 homeodomain of *Drosophila*, enriched with $^{15}$N and $^{13}$C, has been studied by aqueous, multi-dimensional NMR. A model structure has been determined for the unbound protein using NOE-derived distance constraints. The model shows the helix-turn-helix (HTH) motif, in common with the other structurally determined homeodomains, though with less helical content, most notably the lack of the extension of the third helix. The consensus DNA binding site of NK-2 AAGTG differs from the TAAT sequence common to the binding sites of other structurally determined homeodomains to date. Using multi-dimensional NMR of NK-2 bound to a 16 base pair DNA oligomer containing the AAGTG binding site, the interactions between specific residues and the DNA have been determined. Methylation protection experiments have also been performed, indicating those portions of the DNA in contact with the protein. These results are compared with previously determined DNA/homeodomain interactions and mechanisms of sequence specific binding are discussed.

**M-Pos42**

**LASER UV-CROSSLINKING AND STOPPED-FLOW FLUORESCENCE STUDIES OF TBP/DNA INTERACTION.**
((Roberta A. Knittle, Gina M. Perez-Howard, P.A. Weil and Joseph M. Beechem)) Vanderbilt University, Dept. of Molecular Physiology and Biophysics. Nashville, TN 37232.

The association of TATA-box Binding Protein (TBP) with its DNA binding site (TATAAAA) results in the formation of an 80° bend and almost complete flattening of the minor groove. This initial binding and associated DNA conformational transition is the nucleating event in the formation of a transcription pre-initiation complex on all eukaryotic Polymerase II promoters. We have determined that laser-UV (266nm) crosslinking can be utilized to generate crosslinked TBP-DNA adducts on the TATA box. Sufficient adduct is produced by our method to permit peptide analysis of the crosslinked sites on TBP. Detection of protein in the complexes was demonstrated by silver stain and shown to contain TBP by Western blot analysis. Co-migration of these species with the radioactive signal from a probe internally labeled through the TATA sequence after nuclease digestion indicates crosslinking to the TATA box was achieved. Stopped-flow fluorescence anisotropy studies using end-labeled Rhodamine-X DNA reveal multi-phasic binding to DNA. Attempts are being made to perform UV crosslinking on the same time scale as the spectroscopic study in order to chemically identify intermediates in the association phase of binding. RAK supported by the Mol. Endo. Training Program (DK07563).

M-Pos43

## KINETICS OF ADENINE NUCLEOTIDE BINDING TO THE E.coli REP HELICASE

((Keith J.M. Moore and Timothy M. Lohman.)), Dept. of Biochemistry and Molecular Biophysics., Washington University School of Medicine., Box 8231., 660 S. Euclid Ave., St Louis, MO 63110. (Spon. by T. Lohman)

DNA helicases catalyze the unwinding of duplex DNA and translocate along the duplex in reactions that are coupled to ATP binding and hydrolysis. While the E.coli Rep helicase is a stable monomer in the absence of DNA, it is induced to dimerize upon binding DNA, with a concomitant increase in ATPase activity. As a basis for understanding how the hydrolysis of ATP is coupled to DNA unwinding, we are investigating the kinetics and mechanism of ATP binding and hydrolysis by the Rep monomer (P) and the various dimer species. These stopped flow studies monitor changes in the intrinsic protein fluorescence and/or changes in energy transfer from Trp residues in Rep to the fluorescent 2'(3')-[O-(N-methylanthraniloyl)]- (mant) derivatives of adenine nucleotides. We have characterized the binding of ATP by the Rep monomer (6 mM NaCl, pH 7.5, 4°C) as a basis for understanding the ATPase of the more complex dimeric species. We have used a kinetic competition approach to follow ATP binding in the presence of mantATP. Relatively rapid binding of ATP to P (step 1) is followed by a slow conformational change (step 2) ; i.e $P + ATP \leftrightarrow P.ATP \leftrightarrow P^*.ATP$ where $k_{+1} = 7.2 (\pm 0.2) \times 10^6\ M^{-1}\ s^{-1}$, $k_{-1} = 1.2 (\pm 0.4)\ s^{-1}$, $k_{+2} \approx 0.4 (\pm 0.2)\ s^{-1}$, $k_{-2} \approx 0.09 (\pm 0.02)\ s^{-1}$. Mant-nucleotide binding also follows a similar mechanism. These approaches are being extended to investigate the ATPase activity of Rep dimers bound to DNA.

M-Pos44

## THERMODYNAMIC ANALYSIS OF THE INTERACTION BETWEEN THE *DROSOPHILA* HEAT SHOCK FACTOR DNA BINDING DOMAIN AND ITS COGNATE SEQUENCE.

((S-J. Kim, T. Tsukiyama, M. S. Lewis and C. Wu)) LB, NCI and BEIP, NCRR, NIH, Bethesda, MD 20892 (Sponsored by L. Holladay)

Heat shock transcription factor (HSF) mediates the transcriptional activation of heat shock genes by binding to cognate elements known as heat shock elements with high affinity and specificity. High affinity binding of HSF is dependent on the formation, following heat shock, of an HSF homotrimer. In order to study the interaction of monomeric HSF with a synthetic 13 base pair binding site containing a single core -GAA- recognition element, we have over-expressed and purified a polypeptide encompassing the DNA-binding domain of HSF (dHSF(33-163)). We have demonstrated that this polypeptide can bind to the cognate sequence with relatively high affinity and specificity. We have studied these interactions by equilibrium analytical ultracentrifugation using a multi-wavelength scan technique. The values of the thermodynamic parameters were obtained from the temperature dependence of the values of *ln*K for the interactions. In 0.05 M KCl buffer, pH 6.3, at 10° C, the values of $\Delta G^o$, $\Delta H^o$, and $\Delta S^o$ were, respectively, -9.81 kcal mol$^{-1}$, -7.52 kcal mol$^{-1}$ and 8.10 cal mol$^{-1}$ K$^{-1}$ for the wild type DNA sequence and -7.92 kcal mol$^{-1}$, -10.54 kcal mol$^{-1}$ and -9.27 cal mol$^{-1}$ K$^{-1}$ for a mutant DNA sequence with -CAA- replacing -GAA-. The interaction with this DNA demonstrated much greater salt concentration dependence, $\Delta\Delta G^o$ increasing from 1.89 kcal mol$^{-1}$ in 0.05 M KCl to 3.15 kcal mol$^{-1}$ in 0.10 M KCl.

M-Pos45

## THERMODYNAMICS OF THE BASE SPECIFIC INTERACTIONS OF *E.coli* SINGLE STRANDED BINDING PROTEIN WITH DNA.

((Marilyn E. Ferrari, and Timothy M.Lohman)) Dept. of Biochem. & Mol. Biophysics, Washington Univ.School of Med., St. Louis, MO 63110.

Single stranded DNA binding proteins (SSB's) are essential for DNA replication in procaryotes and eucaryotes, and also function in recombination and repair. Although SSB's are usually referred to as "non-specific" binding proteins with regard to DNA sequence, several SSB's from both procaryotes and eucaryotes bind with greater affinity to polydeoxypyrimidines relative to polyd(A). To further understand the basis of this, we have compared the thermodynamics of the interaction of *E.coli* SSB with pyrimidine oligonucleotides ($dT(pT)_N$,$dC(pC)_N$) vs.$dA(pA)_N$ (N=34,55 and 69). *E.coli* SSB is a homotetramer and binds single stranded nucleic acids in at least four distinct binding modes, differing in the number of nucleotides bound per SSB tetramer (n) where n=35,40,56, or 65. We observe differences between the binding enthalpy ($\Delta H_{obs}$) for the SSB-d(pyr) and SSB-$dA(pA)_N$ interactions. Linear van't Hoff plots are obtained for the interaction of SSB with $dT(pT)_N$ and $dC(pC)_N$ and $\Delta H_{obs}$ is negative (-50 to -100 Kcal/mol). However, van't Hoff plots for the SSB-$dA(pA)_N$ binding are non-linear with a maximum in the equilibrium constant near 25°C. $\Delta H_{obs}$ is positive at lower temperature, and negative at higher temperature. The observed curvature for the SSB- $dA(pA)_N$ interaction is not due to dissociation or disassembly of the SSB tetramer at 37°C, nor the formation of other SSB binding modes. Our results are consistent with a model in which the unstacking transition in the $dA(pA)_N$ is coupled to SSB binding.

M-Pos46

## COOPERATIVE BINDING OF *Escherichia coli* SSB TETRAMERS TO SINGLE STRANDED DNA IN THE $(SSB)_{35}$ BINDING MODE.

((M. E. Ferrari†, W. Bujalowkski§, and T.M.Lohman†)) †Dept. of Biochem. & Mol. Biophysics, Washington Univ.School of Med., St. Louis, MO 63110. §Dept of Human Biological Chem. & Genetics, Univ. of Texas Medical Branch, Galveston, TX 77550.

*E. coli* SSB tetramers can bind to single stranded (ss) DNA in at least three distinct binding modes, $(SSB)_n$, where the number of nucleotides occluded per tetramer (n), can be 35, 56 or 65 (25°C, pH 8.1). Stability of the modes is modulated by primarily the salt concentration and type, and free SSB concentration. Two different types of positive cooperative binding of have been observed, which correlate with different SSB binding modes. The $(SSB)_{65}$ mode dominates at [NaCl] > 0.2 M, and displays a cooperative binding "limited" to octamer formation. At lower [NaCl], "unlimited" cooperative binding is observed in which long SSB clusters can form. The "unlimited" cooperativity appears to be linked to the $(SSB)_{35}$ binding mode; however, this has not been verified. To estimate the nearest-neighbor cooperativity parameter in the $(SSB)_{35}$ mode, we examined the equilibrium binding of SSB to the oligodeoxynucleotide, $dA(pA)_{69}$ under conditions where a mixture of 1:1 and 2:1 complexes form. The 2:1 complex serves as a model for cooperative binding in the $(SSB)_{35}$ binding mode. SSB tetramers bind in this mode with a minimum nearest-neighbor cooperativity parameter of $\omega_{35}=1.0 \times 10^5$ (0.125 M NaCl, pH 8.1, 25°C), suggesting that the $(SSB)_{35}$ mode is able to form long clusters on ss-DNA. If the ability of SSB to form uninterrupted protein clusters on ss-DNA is important in DNA replication, then it is likely that the $(SSB)_{35}$ mode functions in this capacity.

M-Pos47

## SMALL-ANGLE X-RAY SCATTERING OF FD GENE 5 PROTEIN: NUCLEIC ACID COMPLEXES.

((D.M. Gray, C.W. Gray, B.L. Mark, M.D Powell, & M.R. Vaughan)) Molecular and Cell Biology, The University of Texas at Dallas, Box 830688, Richardson, TX 75083-0688. ((G.A. Olah, D.L. Kergil, T.R. Sosnick, & J. Trewhella)) Isotope and Nuclear Chem. Div., Los Alamos National Lab., Los Alamos, NM 87545.

Small-angle X-ray scattering profiles have been obtained for five helical complexes formed by the fd gene 5 protein (g5p) and fd DNA, poly[d(A)], or poly[r(A)] in solution. Complexes at a [protein monomer]/ [nucleotide] ratio of 1/4 were formed with all three nucleic acids. Additional complexes with fd DNA and poly[d(A)] were studied that had [protein]/[nucleotide] ratios of 1/3 and 1/2.5, respectively. Guinier analysis of the data showed a significant variation among the complexes in their cross-sectional radius of gyration (Rc) and mass per unit length values. The complex with the largest Rc (34.5 ± 0.4 Å) and smallest mass per unit length was the g5p:poly[d(A)] complex at a 1/2.5 [protein monomer]/[nucleotide] ratio. The g5p:poly[r(A)] complex, on the other hand, had the smallest Rc (26.3 ± 0.3 Å) and the largest mass per unit length. Therefore, the packing and arrangement of protein dimers along the helix axis is dependent on the composition of the nucleic acid substrate and the [protein]/[nucleic acid] stoichiometry. A new Monte Carlo method has been developed to model the complexes, from which the parameters of radius, pitch, and rise per dimer subunit are derived.

This work was supported by NIH Grant GM19060, Grant AT-503 from the Robert A. Welch Foundation, and DOE/OHER Project KP-04-01-00-0

M-Pos48

## NUCLEOCAPSID PROTEINS FROM EIAV AND AMV SHOW SIGNIFICANT DIFFERENCES IN THE WAY THEY INTERACT WITH NUCLEIC ACIDS*

**((Craig A. Gelfand†, Bruce Woodson‡, Ronald Montelaro‡, & Joyce E. Jentoft†)) †Dept. of Biochemistry, Case Western Reserve University, Cleveland, OH 44106, & ‡Dept. of Molecular Genetics and Biochemistry, University of Pittsburgh, Pittsburgh, PA 15213.**

**Retroviral nucleocapsid proteins (NCs), found in histone-like association with the RNA genome, are essential proteins during many processes in the viral life cycle. In this study, we present nucleic acid (NA) binding parameters for NC from equine infectious anemia virus (EIAV). EIAV NC binding to poly(rA) can be monitored by the change in the circular dichroism spectrum of the NA. Stoichiometric binding conditions show EIAV NC to have an occluded site size of 8 bases per NC, while binding in 150mM NaCl shows $K_{obs}$ to be 1.1±0.2 x $10^4$ $M^{-1}$ with cooperativity, ω, of 150±10. NaCl-induced dissociation of the NC-NA complex shows the thermodynamic association constant, $K_T$, to be 40 $M^{-1}$. These findings directly contrast the binding parameters from avian myeloblastosis virus (AMV) NC[1]: $K_T$=630 $M^{-1}$, ω=25. Apparently, NCs from lentiviridae (i.e. EIAV) and oncoviridae (i.e. AMV) utilize different modes of interaction to achieve high affinity NA binding.**

*A contribution from the Protein Group at Case Western Reserve University.

[1]Gelfand et al, *J. Biol. Chem.* 268 (1993) 18450-18456.

**M-Pos49**

**BINDING OF YEAST RIBOSOMAL PROTEIN L32 TO ITS PRE-mRNA.** (Hu Li and Susan White) Bryn Mawr College, Bryn Mawr, PA 19010.

The specific interaction between yeast r-protein L32 and the 5' splice site of its pre-mRNA is critical to the autoregulation of L32. When the L32 protein is present in excess, it binds to its own pre-mRNA, inhibits splicing and thus prevents formation of the mature RNA. Production of additional L32 protein is thereby abolished [Eng and Warner, (1991) Cell, 65, 797-804]. The RNA binding target is thought to contain two short helical regions separated by an asymmetric loop composed solely of purines.

Small RNAs which are intended to reproduce the essential protein recognition features have been synthesized. Both enzymatic and chemical susceptibilities support the stem-loop-stem secondary structure model and further indicate that the unpaired loop G's and A's have reactivities intermediate between those of single and double-stranded nucleotides. The smallest RNA which we have tested for RNA binding is a duplex which consists 24 nucleotides. The binding affinity of these RNAs to the L32-Maltose Binding Protein has been measured using both electrophoretic bandshifts and filter binding.

**M-Pos50**

**ELECTRON CRYOMICROSPCOPY OF 50S RIBOSOMAL SUBUNITS CRYSTALLIZED ON PHOSPHOLIPID MONOLAYERS.** ((Agustin J. Avila-Sakar[1], Ting-Lu Guan[2], Talmon Arad[3], Michael F. Schmid[2], Tim W. Loke[2], Ada Yonath[3,4], Jutta Piefke[5], Francois Franceschi[5] and Wah Chiu[1,2]))

[1]Dept. of Mol. Physiol. & Biophys., Baylor College of Medicine, Houston, TX
[2]Verna and Marrs McLean Dept. of Biochemistry, Baylor College of Medicine, Houston, TX
[3]Dept. of Structural Biology, Weizmann Institute of Science, Rehovot, Israel
[4]Max-Planck-Laboratory for Ribosomal Structure, Hamburg, Germany
[5]Max-Planck-Institute for Molecular Genetics, Berlin, Germany

Electron images of frozen-hydrated 50S ribosomal subunits of *B. stearothermophilus*, crystallized on a negatively charged phospholipid monolayer, were recorded at 100 kV under low dose and low temperature conditions. The Fourier spectra of 76 image arrays reveal unit cell spacings of a = 371 Å, b = 152 Å, γ = 96°. Some of the image arrays display *p2* symmetry with phase residuals of less than 25°. The mean figure of merit of the merged structure factors from these image arrays out to 20 Å resolution is greater than 0.87. The fall-off of the amplitudes as a function of spatial frequency suggests that the present resolution extends beyond 20 Å. A projection density map to 20 Å resolution was computed from the merged data. There are two ribosomal subunits per unit cell, related by a 2-fold rotational axis normal to the plane of the projection. The map shows details not previously seen in studies of the 50S ribosomal subunit.
Our study demonstrates the feasibility of producing two-dimensional crystalline arrays of 50S ribosome subunits from *B. stearothermophilus* suitable for the reconstruction of its three-dimensional structure beyond 20 Å resolution.

This work is being supported by NIH, the Kimmelman Center at the Weizmann Institute, the Robert A. Welch Foundation and the W. M. Keck Foundation.

**M-Pos51**

THREE-DIMENSIONAL RECONSTRUCTION OF MAMMALIAN 40S RIBOSOMAL SUBUNIT EMBEDDED IN ICE.
(( S. Srivastava, A. Verschoor, M. Radermacher and J. Frank)) Wadsworth Center for Labs and Research, NYS Dept. of Health, Albany, NY 12201.

We have performed a three-dimensional reconstruction of the mammalian 40S small ribosomal subunit embedded in ice, using the random conical reconstruction method to analyze lateral-orientation particle images. The characteristic features of the subunit can readily be identified: the head with its prominent beak structure, the body portion with its two back lobes protruding in the direction opposite to the beak, and the two feet that comprise the base of the subunit.

Overall, there is good agreement with a previous reconstruction from a negatively stained specimen (Verschoor et al. 1989). One notable new observation that emerges, however, is the degree of morphological resemblance of the platform/ lobe structure of the upper body to the well characterized platform region of the 30S small subunit of the eubacterial ribosome. This brings into question the assumption in the literature that, in evolutionary terms, the two back lobes of the 40S subunit substitute for, and are functionally homologous to, the platform structure of the 30S subunit. The back lobes in the new 40S structure appear as only minor features, perhaps representing sites of insertions (relative to the 16S rRNA sequence of the 30S ribosomal subunit) in the 18S rRNA of the 40S subunit.

Refinement of the reconstruction should help to elucidate the details of this crucial translational domain at higher resolution.

Ref: A. Verschoor, N.-Y. Zhang, T. Wagenknecht, T. Obrig, M. Radermacher and J. Frank. , (1989) 209, 115./ Supported by NIH GM29169 ( to J.Frank).

## NMR AND ESR

**M-Pos52**

NMR STUDIES OF DESIGNED AMPHIPATHIC PEPTIDES.
((Karol Maskos and Kathleen M. Morden)) Dept. of Biochemistry, Louisiana State University, Baton Rouge, LA 70803

A nuclear magnetic resonance analysis of the following synthetic peptides has been conducted

I. $NH_2$-(KLGKKLG)3-$CONH_2$
II. $NH_2$-(KLAKKLA)3-$CONH_2$
III. $NH_2$-(KPAKPAK)3-$CONH_2$

NMR spectra have been obtained in 15% and 30% HFIP at different temperatures. These conditions mimic a membranelike environment and under these conditions the peptides display CD spectra indicative of helical secondary structure. Using TOCSY and DQF COSY experiments all resonances of the main chain and side chain protons have been assigned except for those of the N-terminal lysine. Secondary structure connectivity diagrams have been established on the basis of NOESY data. 2D-TOCSY experiments were used for chemical shift analysis and for the study of exchange behavior of labile protons. These data together with the $J_{NH\alpha}$-coupling constants in conjunction with CD experiments, allow the characterization of conformational ensembles exhibiting a high degree of helicity.

Supported by NSF/LEQSF (1992-96)-ADP-01.

**M-Pos53**

**The Determination of the Secondary Structure of a 16 Residue Peptide via N.M.R.**
((Paul Hanson, Doug Brooks, Siobhan Miick, Glenn Millhauser)) Department of Chemistry and BioChemistry, University of California, Santa Cruz , Ca., 95064

Previous EPR work with spin labeled peptides has shown that these peptides are more structured towards the N-terminus as well as also having $3_{10}$ structural characterstics(Miick, et al., Biochemistry 1993). In this work, we report the results of 2D N.O.E. epxeriments on the non-spin labeled analogue of those peptides.

N.O.E. evidence gathered from these experiments provides enough data in the amide region to make assignments to the first five residues only, starting from the acetyl group located at the N-terminus (Lockhart, Kim, Science, 260(9), April 9, 1993). The remaining residues are unassignable due to spectral overlap. The data from these first five residues suggest that the N-terminus is more ordered than the remainder of the peptide which is agreement with previous E.S.R. experiments(Miick, et al., Biochemistry 1993). However, the long range N.O.E. data are inconclusive due to the poor dispersion of the α and β regions of the alanines. As a result of this lack of dispersion, the crucial assignments for determination of the structure from the N.O.E. cross peaks did not provide any new information regarding the question of the peptide being $3_{10}$ or α-helical in its structure.

M-Pos54

**NMR STRUCTURE DETERMINATION OF A PEPTIDE FRAGMENT CORRESPONDING TO THE C-TERMINUS OF GP41 OF HIV-1 IN A MEMBRANE MIMETIC ENVIRONMENT**

((B.W. Koenig*, K. Gawrisch** and J.A. Ferretti*))
NIH, Bethesda, MD 20892; * NHLBI, ** NIAAA

We have shown previously that the peptide fragment RVIEVVQGACRAIRHIPRRIR undergoes a structural change from a disordered state in solution to an ordered structure upon binding to negatively charged lipid bilayers (Biochemistry 32 (1993) 3112 - 3118).
Here we report an NMR structural analysis of the peptide in a membrane mimetic environment. Both TOCSY and NOESY experiments were carried out with 10 mM peptide dissolved in a 300 mM Sodium Dodecyl Sulfate (SDS) micellar solution, at 60 °C. The NOESY spectra confirm the existence of an α-helical structure. However, the relative intensity of $d_{\alpha\alpha}$ vs. $d_{\alpha N}$ crosspeaks indicates that the peptide is in fast exchange between at least two conformations. These results are in agreement with CD - measurements which indicate a α-helical content of approximately 50% under identical conditions. Rotational reorientation correlation times of peptide were estimated from $T_1$ and $T_2$ measurements at 600 MHz and 360 MHz. The correlation times are in the expected range for small micelle - peptide complexes, thus confirming peptide binding to SDS. We suggest that both events are related to an interaction of the C-terminus of gp41 with membranes.
(B.W.K. acknowledges financial support by a grant from the German Academic Exchange Service)

M-Pos55

**STRUCTURE OF A C-TERMINAL ALPHA HELIX CAP IN A SYNTHETIC PEPTIDE**

((Hongxing X. Zhou†, Pingchiang C. Lyu‡, David E. Wemmer‡, and Neville R. Kallenbach†)) †Department of Chemistry, New York University, New York, NY 10003; ‡Department of Chemistry, University of California at Berkeley, CA 94720.

The peptide bonds at the ends of short α helices cannot form H-bonds to donors or acceptors in the backbone. Instead, polar side chains can interact with unbonded NH groups to stabilize the N terminal ends of α helices in peptides or proteins. The predominant interaction at the C terminus in proteins involves an unusual left handed ($\alpha_L$) conformation of the backbone, which allows H-bonding between an extrahelical NH group and a CO in the helix. The amino acid asparagine at the C terminus is found to stabilize the helical structure in a synthetic model peptide. We show here, using 2D $^1$H NMR, that the side chain of asparagine interacts with a main chain CO three residues in the N direction along the chain, forming a C terminal cap structure. This structure is seen for the first time in a model peptide, and shares with the N-terminal capping structure that has recently been determined in a related peptide model the common feature that a pair of H-bonds participate in initiation or termination of α helical structure.

This research was supported by grants from NIH and NSF.

M-Pos56

**$^1$H NMR CHARACTERIZATION OF HEME-HEME OXYGENASE.**

((G. Hernández[1,3],A. Wilks[2],P. R. Ortiz de Montellano[2], and G. N. La Mar[1]))
[1] Department of Chemistry, University of California, Davis, CA 95616. [2] Department of Pharmaceutical Chemistry, School of Pharmacy and Liver Center, University of California, San Francisco, CA 94143-0446. [3] Present Address: Los Alamos National Laboratory. Spectroscopy and Biochemistry, INC 14, MS C345, Los Alamos, NM 87545. (Spon. by P. A. Seeger)

Heme oxygenase is a membrane-bound 32 kDa protein which catalyses the oxidation of heme at the a-methene bridge to form biliverdin at the expense of NADPH and molecular oxygen. The enzyme binds heme yielding an enzyme-substrate complex. It has been suggested that the attack of the methene bridge by an iron bound to oxygen molecule is controlled by the protein environment based on the selectivity of the heme cleavage observed in model systems with myoglobin and hemoglobin. An active soluble 30 kDa form of the rat liver heme oxygenase has been expressed and several hemins added as a substrate. $^1$H NMR spectra of protohemin IX and deuterohemin IX heme oxygenase complexes suggested two different molecular species. Protohemin III and deuterohemin III were added as a substrate to elucidate structural homogeneity because these hemins present two fold symmetry about the a-g axis. $^1$H NMR spectra of their complexes with heme oxygenase showed only one dominant molecular species suggesting that the two molecular species are due to the presence of the heme in two different environments. 2D NMR analysis combined with assignments provided by selectively deuterated hemins confirmed that the heme is present in two different environments.

M-Pos57

**3D NMR STUDIES OF GIANT RAGWEED ALLERGEN 5**

((G.L. Warren, A.T. Brunger, G.A. Petsko and C.J. Turner))
Howard Hughes Medical Institute and Department of Biophysics and Biochemistry, Yale University, New Haven, CT 06511; Rosenstiel Basic Medical Sciences Research Center, Brandeis University, Waltham, MA 02254; Francis Bitter National Magnet Lab, MIT, Cambridge, MA 02139. (Spon. by K.V. Lakshmi)

We have undertaken 3D homonuclear proton NMR studies of *Amb. t.* V, a small 40 residue protein with 4 disulphide bonds which elicits an allergic response in humans (Hay Fever). Using 3D TOCSY-NOESY experiments we have unambigously identified 3 out of 4 disulphide bonds (C5-C35, C11-C26,, and C18-C28). Structure calculations have been undertaken using three methods: Distance Geometry/Simulated Annealing (DG/SA), intensity modified DG/SA and relaxation matrix refinement using an extended version of the program X-PLOR. The quality of the structures derived from, and the computational efficiency of, these methods are compared.

M-Pos58

ONE-DISULFIDE INTERMEDIATES OF APAMIN EXHIBIT NATIVE-LIKE STRUCTURE. ((Xiaobing Xu and J.W. Nelson)) Department of Biochemistry, Louisiana State University, Baton Rouge, LA 70803.

The conformations of three model peptides analogous to the one-disulfide folding intermediates and fully reduced apamin were characterized using nuclear magnetic resonance (NMR). Apa-2 contains the native disulfide bond between Cys3 and Cys15 in apamin with other cysteines replaced by alanines. Apa-1 contains the native disulfide bond between Cys1 and Cys11. Apa-S has all cysteines replaced with serines, mimicing fully reduced apamin. Comparing NOE cross peaks and coupling constants for amide protons in the peptide analogs with those in native apamin indicates that a significant population of Apa-2 possesses the native-like structural elements of apamin. Some random coil conformations were also observed in Apa-2. Apa-1 contains a short α-helical structure from Ala9 to Arg13 which is similar to the N-terminal of the α-helix in native structure. Some short and unstable local secondary structures corresponding to the reverse turn and helical regions in the native structure were also detected. Larger portions of Apa-1 exist in the form of random coil conformation compared to Apa-2. Apa-S displays mainly random coil conformation with some localized helical structure from Glu7 to Arg14.
The formation of the first disulfide bond in apamin seems to be very important in initiating the folding process and stabilizing the native like structure. Formation of one disulfide bond presumably reduces the conformation entropy and stabilizes the native structure of apamin. For a small peptide such as apamin, the position of disulfide bond is important in determining the conformations of folding intermediates, as evidenced by Apa-2 containing significantly more native like conformations than Apa-1. This research was supported by NIH grant GM 39615.

M-Pos59

**DEVELOPMENT OF TOOLS FOR ORIENTED SAMPLE NMR APPROACHES TO MEMBRANE PROTEIN STRUCTURE.** ((James P. Schwonek, Geoffrey C. Landis and Charles R. Sanders, II)) Dept. of Physiology and Biophysics, Case Western Reserve University, Cleveland, Ohio 44106. (Spon. by Thomas Gerken).

It is now well established that oriented sample NMR (OSNMR) can be used to elucidate membrane protein structure (Ketchem, Hu, and Cross; *Science* **261**, 1457-1460, 1993). In this poster, we present progress in the following areas related to future development and application of this approach:

(i). Development of solvent systems suitable for transmembrane polypeptides (which are often very difficult to synthesize, purify, and handle due to their propensity to aggregate).

(ii). Reconstitution of surface-associating and transmembrane polypeptides in magnetically orientable phospholipid systems. Evaluation of such reconstitutions in terms of both protein function and spectroscopic suitability for OSNMR studies.

(iii). Development of energy/force field functions suitable for computer modeling of membrane proteins in a bilayer environment.

(iv). Development methods for translating OSNMR data into explicit information on molecular structure and dynamics.

(v). Proposal of a general algorithm which we hope to apply to polytopic membrane proteins. This algorithm is based in part upon the Popot-Engelman model (*Biochemistry* **29**, 4031-4037, 1990) for the folding of membrane proteins.

M-Pos60

AUTOMATIZED FITTING OF THE SIMULATED NOESY SPECTRA TO THE EXPERIMENTAL ONES BY MEANS OF A GLOBAL OPTIMIZATION TECHNIQUE.
((I.P. Sugar,* Y. Xu and N.R. Krishna)) *Department of Biomathematical Sciences, Mount Sinai School of Medicine, New York, NY 10029; NMR Core Facility, University of Alabama at Birmingham, Birmingham, AL 35294.

A new method of structure refinement based on optimization of the variable target function (Sugar and Xu, Progress in Biophysics and Molecular Biology, 1992, 58, 61-84) is tested in this work. In the test calculations, by using simulated experimental data for model proteins of known structure, we have *a priori* knowledge of the global minimum of the target function and R-factor, enabling us to make comparisons between the target values and the results of the optimizations.
The global minimum of the target function was attained after a single or several consecutive optimizations depending on the initial set of optimization parameters. The success of the variable target function method in the polypeptide structure determination depends on the number and distribution of the constraints (integrated intensities of the resolvable off-diagonal peaks of NOESY spectra); namely, the constraints should be larger in number than the dihedral angles, and they should be distributed over them homogeneously. The method *may* fail to determine the values of unconstrained dihedral angles; however, according to the test calculations, the new structure refinement method makes possible high resolution polypeptide structure determination even in the case of 30% relative standard deviation of the integrated peak intensities.

M-Pos61

Solution Structure of a β-toxin from *Centruroides sculpturaus Ewing*

(( Patricia L. Jackson, Dean D. Watt, and N. Rama Krishna))
University of Alabama at Birmingham, Birmingham, Al 35294; Creighton University, Omaha , NE 68178.

We have determined the first detailed solution state structure of a β-toxin (CsE-I) from the venom of the New World scorpion *Centruroides sculpturatus Ewing* (CsE). In the past, structures have been determined for the α-toxins CsE-v3 and CsE-v1. Both bind the α-subunit of sodium channels, and inhibit the inactivation of the sodium current. In contrast, CsE-I binds to a different site on the sodium channel and effects the activation of the sodium current without influencing the inactivation. There is only about 50% sequence homology between CsE-I and the α-toxins, however CsE-I contains a comparable number of residues and identically conserved disulfide bridges. Sequence-specific assignments have been made using 2D-NMR spectroscopy at 600 MHz. A number of short, medium, and long range NOESY contacts, slowly exchanging amide hydrogens, and coupling constants from phase-sensitive COSY spectra have been evaluated and used in structural determination. A hybrid distance geometry-dynamical simulated annealing protocol has been used to generate a number of structures with no constraint violations. A comparison will be made of the solution structure of the β-toxin and the α-toxin.

M-Pos62

## THE STRUCTURE AND DYNAMICS OF APO-CALMODULIN EXAMINED BY MULTINUCLEAR NMR.

((Bryan E. Finn[1], Torbjörn Drakenberg[1,2], and Sture Forsén[1]))
[1]Department of Physical Chemistry 2, Chemical Center, University of Lund, POB 124, S-221 00 Lund, Sweden and [2]Chemical Laboratory, VTT, POB 204, SF-02151 Espoo, Finland

The calcium induced activation of EF-hand calcium binding proteins such as calmodulin and troponin C has been the subject of much interest due to their many regulatory roles in cell metabolism. In order to understand the structural changes induced by the binding of calcium to calmodulin, which possesses four helix-loop-helix EF-hands, we studying the structure of one domain of calmodulin which is composed of the two carboxy-terminal EF-hands . Using multidimensional heteronuclear NMR combined with distance geometry methods, we are examining the structure and dynamics of the apo form. We have found that the structure and of the apo form of this domain differs substantially from that it possesses in the $Ca^{2+}$ activated form of calmodulin. In addition, it is found that the dynamical behavior also differs greatly from that of the $Ca^{2+}$ activated protein.

M-Pos63

DYNAMIC STRUCTURAL CHANGES OF MALEIMIDE SPIN-LABELED CALMODULIN.
((Joan Gao, Long Huynh, and Diana J. Bigelow)) Dept. of Biochemistry, University of Kansas, Lawrence, KS 66045

We have covalently attached a maleimide spin label (MSL) to a single cysteine (Cys 27) located in the hydrophobic calcium binding domain I of wheat germ calmodulin (CaM). This method for spin labeling does not (1) alter the ability of calmodulin to activate the Ca-ATPase of erythrocyte plasma membranes nor does it (2) result in any fraction of intermolecular crosslinked species. Conventional EPR spectra of MSL-CaM in aqueous media exhibit apparent correlation times in the subnanosecond time-range; these motions are sensitive to both calcium and viscosity of the media. At high viscosities that approximate that of biological membranes, the EPR spectrum exhibits two motional populations: *one*, characterized by subnanosecond probe motions, and *the other*, characterized by slower motions representing overall molecular tumbling. The abundance of the subnanosecond component is sensitive to both temperature and calcium concentration. The calcium concentration dependence for probe motion is identical to that observed for the calmodulin-induced activation of the plasma membrane, suggesting that binding of calcium to calmodulin results in increased solvent accessibility at Cys 27 in calcium binding domain I.

M-Pos64

INTRAMOLECULAR DISTANCE FLUCTUATIONS IN MODELS, PEPTIDES, AND PROTEINS.
((D. S. Cafiso, R. G. Bryant, C. North)) Department of Chemistry, University of Virginia, Charlottesville, VA 22901

The proton-proton dipole-dipole coupling is widely used as an intramolecular ruler to define distances for molecular structure determinations. Averaging over distance fluctuations is not a significant problem when at short distances. The longer range electron-nuclear dipole-dipole coupling permits characterization of larger scale intramolecular flexibility. The results of this method are demonstrated for rigid and flexible peptides, and calmodulin. The effects of internal flexibility on the electron induced nuclear relaxation cause the distances derived from relaxation data to be too short compared with a linearly averaged distance because of the very strong $r^{-6}$ dependence of the dipolar coupling. The effects of segmental flexibility are, therefore, obvious. The weakness of the approach is that there is not a unique dynamical model or trajectory derivable from the observations that yields the averaged structure from reference or model structures.

M-Pos65

FUNCTIONAL CHARACTERISTICS OF THE SUGAR-$H^+$ SYMPORT PROTEINS FROM MAGIC-ANGLE SPINNING NMR.
((Paul J.R. Spooner, Anthony Watts and Peter J. F. Henderson[¶])). Departments of Biochemistry, University of Oxford, South Parks Road, Oxford OX1 3QU and [¶]University of Leeds, Leeds LS2 9JT.
Work has been continued to access and combine structural and dynamic information on the membrane proteins responsible for sugar-$H^+$ symport, using magic-angle spinning (MAS) NMR. Inner-membrane vesicles of *Escherichia coli* with the galactose-$H^+$ symport protein, GalP, over-expressed to levels above 50% of total protein were pelleted to provide around 26mg (~0.5μmol) of this protein for each analysis. The detection of $^{13}C$-labelled glucose substrate weakly bound to the membranes in their normal "fluid" state was most striking in terms of measuring sensitivity and spectral resolution, showing that the membranes in this native state present a binding environment of high structural homogeneity. Studies incorporating specific inhibitors of sugar transport and alternate substrates showed that this binding was due to specific interactions with GalP protein alone. Apart from providing structural information on substrate recognition, observations can report explicitly on the dynamics of conformational events associated with substrate translocation. These studies not only demonstrate the feasibility of conducting structural analyses on this class of proteins by NMR but that there are distinct advantages in designing strategies for the functional protein in its native membranes. These advanced strategies involve observations on labelled protein where substrate is used as a "spectral filter" to derive more detailed information on the structure and conformational dynamics within the carrier-center of the protein.

This work is supported by SERC and The Wellcome Trust.

M-Pos66

SHORT PEPTIDE ROTATIONAL DYNAMICS FROM $^{13}C$ AND $^{15}N$ NMR RELAXATION AND MOLECULAR DYNAMICS SIMULATIONS.

((V.A. Daragan, D.V. Mikhailov, K.H. Mayo)) University of Minnesota, UMHC, Box 609, Minneapolis, MN 55455.

Backbone motional dynamics in tri- and diglycine have been studied by $^{15}N$ NMR relaxation and $^{13}C$ NMR multiplet relaxation. Six dipolar auto- and three dipolar cross-correlation times were determined as a function of pH, ionic strength and temperature. Significant pH dependence in correlation times for the C-terminal glycine and more so for the N-terminal glycine, indicate the importance of the ionization state on the internal mobility of terminal backbone positions. Various motional models were used to fit experimental and molecular dynamics data. For terminal glycines, rotational jump models which allow for diffusive-like fluctuations within potential minima best explain the experimental data. For the central glycine, no model or model-free approaches can adequately describe experimentally determined correlation times. To do this, coupling between overall tumbling and $\varphi$, $\psi$-internal rotations must be considered. A simple model describing this coupling is proposed. Using strongly coupled overall and internal rotations, Monte-Carlo computer simulations show good agreement with experiment.

This project has been supported by an NSF/NAS Research Grant.

M-Pos67

CROSS CORRELATION EFFECTS IN $^{13}C$-NMR RELAXATION MEASUREMENTS ON GLYCINE AND LYSINE RESIDUES.

((L. Zhu and M. D. Kemple)) Department of Physics, IUPUI, Indianapolis, IN 46202-3273.

$^{13}C$ (and $^{15}N$)-NMR relaxation measurements have proven useful for the study of peptide and protein dynamics in aqueous solution. Most often the particular nucleus probed has only a single attached proton. However, in the case of the $\alpha$-carbon of glycine and the side chain carbons of lysine for example, there are two attached protons. To properly interpret the relaxation results cross correlation between the motions of the two C-H vectors must be considered. With physically plausible values for the strength of the spectral density arising from cross correlation, the contribution of cross correlation to the measured relaxation quantities, $T_1$, $T_2$, and the NOE, are less than the uncertainties in the measurements as they are normally performed (for example with proton saturation during the recovery period in a $T_1$ experiment) when the motion is isotropic. The range of possible errors in the relaxation values caused by the neglect of cross correlation will be given as a function of the rotational correlation time and other relevant parameters for both isotropic and anisotropic motion. This work was supported in part by NSF grant DMB-9105885.

M-Pos68

COMPARISON OF MOTIONAL PARAMETERS OBTAINED FROM $^{13}C$-NMR AND FLUORESCENCE-ANISOTROPY MEASUREMENTS OF MELITTIN IN SOLUTION.

((P. Buckley, P. Yuan†, M. D. Kemple†, and F. G. Prendergast)) Dept. of Biochemistry and Molecular Biology, Mayo Foundation, Rochester, MN 55905, and †Dept. of Physics, IUPUI, Indianapolis, IN 46202-3273.

Melittin is a 26-residue, cytolytic peptide which assumes a random coil structure in water at low pH and forms a tetramer of bent helices at high pH and modest salt concentration. From $^{13}C$-NMR relaxation measurements of melittin isotopically enriched with $^{13}C$ at several backbone and side chain positions we have determined the overall rotational correlation times ($\tau_m$), and the order parameters ($S^2$) and effective correlation times ($\tau_e$) for the internal motion of the relevant C-H vectors using the formalism of Lipari and Szabo for the random-coil and the tetrameric peptide in aqueous solution. Corresponding parameters were also extracted from tryptophan time-resolved and steady-state anisotropy measurements on melittin. The $\tau_m$ value obtained from time-resolved anisotropy was smaller than that found from NMR for the tetramer while the $S^2$ and $\tau_e$ values for trp were in reasonable agreement for both the monomer and the tetramer. Results of dynamics measurements for melittin in a lipid environment (micellar) will also be given. This work was supported in part by NIH grant GM34847 and NSF grant DMB-9105885.

M-Pos69

CAN $^{19}F$ NMR SPIN-LATTICE RELAXATION BE USED TO DESCRIBE ANESTHETIC MOTION IN MICELLES AND LAMELLAR MEMBRANES?

((B.S. Selinsky and C.L. Strohbeck)) Chemistry Department, Villanova University, Villanova, PA 19085.

The mechanism of action of inhalation anesthetics is poorly understood. A sensitive probe of anesthetic motion would facilitate an understanding of anesthetic partitioning into membranes, anesthetic-lipid interactions, and anesthetic-protein interactions. NMR spin-lattice relaxation is a potentially useful probe of anesthetic motion. To evaluate spin-lattice relaxation as a motional probe, a systematic analysis of $^{19}F$ and $^{13}C$ spin-lattice relaxation of the inhalation anesthetic *enflurane* (2-chloro-2-fluoro-1,1-difluoroethyl difluoromethyl ether) has been performed. $^{13}C$ $T_1$ relaxation has been used extensively to describe the motion of small molecules, as the relaxation mechanism is almost exclusively dipolar. Rotational correlation times ($\tau_c$) derived from the $^{13}C$ $T_1$ relaxation of enflurane in different organic solvents agree closely with $\tau_c$s calculated from solvent viscosity. However, the $\tau_c$s calculated from $^{19}F$ $T_1$ relaxation times do not agree with those calculated from solvent viscosity when relaxation is analyzed assuming a strictly dipolar relaxation mechanism. Therefore, $^{19}F$ $T_1$ relaxation of enflurane has a large contribution from non-dipolar mechanisms, making the calculation of molecular motion problematic.

M-Pos70

CHARACTERIZATION BY FTIR AND NMR SPECTROSCOPIES OF THE INTERACTIONS BETWEEN CYTOCHROME C AND LIPID BILAYERS.

((Mario Laviolette and Michèle Auger)), CERSIM, Département de chimie, Université Laval, Québec, Québec, Canada, G1K 7P4.

Cytochrome c is an extrinsic protein from the internal membrane of the mitochondria. This protein acts like an electron carrier in the respiratory chain. We have investigated the interactions between bilayers of dimyristoyl-phosphatidylglycerol (DMPG), dimyristoylphosphatidylcholine (DMPC) and cytochrome c by Fourier transform infrared spectroscopy. The results indicate that the protein interacts only with negatively charged phospholipids, such as DMPG. More specifically, we observe a large increase in the gel to liquid-crystalline phase transition temperature of the anionic lipid upon interaction with cytochrome c. Moreover, the observation of the phospholipid carbonyl and phosphate bands allows the determination of the degree of hydration of these functional groups. On the other hand, the amide I region indicates that the protein is undergoing a conformational change when interacting with anionic phospholipids. Furthermore, we have studied our systems by one and two-dimensional solid-state $^{31}P$ NMR. A combination of $T_1$, $T_2$ and 2D exchange measurements allows us to probe molecular motions in the frequency range of 1-$10^{10}$ $s^{-1}$. Results will be presented for different lipid systems in the absence and presence of cytochrome c.

M-Pos71

DYNAMICAL PROPERTIES OF PHOSPHOLIPID MEMBRANES EXPLORED WITH $^{13}C$ NMR SPECTROSCOPY.

((Christine Le Guernevé and Michèle Auger)), CERSIM, Département de chimie, Université Laval, Québec, Québec, Canada, G1K 7P4.

Model membranes have been studied by natural abundance $^{13}C$ magic angle spinning (MAS) NMR spectroscopy at 75 MHz (7.05T). MAS, high-power proton decoupling and cross-polarization (CP) allow the obtention of highly resolved solid state spectra in which many of the narrowed peaks can be identified and assigned to individual atomic sites. The molecular motions of lipid bilayers of dimyristoylphosphatidylcholine (DMPC) with and without cholesterol have been investigated using relaxation techniques. The $^1H$ and $^{13}C$ spin-lattice relaxation times ($T_1$), which are sensitive to very fast motion (with rates between $10^7$ to $10^{10}$ $s^{-1}$) and the spin-lattice relaxation times in the rotating frame ($T_{1\rho}$), which are sensitive to slower rate motions (with rates between $10^4$ to $10^6$ $s^{-1}$) have been measured for the polar head group, the interfacial region and the acyl chains of the lipid bilayers. Preliminary results indicate that very interesting informations can be obtained on the changes in membrane structure, on order fluctuations and types of motions. Specifically, the $^{13}C$ $T_{1\rho}$, which have been determined for the different carbon atoms, seem to be a sensitive probe to characterize and compare the molecular motions of each individual carbon sites. The technique can be applied to the study of the effect of protein incorporation on slow and fast molecular motions in lipid bilayers.

M-Pos72

POLARIZED NMR SIGNALS RESULT FROM CYCLIC ELECTRON TRANSFER IN Q-DEPLETED REACTION CENTERS ((A. McDermott, M. Zysmilich)) Columbia University, Department of Chemistry NY NY 10027 (Sponsored by A. McDermott)

We report a rare example of Chemically Induced Dynamic Nuclear Polarization (CIDNP) in the solid state, which we have observed in the NMR spectra of $^{15}N$-labeled photosynthetic reaction centers. In simple echo-detected Bloch decay spectra collected under magic-angle spinning (MAS) with or without proton decoupling, we detect nuclear polarizations for the nitrogens in the tetrapyrroles of the bacteriochlorophyll special pair ("P") that are far from Bolzmann equilibrium. The resulting NMR lines are emissive and approximately -300 times the intensity of the thermally relaxed nuclei. We do not observe the polarization if the quinones are present and pre-oxidized. Such signals are mechanistically related to the previously reported polarized EPR signals (CIDEP) in that they result from a transient non-equilibrium mixing of the singlet and triplet states of the initially formed charge transfer pair, $P^+I^-$. The fact that we observe strongly polarized $^{15}N$ signals indicates that the kinetics for the mixing of the singlet and triplet states has some contribution from the hyperfine coupling between the electron in the radical and the nitrogens of the tetrapyrrole. We are attempting to assign both the detailed mechanism for developing polarization and the chemical origin of each line in the spectrum of P and I in order to determine the electron densities in the various macrocycles for the radical pair.

M-Pos73

THE STUDY OF THE LIGAND-BINDING SITE OF GLUTAMINE-BINDING PROTEIN OF *ESCHERICHIA COLI* USING REDOR-NMR

((N. Tjandra*, A. W. Hing†, P. F. Cottam*, J. Schaefer†, C. Ho*.))
*Dept. of Biological Sciences, Carnegie Mellon University, Pittsburgh, PA 15213 and †Dept. of Chemistry, Washington University, St. Louis, MO 63130.

Glutamine-binding protein (GlnBP) is an essential component of the glutamine permease in *Escherichia coli*. The determination of its structure is essential for understanding the complex mechanism of active transport of L-glutamine across the cytoplasmic membrane of *E. coli*. A rotational double-resonance nuclear magnetic resonance experiment (REDOR-NMR) on the solid form of GlnBP complexed with L-Gln has been used to avoid complications arising from the dynamic properties and spectral overlaps encountered in determining the inter-nuclear distances in a large complex protein molecule by solution-state NMR techniques. This method, combined with strategically placed isotopic labels, has been shown to be very effective in obtaining model-independent inter-nuclear distances, and thus detailed structural information on the ligand-binding site of GlnBP. The existence of a single histidine residue (His156) at the binding site provides a perfect probe for distance measurements between GlnBP and L-Gln. REDOR distances up to 6.3 Å have been observed between $^{13}C$ labels in L-Gln and $^{15}N$ labels in His156. These distances have been used as constraints in molecular dynamic (MD) calculations of the complex using the unliganded crystal structure of GlnBP as the starting point. The results clearly show consistency between the REDOR-measured and MD-calculated distances. The significance of these findings to the understanding of ligand specificity in active transport will be discussed. [Supported by NIH grant (GM-26874) and NSF grant (DMB-8816384)].

M-Pos74

ASSIGNMENT OF THE METHIONINE BACKBONE NMR RESONANCES IN GLUTAMINE-BINDING PROTEIN OF *ESCHERICHIA COLI*

N.Tjandra, J. Yu, L.M. Smith, V. Simplaceanu, P.F. Cottam, and C. Ho
Department of Biological Sciences, Carnegie Mellon University, Pittsburgh, PA 15213.

Heteronuclear multi-dimensional NMR experiments have been carried out to establish backbone resonance assignments of all methionine residues in the glutamine-binding protein (GlnBP) of *E. coli*, a periplasmic protein of 226 residues. These experiments were done in order to provide additional, unambiguous markers along the polypeptide backbone for sequential assignment of the protein-ligand complex. Even though spectra from HNCA, HNCO, HN(CO)CA, HCACO, and HCA(CO)CA experiments on $^{13}C$ and $^{15}N$ uniformly labeled GlnBP have been obtained, and His and Trp residues have been assigned as markers [Tjandra *et al.* J.Biomolecular NMR 2,149-160, (092)], it is very difficult to achieve complete sequential assignments due to the high degree of degeneracy of the resonance peaks in the spectra. Additional markers are needed. Methionine was chosen because there are only three methionyl residues in the primary structure of GlnBP (Met48, Met93 and Met144). The unique pairing of each methionine to one adjacent residue can be exploited to distinguish among the resonances arising from the methionyl residues. $^{13}C$, $^{15}N$ edited proton spectra of [$^{13}C'$, L-Pro], [$^{15}N$, L-Met] doubly labeled GlnBP complexed with L-Gln (GlnBP+L-Gln) have been obtained to assign Met48. Similarly [$^{13}C'$, L-Tyr], and $^{15}N$ uniformly labeled GlnBP+L-Gln have been used to assign Met144. The remaining Met93 can be assigned by comparing the above spectra with the spectrum from the HMQC experiment on [$^{15}N$, L-Met] labeled GlnBP+L-Gln. With this additional information, we are moving toward the complete backbone assignment of GlnBP. [ Supported by a grant from NSF (DMB-8816384)].

M-Pos75

FACTORS THAT DETERMINE THE EPR SPECTRA OF NITROXIDE SIDE-CHAINS IN SPIN LABELED PROTEINS AND ANALYSIS BY MOLECULAR DYNAMICS SIMULATION

((Christian Altenbach, Heinz-Jürgen Steinhoff, Duncan A. Greenhalgh, H. Gobind Khorana, Wayne L. Hubbell)) Jules Stein Eye Institute and Department of Chemistry and Biochemistry, UCLA, Los Angeles, CA 90024-7008, and the Department of Biology and Chemistry, Massachusetts Institute of Technology, Cambridge, MA 02139.

Site directed spin-labeling was used to introduce single nitroxide spin-labels along the outside surface of the transmembrane D-helix in bacteriorhodopsin. EPR spectra of frozen samples were fitted to a powder line shape to determine the magnetic parameters. $A_{zz}$ was found to be a function of depth in the membrane through its dependence on solvent polarity. Room temperature spectra as a function of position, side-chain structure and phospholipid composition can be rationalized with the known protein structure, but these spectra cannot be fit with single-component motional models. The relation between the motional restriction of the spin label and the local protein structure was investigated by molecular dynamics techniques. For this purpose EPR spectra were computed from trajectories of the nitroxide reorientational motion for different model peptide structures. Results suggest that the EPR spectrum of a spin labeled side-chain reflects tertiary interactions of the nitroxide, and is a sensitive indicator of small conformational movements in the protein.

M-Pos76

SITE-DIRECTED SPIN LABELING STUDIES OF THE BACTERIORHODOPSIN PHOTOCYCLE

((Heinz-Jürgen Steinhoff, Ramin Mollaaghababa, Gobind Khorana, Wayne L. Hubbell)) Jules Stein Eye Institute and Department of Chemistry and Biochemistry, UCLA, Los Angeles, CA 90024-7008, and the Department of Biology and Chemistry, Massachusetts Institute of Technology, Cambridge, MA 02139. (Spon. by B. Yazejian).

It is generally agreed that proteins operate through time-dependent structural changes, and one major goal of protein biophysics is to establish methods to study these transitions. Genetic engineering technology has made it possible to introduce an amino acid with a nitroxide side-chain at any desired postion in a protein sequence. This recently introduced method of site-directed spin labeling has been applied to study the structural dynamics of bacteriorhodopsin during the photocycle. Time courses of the structural changes after photoexcitation have been obtained with time-resolved electron paramagnetic resonance (EPR) spectroscopy. Light-dark EPR difference spectra have been measured directly using periodic photoexcitation and phase sensitive demodulation. The results indicate localized motions of the E, F or G helices during the reaction pathway which follows the decay of the M intermediate.

M-Pos77

PHOSPHORYLATION INDUCES A SIGNIFICANT CONFORMATIONAL CHANGE IN A PHOSPHOLAMBAN PEPTIDE. ((R. Mortishire-Smith*, S. Pitzenberger#, V.M. Garsky#, C. Burke#, H. Mach#, C.R. Middaugh#, and R.G. Johnson, Jr.#)) Merck Sharp & Dohme Research Labs, Harlow, U.K.* and Merck Research Labs, West Point, PA 19486#. (Spon. by R. Johnson)

Phospholamban is a 52 amino acid cardiac sarcoplasmic reticulum protein found in stoichiometric amounts with the calcium ATPase, whose activity is inhibited when bound to PLB. During β–adrenergic stimulation of the heart, PLB is phosphorylated at serine 16 by protein kinase A or at threonine 17 by calcium-calmodulin dependent protein kinase resulting in dissociation of PLB from the ATPase and therefore stimulation of the pump. An understanding of the PLB-calcium ATPase interaction would be aided by knowledge of the solution structure of PLB. Therefore, the effect of phosphorylation upon the conformation of the N-terminal portion of PLB [PLB(1-25)] was investigated by homonuclear NMR spectroscopy and circular dichroism. Complete chemical shift assignments were obtained for both PLB(1-25) and pSer$^{16}$-PLB(1-25) in 30% TFE/$H_2O$ by conventional techniques. Using sequential and medium range NOE connectivities and secondary $C_\alpha$-H shifts as criteria, residues 1-17 in PLB(1-25) appear to form a regular alpha helix with the remaining 8 residues essentially unstructured. Phosphorylation at serine 16 induces an unwinding of the helix at the C-terminal end by approximately 1.5 turns. The results are in agreement with the available CD data where in 30% TFE-$H_2O$, the helical content based on molar CD at 222 nm is 60% for PLB(1-25) and 25% for pSer$^{16}$-PLB(1-25). Experiments to determine the full three-dimensional structure of PLB(1-25) and pSer$^{16}$-PLB(1-25) are in progress. These data contradict several previously proposed models for the N-terminal domain of PLB; a new model will be advanced.

**M-Pos78**

MICROSCOPIC MAGNETIC RESONANCE IMAGING AND SPECTROSCOPY OF LACTATE. ((J.A. Kmiecik, C.D. Gregory, Z.-P. Liang, and M.J. Dawson)) Dept. Physl. & Biophys. and College of Medicine, University of Illinois at Urbana-Champaign. (Spon. by P.C. Lauterbur)

The production of maps depicting local concentrations of specific tissue metabolites using magnetic resonance (MR) spectroscopic imaging can provide insights into normal and abnormal tissue function. In the brain, the discovery that lactate levels rise during sensory stimulation (Prichard, J. *et al.* 1991, *Proc. Natl. Acad. Sci. USA* **88**, 5829) suggests that MR spectroscopy and imaging of lactate in activated areas of the brain may complement studies of brain activation by MR functional imaging, provided that practical problems such as overwhelming water and lipid signals, spatial localization, and low intrinsic sensitivity are overcome. To test the ability of MR imaging and spectroscopy to provide localized measurements of lactate levels in activated brain, and also to determine the limits of spatial resolution with these methods, phantom studies were performed using a home-built microscopy RF/gradient probe in a 7 tesla GE/Tecmag imaging spectrometer.

Test objects included various concentrations of lactic acid, water, and corn oil in capillary tubes of size ranging from 300μm-1250μm in diameter by 1cm in length. Spectral editing for selection of the lactate methyl signal was provided by the use of a double-quantum coherence filter sequence. Spectroscopic spatial localization, when used, was accomplished by the Spectral Localization by Imaging (SLIM) technique (Hu, X. *et al.* 1988, *Mag. Res. Med.* **8**, 314) and lactate map resolution enhancement was provided by Reduced-encoding Imaging by Generalized series Reconstruction (RIGR).

Spectra from the phantoms using the double-quantum coherence filter showed remarkable suppression of water and lipid signals. Three-dimensional lactate-map images also revealed suppression of water and lipid, and sensitivity for moderate levels of lactic acid was good even at microscopic spatial resolution (on the order of a few micrometers in-plane).

The ability of SLIM and RIGR to improve sensitivity and spatial localization in now being evaluated and the extension of the technique to the spatially localized measurement of lactate in living tissues is underway.

**M-Pos79**

$^1$H Spectroscopy of Living Toad Retina (D.C. Brown, C.D. Gregory, T.G. Ebrey and M.J. Dawson) Center for Biophysics, University of Illinois, Urbana, IL 61801. (Spon. by M.J. Dawson)

Nuclear magnetic resonance spectroscopy of isolated perfused retina allows determination of the concentrations of metabolites and how these change as a result of experimental manipulation. This is useful in studying the relation between metabolism and phototransduction, and because the retina serves as an easily accessible piece of the central nervous system. We use proton NMR spectroscopy with the jump and return echo pulse sequence to suppress the water signal (Sklenar and Bax, J. Mag. Res. 74:469, 1987). The theoretical relation between metabolite concentration and signal intensity has been confirmed experimentally in model solutions. In these studies, eight to ten isolated *Bufo marinus* retinae are superfused with physiological salt solution at room temperature in a 10 mm NMR tube and spectra are acquired at 300 MHz at 10 min intervals. The largest peaks appear in the positions of lactate, glutamate and taurine, and they represent approximately the concentrations of these compounds which would be expected in the normal toad retina. Other evidence for the assignments of these peaks will be presented. Preliminary data from a perfused single retina will also be shown.

**M-Pos80**

ANALYSIS OF THE RELATIONSHIP BETWEEN FORCE AND METABOLISM IN FROG GASTROCNEMIUS USING $^1$H NMR SPECTROSCOPY. ((D. Shen, C.D. Gregory, L.E. Ford*, M.J. Dawson)) Dept. of Physiology & Biophysics, Univ. of Illinois at Urbana-Champaign, IL 61801. *Dept. of Medicine, Univ. of Chicago, IL 60637 (Spon. By W.W. Sleator)

We are using proton NMR spectroscopy of living, contracting muscle to study the relationship between mechanical function and metabolism in fatiguing skeletal muscle. The water suppression sequence consists of a hard 1,1 excitation pulse immediately followed by a 1,1 refocusing pulse (Sklenar and Bax, J. Mag. Res. 74:469, 1987) which yields spectra that require minimal phase and baseline correction. This sequence provides reasonable quantitative accuracy in studies of model solution (~10%). Frog gastrocnemius muscles are superfused with Ringer's solution within a 20 mm NMR tube in which they are stimulated electrically (1s tetanus per min for 60 min) and isometric force is recorded. $^1$H NMR spectra are recorded on a 300 MHz wide-bore spectrometer and the timing of the experiment is controlled by a personal computer-based data acquisition system which controls stimulation of the muscles, records the mechanical responses, and interfaces with the NMR data collection. As the muscle fatigues under anaerobic conditions, there is a linear relation between (total force x number of contractions) and [lactate]. There is a similar increase in intensity of a peak slightly lower in frequency than that of lactate; the identity of this peak and its significance is now under investigation.

**M-Pos81**

DYNAMICS OF NMR CONTRAST AGENT UPTAKE BY TUMORS. ((Lorinda Opsahl and E.E. Uzgiris)) General Electric Research and Development Center, Schenectday, NY 12309

The time course of tumor uptake of $T_1$ relaxing agents gadolinium diethylenetriaminepentaacetic acid, (Gd-DTPA) and Gd-DTPA-polylysine, (Gd-DTPA-polyL), has been measured in vivo using NMR imaging. Measurements are taken on mammary carcinoma tumors, 1-2 cm in diameter, 5-10 days after subcutaneous implantation in 160 gm female Fisher 344 rats. The gadolinium contrast agents are intravenously injected at a dose of 0.1 mmole(Gd)/kg and $T_1$ weighted images are obtained at 3 minute time intervals following injection. Gd-DTPA is taken up nonspecifically by tumor tissue following injection, showing a relatively fast uptake and removal, as reported elsewhere in the literature. By comparison, Gd-DTPA-polyL has a much slower uptake, being excluded from normal tissue, yet showing contrast enhancement on the tumor periphery of greater than 40% increase in $T_1$ weighted image intensity. This behavior is modeled based on difference in the kinetics of uptake as well as clearance through the reticuloendothelial system, kidneys ,and liver.

**M-Pos82**

SATURATION RECOVERY EPR OF NITROUS OXIDE REDUCTASE. A STUDY OF THE UNUSUALLY FAST RELAXATION OF THE MIXED VALENCE CENTER IN NITROUS OXIDE REDUCTASE ((S. Pfenninger, W.E. Antholine, J.-J. Yin, J.S. Hyde, P.M.H. Kroneck[§], and W.G. Zumft[‡])) Biophysics Research Inst., Medical College of Wisconsin, Milwaukee, WI 53226, [§]Univ. Konstanz, Konstanz, FRG, and [‡]Univ. Karlsruhe, Karlsruhe, FRG.

Temperature-dependent saturation-recovery data for the binuclear mixed valence [Cu(1.5)...Cu(1.5)], S=1/2 center of nitrous oxide reductase, $N_2OR$, are similar to data for the $Cu_A$, binuclear, mixed valence center in cytochrome *c* oxidase, COX, if the data are fit to a single exponential. But, the saturation recovery curves are best fit to at least double and sometimes triple exponentials for both $N_2OR$ and COX at most magnetic fields in both the $g_{\parallel}$ and $g_{\perp}$ regions. The shorter relaxation time is almost field-independent compared with the long relaxation time, which varies about a factor of five over the spectrum. Temperature-dependent $T_1$ data are fit to Orbach and/or Raman processes from 10 to 50 K. Results are discussed in terms of vibronic couplings to low-lying excited states, $M_I$-values, field dependence, allowed and forbidden transitions, cross relaxations, spectral diffusion, and superposition of spectra. These data are compared with data from a well-defined pyramidal square-planar cupric complex in which the relaxation is slower. These recovery curves are also better fit by at least double exponentials. This work is supported by NSF grant DMB9105519.

**M-Pos83**

THE DETERMINATION OF THE ORIENTATION OF A NITROXIDE SPIN-LABEL RELATIVE TO BAND 3 PROTEIN OF THE HUMAN RED BLOOD CELL ((E.J. Hustedt and A.H. Beth)) Department of Molecular Physiology and Biophysics, Vanderbilt University, Nashville, TN 37232

The stilbene dilsulfonate derivative, spin-labeled DADS maleimide (SL-$H_2$DADS-MAL), has proven to be a useful probe of the rotational mobility of Band 3, the anion exchange protein in the human red blood cell membrane. Saturation Transfer EPR (ST-EPR) spectra are sensitive to both the rate of rotational diffusion and the orientation of the nitroxide with respect to the diffusion tensor. The orientation of the nitroxide A- and g-tensors with respect to a vector perpendicular to the cell membrane has been determined from linear EPR spectra of SL-$H_2$DADS-MAL labeled Band 3 in whole red blood cells preferentially oriented by flow. Two independent methods of analyzing the data have been used to give essentially equivalent results. First, the spectra were fit assuming a variable percentage of cells are perfectly aligned biconcave disks with the remainder totally disordered[1]. Secondly, an model-independent determination[2] of the membrane normal orientation distribution was obtained from cells labeled with the spin-labeled stearic acid, 5-NS. This membrane normal distribution was then used to fit the spectra of cells labeled with SL-$H_2$DADS-MAL. Fits to ST-EPR data, assuming Band 3 undergoes uniaxial rotational diffusion in the membrane, have determined the rate of rotational diffusion and the orientation of the nitroxide to the diffusion axis (Hustedt & Beth, poster at this meeting). The orientation of the nitroxide with respect to the diffusion axis is in excellent agreement with the orientation of the nitroxide to the membrane normal. This strongly suggests that the motion of SL-$H_2$DADS-MAL Band 3 observed by ST-EPR is uniaxial rotational diffusion about the membrane normal. *Supported by NIH grants R01 HL34737 & T32 DK07186.*

1) Bitbol and Letterier, *Biorheology 19*, 669-680 (1982).
2) Burghardt and Thompson, *Biophys. J. 48*, 401-409 (1985).

M-Pos84

**THE ROTATIONAL DIFFUSION OF BAND 3 IN INTACT RED BLOOD CELL MEMBRANES AS MEASURED BY SATURATION TRANSFER EPR SPECTROSCOPY** ((E.J. Hustedt and A.H. Beth)) Department of Molecular Physiology and Biophysics, Vanderbilt University, Nashville, TN 37232

Algorithms have been developed for the rapid computer simulation of Saturation Transfer EPR (ST-EPR) spectra of a nitroxide undergoing uniaxial rotational diffusion. These algorithms have been incorporated into a general non-linear least-squares analysis program based on the Marquardt-Levenberg algorithm[1]. Excellent fits to 100kHz, 50kHz, and 25kHz ST-EPR spectra of SL-$H_2$DADS-MAL labeled Band 3 in whole red blood cells at 37°C have been obtained with a best fit characteristic uniaxial rotation time ($r_{parallel} = 1/6D_{parallel}$) on the order of 10$\mu$sec. The best fit orientation of the nitroxide A- and g-tensors with respect to the rotation axis is in close agreement with the orientation of the nitroxide with respect to the membrane normal as determined from linear EPR spectra of preferentially oriented cells (Hustedt & Beth, poster at this meeting). This strongly suggests that the rotation observed by ST-EPR is uniaxial rotation of Band 3 about the membrane normal. The fact that the spectra for all three modulation frequencies can be fit using a single characteristic rotation time suggests that only a small fraction, if any, of Band 3 exists in a low mobility or immobile state[2]. The ST-EPR spectra of SL-$H_2$DADS-MAL labeled Band 3 in ghost membranes at 37°C demonstrate that Band 3 is slightly more mobile in ghost membranes than in whole cells. *Supported by NIH grants R01 HL34737 & T32 DK07186.*

1) Hustedt *et al., Biophys. J. 64*, 614-621 (1993).
2) Beth & Robinson in *Biological Magnetic Resonance Volume 8: Spin Labeling Theory and Applications* (Berliner and Reuben, eds.), Plenum Press, NY (1985).

M-Pos85

**STRUCTURE-FUNCTION CORRELATIONS IN LOWER VALENCE STATES OF BIS-(DIMETHYLGLYOXIMES): IMPLICATIONS FOR COBALAMINS.** ((M.D. Wirt,[a] E. Scheuring,[c] C.J. Bender[a], M.R. Chance[c], and J. Peisach[a*])) *Depts. of Molecular Pharmacology[a] and Physiology and Biophysics[c], Albert Einstein College of Medicine, Bronx, NY 10461*

We present the first direct structural data, obtained from x-ray edge and extended x-ray absorption fine structure (EXAFS) spectroscopy, that demonstrates an unambiguous shortening of the Co-N(axial) distance to pyridine upon homolytic cleavage of the Co-C bond in *trans*-bis-(dimethylglyoximato)methylpyridine cobalt(III), (Co(III)(dmg)$_2$Me(py)). Solution phase structures of the Co(I) and Co(II)(dmg)$_2$(py) complexes indicate a five-coordinate structure where the Co-N(axial) distance is shortened by approximately 0.1Å with respect to the Co(III)(dmg)$_2$Me(py) species. The Co(II)(dmg)$_2$(py) results parallel those seen upon homolytic cleavage of adenosylcobalamin forming Co(II) $B_{12}$. Additionally, the ab-initio EXAFS code FEFF (v. 5.05) is used to simulate theoretically generated Chi data for cobaloximes. Lastly, we have demonstrated our ability to employ Electron-Spin Echo Envelope Modulation (ESEEM) spectroscopy to determine previously inaccessible in-plane (equatorial) Co-N coupling parameters of dimethylglyoxime complexes. Extension of our preliminary ESEEM studies of $B_{12}$ models to free Co(II) cobalamins and enzyme bound Co(II) cofactors will provide unique insight into properties of the corrin ring and orientation of the benzimidazole base that may influence Co-C bond reactivity. This research is supported by USDA Grant 91-37200-6897 (MRC) and NIH Grants RR-02583 and GM40168 (JP).

M-Pos86

CHARACTERIZATION OF THE $MN^{2+}$ BINDING SITES OF CALCINEURIN BY NMR PROTON RELAXATION ENHANCEMENT AND EPR. ((A. Haddy*, R. R. Sharp† and F. Rusnak*)) *Hematology Research, Mayo Graduate School of Medicine, Rochester, MN 55905 and †Chemistry Dept., University of Michigan, Ann Arbor, MI 48109.

The protein phosphatase calcineurin contains endogenous Fe and Zn in approximately stoichiometric amounts and is activated by $Mn^{2+}$. Properties of the $Mn^{2+}$ binding sites of one recombinant and two native bovine calcineurin preparations were characterized by NMR water proton relaxation enhancement (NMR-PRE) and Q-band (34 GHz) EPR. NMR-PRE showed the presence of two $Mn^{2+}$ binding sites: one high affinity with low enhancement ($\leq$0.25) and the other lower affinity with high enhancement ($\geq$5). Q-band EPR also revealed two $Mn^{2+}$ binding sites. In calcineurin preparations showing the low NMR-PRE enhancement site, the first equivalent of $Mn^{2+}$ added was EPR silent for T>150 K, while addition of a second equivalent yielded a nearly isotropic six-line signal. The six-line signal dominated in a calcineurin preparation that showed primarily the high NMR-PRE enhancement site even when one equivalent of $Mn^{2+}$ was added. Metal analysis revealed that this preparation contained 1.8 equivalents of Fe, whereas those showing the low enhancement site contained 0.75-0.9 equivalent of Fe. These results indicate that $Mn^{2+}$ bound at the low enhancement site was inaccessible to exchangeable $H_2O$ and EPR silent, perhaps due to a nearby paramagnetic species such as $Fe^{3+}$. $Mn^{2+}$ bound at the high enhancement site, however, was $H_2O$ accessible and characteristic of a monomer in an essentially octahedral environment.

M-Pos87

**A MODEL-FREE APPROACH FOR MONITORING THE DYNAMICS OF DNA BY NITROXIDE SPIN LABELS.** ((R.S. Keyes and A.M. Bobst)) Department of Chemistry, University of Cincinnati, Cincinnati, OH 45221.

The highly dynamic nature of DNA contributes to its ability to undergo a large number of conformational substates. Attempts to separate the various dynamic modes have resulted in complex methods of analysis involving well-defined models. In contrast to these approaches, we have followed an interpretive framework that reduces the multiple dynamics to two classes of motions [1]. The first involves overall diffusion of the macromolecule which can be modeled as a simple hydrodynamic object (e.g., cylinder). The second type of motion consists of the various internal dynamics which are subsumed into an order parameter without requiring a model. These include length independent motions (e.g., base oscillations) and length dependent motions (e.g., bending and twisting). By taking this simplified approach, analyses can be performed on complex systems including plasmids and protein-nucleic acid complexes.

The EPR spectra of several DNA oligomer and polymer systems spin labeled with nitroxides of various tether lengths were analyzed by combining two simulation methods to extract the magnetic and motional parameters. The internal dynamics were examined according to the model-free approach of Lipari and Szabo [2] as implemented by Eimer et al. [3]. Supported in part by NIH GM 27002.

1. Hustedt, E.J., Spaltenstein, A., Kirchner, J.J., Hopkins, P.B. & Robinson, B.H. (1993) Biochemistry **32**, 1774-1787.
2. Lipari, G. & Szabo, A. (1982) J. Am. Chem. Soc. **104**, 4559-4570.
3. Eimer, W., Williamson, J.R., Boxer, S.G. & Pecora, R. (1990) Biochemistry **29**, 799-811.

## BACTERIORHODOPSIN AND RHODOPSIN

M-Pos88

PHOTOVOLTAGE OF THE BLUE FORMS OF BACTERIORHODOPSIN AND ITS MUTANTS.
((S. Moltke, M.P. Krebs†, R. Mollaaghababa†, H.G. Khorana† and M.P. Heyn)) Biophysics Group, FU Berlin, D-14195 Berlin, † MIT, Cambridge, MA 02139

The laser-flash induced photovoltage generated by bacteriorhodopsin in purple membranes adsorbed to a polyethylene support was investigated for wildtype and mutants at positions 82, 85, 212 and 96. Since some of the mutants show color-changes of the chromophore with pKs very different from those known to occur in wildtype, the voltage was recorded between pH 0 and pH 11. A clear correlation between the blue color of the chromophore and the disappearance of net charge-transport could be established. Those mutants, which are blue at physiological pH, show components in the electrical signal not seen in the blue form of the wildtype. They can be interpreted as the deprotonation and subsequent reprotonation of some unknown group to and from the extracellular side. This group might be the ultimate proton release group in bR. It is able to deprotonate without the concommitant deprotonation of the Schiff base. While the mutant D212N is the only one to be optically and electrically blue at high pH, the inactive mutants D85N and D85A can be reactivated by raising the pH: above pH 10 the mutants D85N and D85A show net charge transfer with the sign of the wildtype pumping signal up to the passive system discharge time of 1 s.

M-Pos89

MOVEMENT OF THE TRANSITION DIPOLE MOMENT IN THE PHOTOCYCLE OF BACTERIORHODOPSIN MEASURED BY TIME RESOLVED ABSORPTION ANISOTROPY OF ORIENTED IMMOBILIZED PURPLE MEMBRANES.
((H. Otto, Ch. Zscherp, B. Borucki and M.P. Heyn)) Biophysics Group, Freie Universität Berlin, D-14195 Berlin.

Purple membranes were oriented in a 14 T magnetic field and immobilized in a gel. To obtain information on the changes in orientation of the transition dipole moment in such samples, photoselection is not required. On the contrary, it is advantageous to excite the sample isotropically. The absorption anisotropy was derived from time traces at 18 wavelengths or from amplitude spectra. In the case of a pure state k the anisotropy should be constant in time and wavelength and described by the simple formula $R_k = S_2 \cdot P_2(\cos\theta_k)$. $S_2$ is the order parameter of the membrane distribution, $P_2$ the second Legendre polynomial and $\theta_k$ the angle between the transition dipole moment in the state k and the membrane normal. The intermediates K, M and O may be separated in time and wavelength from the others allowing a straightforward analysis. Compared with the ground state the transition dipole moment in the O state is tilted nearly 2° away from the normal. To calculate the angles of spectrally superimposed intermediates it is necessary to know all rate constants and therefore to have a model of the photocycle.

**M-Pos90**

INFLUENCE OF EXCITATION ENERGY ON THE BACTERIORHODOPSIN PHOTOCYCLE

((R.W. Hendler[a], Z.S. Dancshazy[b], S.K. Bose[a], R.I. Shrager[c], and Z.S. Tokaji[b])) [a]Laboratory of Cell Biology, NHLBI, NIH, [b]Institute of Biophysics, BRC. Szeged, Hungary, and [c]Laboratory of Applied Studies, DCRT, NIH, Bethesda, MD. 20892.

The kinetics of the bacteriorhodopsin (BR) photocycle were studied by singular value decomposition (SVD) analysis in two different kinds of experiment. In the type 1 experiment, the kinetics of decay of signals at single wavelengths (412 nm and 570 nm) were followed at each of a series of different intensities of laser light. SVD revealed a rank 2 matrix (i.e. kinetics vs. intensity). The transition at low intensity light was due to a simple increase in the amount of cycling BR while that in the high intensity range was due to a change in kinetics of the photocycle, in which the ratio of fast and slow forms of the M intermediate ($M_f$ and $M_s$) decreased with increasing light. In the type 2 experiment, whole spectra were collected as a function of time at a series of increasing laser light intensities. A separate matrix (i.e.spectra vs. time) was analyzed for each intensity. In addition to confirming the inverse relationship between $M_f/M_s$ and light intensity, it was found that $M_f$ decayed directly to the O intermediate, in contrast to $M_s$ which decayed directly to BR.

**M-Pos91**

POSSIBLE ROLE OF MEMBRANE IN CONTROL OF BACTERIORHODOPSIN (BR) PHOTOCYCLE.

((S.K. Bose[a], A. Mukhopaday[a], R.W. Hendler[a], and R.I. Shrager[b])) [a]Laboratory of Cell Biology, NHLBI, NIH, [b]Laboratory of Applied Studies, DCRT, NIH, Bethesda, MD. 20892. (Spon. by M.R. Bunow)

It has long been known that the intensity of actinic light influences the ratio of phenomenologically fast and slow forms of the M intermediate (i.e. $M_f/M_s$) in the BR photocycle. One explanation of the phenomenon suggests that the trimer structure of BR in purple membranes (PM) is a photon-target, susceptible to photon-cooperativity. Indeed, it has been shown that when the trimer structure (monitored by its CD exiton spectrum and sedimentability) is broken down to monomers by Triton treatment, the apparent photocooperative effect is lost (Danshina et al., Photobiol. (1992) 55:735-740). We find, however, that much milder Triton treatment causes the loss of the apparent photocooperativity without destroying trimer structure. We do find a correlation between effects of Triton treatment on the optical properties of the PM suspension and the loss of the apparent photocooperativity. This suggests an important role for the membrane in the ability of light to influence and control the BR photocycle.

**M-Pos92**

SOLID STATE $^{15}N$ and $^{13}C$ NMR STUDY OF BACTERIORHODOPSIN PHOTOINTERMEDIATES

((K.V. Lakshmi, M.R. Farrar, J. Raap, J.A. Pardoen, J. Lugtenburg, R.G. Griffin, and J. Herzfeld)) Depts. of Chem., Brandeis University, Waltham, MA 02254-9110, Francis Bitter National Magnet Lab at MIT, Cambridge, MA 02139-4307, and Rijksuniversiteit te Leiden, 2300 RA Leiden, The Netherlands. (Spon. by S. Pastra-Landis)

SSNMR spectra were obtained of [ε-$^{13}C$,$^{15}N$]Lysine-bR and [12-$^{13}C$]-, [13-$^{13}C$]-, and [14-$^{13}C$]-retinal bR prepared in 0.1 M NaCl at high pH, conditions which favor the accumulation of the M and N photointermediates at low temperature. In SSNMR spectra obtained upon illumination at low temperature, two species are present, both of which decay to $bR_{568}$ upon warming. One species has identical chemical shifts to those obtained previously for M thermally trapped in guanidine·HCl at high pH.[1] For the other species, the [ε-$^{15}N$]Lys-216 and 13-$^{13}C$ chemical shifts indicate that the Schiff base is protonated, the 12-$^{13}C$ chemical shift indicates a 13=14 cis configuration, and the 14-$^{13}C$ and [ε-$^{13}C$]Lys-216 chemical shifts indicate a C=N anti configuration. These results are consistent with those obtained for N at room temperature by time-resolved resonance Raman experiments.[2]

1. Smith, S. O., J. Courtin, E. van den Berg, C. Winkel, J. Lugtenburg, J. Herzfeld, and R. G. Griffin, *Biochemistry 28*:237 (1989).
2. Fodor, S.P.A., J.B. Ames, R. Gebhard, E. M.M. van den Berg, W. Stoeckenius, J. Lugtenburg, & R.A. Mathies, *Biochemistry 27*:7097 (1988).

**M-Pos93**

MOLECULAR MOTIONS IN PURPLE MEMBRANE INVESTIGATED BY QUASIELASTIC INCOHERENT NEUTRON SCATTERING (QINS)

((G. Büldt[1], J. Fitter[1,3], N.A. Dencher[2], R.E. Lechner[3])) [1] Forschungszentrum Jülich, IBI-2, Structural Biology, D-52425 Jülich; [2] Biochemistry Dept., Technische Hochschule, Petersenstr. 22, D-64287 Darmstadt; [3] BENSC, Hahn-Meitner Institut, D-14109 Berlin

QINS yields information on dynamical and geometrical aspects of molecular motions in the time window of $10^{-8}$ - $10^{-12}$ sec and provides information on the trajectories of the incoherently scattering hydrogen atoms. Experiments were performed at 20°C.
Measurements on hydrated Purple Membrane (PM) stacks (lamellar spacing 60 Å) in $H_2O$ and $D_2O$ showed the dynamical behaviour of water molecules, which was analysed parallel and perpendicular to the membrane plane. Translational diffusion was observed only in direction parallel to the membrane surface with a diffusion constant (4.4 $10^{-6}$ $cm^2sec^{-1}$) 5 times smaller than in bulk water. The rotational diffusion of water molecules was also anisotropic with respect to the PM plane.
A comparison of QINS measurements on PM stacks in $D_2O$ at two different levels of hydratation (wet: 900 $H_2O$ per hexagonal unit cell and lamellar spacing of 60 Å; dry: 135 $H_2O$ per unit cell and lamellar spacing of 52.7 Å) showed a strong influence of the extend of hydratation on the dynamics of the protein and lipid. The unharmonious and diffusive motions are reduced in the dry state. The increase of quasielastic scattering, going from the dry to the wet state of the PM, was highly anisotropic showing a larger increase in the direction perpendicular to the membrane plane.

**M-Pos94**

ROLES OF PROTEIN DYNAMICS IN PHOTO-ISOMERIZATION OF RETINAL IN BACTERIORHODOPSIN.

((N. M. Mahoney, M. R. Chance, L. M. Miller, A. Xie)) Albert Einstein Col. of Med., Bronx, NY 10461.

The light-driven proton pumping process in bacteriorhodopsin (BR) and the attractant phototaxis response via sensory rhodopsin I (SR-I), are activated by *all-trans* to *13-cis* photo-isomerization of retinal. The quantum yield of S610, a K-like photoproduct of SR-I, is dramatically reduced as temperature is lowered below 220K, while the quantum yield of K590 from BR is independent of temperature (300K - 80K) [1]. The reduced S610 yield is interpreted as due to steric constraints imposed by the tight retinal binding pocket of SR-I. However, the steric constraints alone can not explain why the photo-isomerization of retinal is not prohibited at temperatures above 220K. We propose that the structural motions of protein *facilitate* photo-isomerization of retinal in SR-I. Thus, protein dynamics are key to the photo-isomerization mechanism. In order to test this hypothesis, we have modified the steric constraints on retinal in BR (reducing the size of the retinal binding pokect) using site-specific mutagenesis. We measure the quantum yield of the K state from 300 to 20 K in order to correlate photo-isomerization with protein dynamics.

[1] B. Yan, A. Xie, G. U. Nienhaus, Y. Katsuta, and J. Spudich. *Biochemistry* **1993**, *32*: 10224-10232.

**M-Pos95**

THE ROLE OF THE LEADER SEQUENCE AND ITS CODING REGION IN EXPRESSION AND ASSEMBLY OF BACTERIORHODOPSIN IN HALOBACTERIUM HALOBIUM

((M. Teintze, Z.-J. Xu, D.B. Moffett and B. Perry)) Department of Chemistry & Biochemistry, Montana State University, Bozeman, MT 59717

Bacterio-opsin is made as a precursor in H. halobium which has 13 additional residues at the aminoterminal. The codons for these residues have been proposed to form a hairpin structure in the mRNA and play a role in ribosome binding and the peptide sequence has a proposed role in membrane insertion of bacteriorhodopsin (BR). We have made mutations in the bop gene region coding for the leader sequence and expressed the mutant genes in an H. halobium mutant lacking wild-type BR. The leader sequence coding region was found to be important for the stability of the mRNA and for its efficient translation. Single base substitutions that did not affect the amino acid sequence caused significant reductions in protein expression. Deletion of the leader region resulted unstable mRNA and almost no BR production. Introduction of a new ribosome-binding sequence within the coding region of the mature protein restored mRNA stability and protein expression. Protein made without the leader peptide was properly assembled in the membrane.
(Supported by NIH Grant GM38142)

M-Pos96

**PROBING OF THE RETINAL-BINDING CAVITY OF BACTERIORHODOPSIN BY CROSS-LINK** ((Y. Feng, B. Katz, J.M. Chapman, C.J. Beischel, D.R. Menick and R.K. Crouch)) Department of Biochemistry and Molecular Biology and Department of Ophthalmology, Medical Univ. of South Carolina, Charleston, SC 29425

The interaction of an introduced cysteine group with a chromophore suitably derivatized with a active leaving group is being used to detect the chromophore binding pocket of bacteriorhodopsin (bR). Cysteine can be introduced to the desired position by site-directed mutagenesis. Since bR has the interesting feature of not having any cysteines present in the native structure, the cysteine will contain the only free sulfhydryl group capable of reacting with the retinal analogue. Based on Henderson's molecular model of bR, we have chosen the positions Met118, Thr121, and Ser141 to be mutated to cysteine individually. The S141C mutant appears not to form any pigment whereas the other two cysteine mutants regenerate well with *all-trans* retinal. By using tritiated 4-bromo-retinal which contains the reactive allylic halide, evidence has been obtained showing a thiol linkage between the cysteine group of M118 position and the chromophore. T121C and the wild-type display similar low levels of cross-linking. The cysteine cross-linking is blocked by the cysteine-specific inhibitor N-methylmelaimide. The sites of cross-linking are being confirmed using mass spectrometry. We conclude that Met118 does contribute to the sites of crosslink around the ring of retinal. Therefore, the application of thiol chemistry presents an opportunity to explore the positions and orientations of amino acids which might be expected to be in close proximity to the retinal chromophore of bR. (Supported by EY04939)

M-Pos97

**MOLECULAR DYNAMICS STUDY OF THE 13-*CIS* PHOTOCYCLE OF BACTERIORHODOPSIN** ((I. Logunov, W. Humphrey, K. Schulten and M. Sheves)) Beckman Institute, UIUC, Urbana, IL, 61801.

The 13-*cis* photocycle of bacteriorhodopsin has been studied by means of molecular dynamics simulations. The structure of 13-*cis*-bacteriorhodopsin was obtained through molecular dynamics refinement and tested by altering substituents of retinal and comparing with available observations. The photoisomerization process was simulated. The resulting structures of the J, K, and L intermediates revealed that the protonated Schiff base points to the cytoplasmic side and, hence, cannot form an M intermediate. Our simulations suggest the possibility that leakage from the 13-*cis* cycle to the *trans* cycle occurs during the initial photoisomerization step.

M-Pos98

TIME - RESOLVED SURFACE POTENTIAL CHANGES IN BACTERIORHODOPSIN.
((U. Alexiev, T. Marti*, M.P. Heyn, H.G. Khorana* and P. Scherrer)) Biophysics Group, Freie Universität Berlin, 14195 Berlin, Germany. *Dept. of Biol. and Chem., MIT, Cambridge, MA 02139, U.S.A.

The pH-sensitive dye 5-iodoacetamidofluorescein was selectively attached to a cysteine residue introduced by site-directed mutagenesis in position 101 on the cytoplasmic surface of bacteriorhodopsin. The light-induced absorbance and surface potential changes were monitored. The mutant V101C shows altered kinetics in the second part of the photocycle with a pronounced slow M-decay component similar to the one observed in wild type at alkaline pH. This component is believed to be the result of a slow N to O transition. The transient negative surface potential detected with fluorescein in position 101 rises with 2.7 ms and decays with 48 ms. The rise time correlates with the fast decay time of the M-intermediate (3 ms) and the potential decays with the slowest M component (45 ms) corresponding to the N-decay. This potential change is equivalent to the transient formation of about one negative charge. The observed charge change in N will be discussed in the context of the transient deprotonation of Asp 96, as suggested by FTIR.

M-Pos99

ELECTROPHORETIC CONVERSION OF BACTERIORHODOPSIN FROM THE PURPLE TO THE BLUE FORM.
((Yuan-chin Ching, Satoshi Takahashi, Ming Yan, Lewis Rothberg, and Denis L. Rousseau)) AT&T Bell Laboratories, Murray Hill, NJ 07974.

Wet films of bacteriorhodopsin purple membrane were formed on glass plates on which electrodes had been deposited. Fields of a few volts per cm resulted in the conversion of purple membrane with a visible absorption maximum at ~560 nm to a blue form with a broader optical transition having a maximum at ~590 nm. Upon incubating the blue sample in a wet atmosphere for 48 hours, the purple form was regenerated. The conversion from the purple to a blue form had a very sharp interface which steadily moved from the anode to the cathode in the presence of the field suggesting a cooperative process. The optical absorption spectra, the FTIR spectra and the resonance Raman spectra of the blue form generated electrophoretically are compared to that formed in solution by cation depletion and by acidification.

M-Pos100

MODIFICATION OF BACTERIORHODOPSIN SURFACE CARBOXYL GROUPS INHIBITS RETINAL BINDING. ((R. Renthal, L. Guerra and R. Rangel)) The University of Texas at San Antonio, San Antonio, TX 78249

How does all-trans retinal enter the binding cavity in bacterio-opsin to form bacteriorhodopsin (bR)? Access from the lipid bilayer is usually assumed to occur. We previously reported slow formation of the 570 nm retinal Schiff base chromophore in bR that had been covalently modified at the membrane surface with quaternary ammonium groups. However, the chromophore regeneration was measured in detergent micelles and involved both a protein folding step and a retinal attachment step. We have now eliminated the folding step by studying chromophore regeneration in purple membrane (PM) sheets. We reacted pPM (PM that had been first treated with papain to remove the C-terminal 17 amino acids) with 1-ethyl-3-trimethylaminopropyl carbodiimide (ETC) at neutral pH. Approximately 2 moles of ETC were incorporated per mole of bR. After bleaching of the chromophore with $NH_2OH$ in the presence of light, regeneration of the 570 nm chromophore was measured. Regeneration of ETC-pPM occurred at less than half the rate of pPM. Furthermore, with ETC-pPM, the binding kinetic step is inhibited: there is a slower rate of retinol binding and also a slower rate of formation of 440 nm intermediate at 5° C. However, the rate of Schiff base formation was not affected by ETC. Amino acid sequence analysis indicates that the major site of ETC modification is Glu 74, which is at the mouth of the proton release channel on the extracellular side of the membrane. (Supported by GM 08194 and GM 07717)

M-Pos101

LOCALIZATION OF AN AMINO ACID RESIDUE IN THE CD LOOP OF BACTERIORHODOPSIN BY X-RAY DIFFRACTION.
((W. Behrens, M.P. Krebs†, R. Mollaaghababa† H.G. Khorana† and M.P. Heyn)) Biophysics Group, FU Berlin, D-14195 Berlin, † MIT, Cambridge, MA 02139.

X-ray diffraction was used to localize a single amino acid in the CD loop of the integral membrane protein bacteriorhodopsin (bR). Exploiting the fact that wild-type bR contains no cysteine, the bR-mutant A103C was labeled with the sulfhydryl specific reagent p-chloromercuribenzoate at a 0.9:1 stoichiometry. The functional properties of A103C and its mercury derivative (photocycle, proton release kinetics, dark adaptation) were similar to those of wild-type and both form the same hexagonal lattice.X-ray diffraction patterns of both the unlabeled and labeled A103C samples were recorded out to the (7,1) peak. The most prominent changes in relative intensities were observed in the (1,0), (1,1), and (4,0) reflections. The calculated two dimensional Fourier difference map shows a clear-cut difference in electron density between helices C and D. Model calculations agree well with the Fourier differences obtained from the refinement implying that the difference in electron density corresponds in strength to that expected for a mercury label.This labeling method using cysteine mutants may be used to monitor structural changes of the protein during the photocycle at well defined positions.

**M-Pos102**

EVIDENCE THAT SCHIFF BASE DEPROTONATION IN BACTERIORHODOPSIN PHOTOCYCLE IS ACCOMPLISHED BY LOWERING IT'S pK ((R. Govindjee, S.P. Balashov, T.G. Ebrey, D. Oesterhelt*, G. Steinberg‡ and M. Sheves‡)) Center for Biophysics and Dep. of Cell and Structural Biology, University of Illinois, Urbana-Champaign IL 61801, USA, *Max-Planck Institut für Biochemie, Martinsried, Germany, ‡Dep. of Org. Chem., Weizmann Inst. of Science, Rehovot, 76100, Israel

At neutral pH the Y57N mutant of bR in which tyrosine 57 was replaced with asparagine shows a flash-induced long lived (500 ms) L- like intermediate but no M-intermediate or proton pumping. We thought that this might be due to an improper $\Delta pK_a$, after light absorption, between the proton donating Schiff base and the proton acceptor, Asp85. In order to check this and repair the defect, we made an artificial analog of Y57N in which the $pK_a$ of the protonated Schiff base (and, presumably, that in the photointermediates) was intrinsically reduced due to the electronic properties of a retinal analog,14-Fluoro retinal. The 14-F,Y57N pigment has absorption maximum at 580 nm in the dark-adapted state. Titration indicates that $pK_a$ of the Schiff base is reduced by 3.4 units in 14-F,Y57N (from 12.1±0.2 in Y57N to 8.7±0.2). The $pK_a$ of D85 is also affected by 14-Fluoro substitution (as indicated by the purple to blue transition). In Y57N the purple to blue transition has two pKs, the first of which is shifted from 3.8 to 5.8 in 14-F,Y57N. *The 14-F,Y57N pigment shows light-induced M formation and proton release, strongly suggesting that light-induced Schiff base deprotonation is accomplished by lowering its $pK_a$ and/or raising the $pK_a$ of D85 during the photochemical cycle.*

**M-Pos103**

SUBSTITUTION OF ARG82 WITH LYSINE IN BACTERIORHODOPSIN: EFFECTS ON THERMAL ISOMERIZATION, PHOTOCYCLE AND PROTON RELEASE. ((S.P. Balashov, R. Govindjee, E. Imasheva, S. Misra, T. G. Ebrey, Y. Feng*, R. K. Crouch*, and D. R. Menick*)) Center for Biophysics and Dept. of Cell and Struct. Biology, UIUC, Urbana, IL 61801, and * Medical Univ. of S. Carolina, Charleston, SC 29425.

Studies on mutants in which Arg82 was substituted with a neutral residue (Ala or Gln) showed that *a)* Arg82 is responsible for the stabilization of the ionized form of Asp85, which acts as a counterion to the Schiff base and as the primary proton acceptor in the photocycle; *b)* protonation of Asp85 controls the rate of thermal isomerization in bR (dark adaptation) and *c)* Arg82 is involved in light-induced proton release. In order to study the role of the positive charge of Arg82 and its guanidinium group more specifically, we substituted Arg82 with Lys which is also positively charged at neutral pH. We found that: *(1)* In the R82K mutant (expressed in *H. halobium*) the $pK_a$ of Asp85 ($pK_a$ of the purple-to-blue transition) is 3.5 compared to 2.6 in the wild type (WT) and 7.2 in R82A (in 150 mM KCl). Thus Lys82 is 80% as effective in shifting the $pK_a$ of Asp85 as Arg82. *(2)* The pH dependence of the rate constant of dark adaptation, $k_{da}$, shows that two groups with $pK_1$=3.9 and $pK_2$=8.0 control $k_{da}$ in R82K between pH 2 and 10 (in the WT, $pK_1$=2.9 and $pK_2$=9.5; in R82A, only one amino acid controls the pH dependence with $pK_1$=7.5). The most straightforward interpretation of these pH dependencies is that $pK_1$ is due to Asp85 deprotonation; $pK_2$ is associated with Lys82 ($pK_a$= 8.0) in R82K and with Arg82 ($pK_a$=9.5) in the WT. *(3)* Flash-induced transient proton release is constrained in the R82A and R82K mutants which indicates that R82 acts as a proton release group. *(4)* R82K mutant (like R82A) shows fast (1 μs) pH independent M formation, lack of accumulation of the O intermediate, fast decay of the bathoproduct of the 13-cis pigment, $K^c$. These features may be due to alteration of hydrogen bonds involving the guanidinium group of Arg82. *(Supported by DOE Grant 88ER13948 to T.G.E., and NIH Grant EY04939 to R.K.C.).*

**M-Pos104**

CALCULATION OF PKA'S OF TITRATABLE GROUPS IN BACTERIORHODOPSIN
((R.V. Sampogna, A-S Yang, B.H. Honig))
Dept. of Biochemistry and Molecular Biophysics, Columbia University, 630 W. 168th Street, NY, NY 10032. (Spon. by A. Nicholls)

The factors governing the pKa's of amino acids are primarily electrostatic. When isolated in solution, the charged and neutral forms of a titrating group are stabilized to differing extents by interactions with the solvent. In the protein, a significant portion of these solvent interactions becomes replaced by interactions with protein dipolar groups, polarizable electrons and other titratable residues. Due to electrostatic effects the protein environment exerts on each residue, individual pKa's of amino acids can be either increased or decreased relative to those isolated in solution. We have used the finite difference Poisson-Boltzmann method to calculate pKa's of titratable groups integral to the proton pumping mechanism of bacteriorhodopsin (bR). Various models of bR have been constructed based on the electron diffraction structure solved by Henderson and coworkers (J.Mol.Biol., 1992, 213, 899-929). These include structures containing a modified arg-82 position, the inclusion of explicit water molecules and a K-like photocycle intermediate. Our calculations provide useful insights into the proton pumping mechanism in bR because they reveal the nature and magnitude of the interactions between titratable groups and their significance to proton transfer.

**M-Pos105**

THE K TO L TRANSITION OF BACTERIORHODOPSIN DOES NOT APPEAR TO BE CONTROLLED BY A PROTON TRANSFER
((Masahiro Kono[1] and Thomas G. Ebrey[1,2])) Biophysics Division[1] and Department of Cell and Structural Biology[2], University of Illinois at Urbana-Champaign, Urbana, IL 61801

Bacteriorhodopsin, a 7-helix membrane protein, acts as a light-driven proton pump. Upon illumination, it undergoes a photocycle which can be schematically represented in the following linear path: bR → K → L → M → N → O → bR where bR represents the ground state and subsequent letters the photointermediates. The K and L intermediates are not different in terms of chromophore isomeric and protonation states; yet the absorbance maximum of the L intermediate is blue shifted from that of the K intermediate indicating a definite change in the structure or interactions of groups near the chromophore. One possiblity is a proton transfer between groups within the protein. It has been suggested that certain residues (Asp-212 or Asp-96) change their protonation states during the K to L transition.

We have characterized the K to L transition optically and electrically in water and deuterium oxide ($D_2O$) and compared the kinetics of these processes. If a proton transfer defines the changes of the protein in forming the L intermediate, then the rate of the K to L transition should be slower in the presence of $D_2O$. We find that these rates do not differ significantly. Therefore, proton transfer appears not to determine changes in the chromophore environment during the K to L transition.

**M-Pos106**

ETHYLGUANIDINIUM SALTS ACCURATELY MODEL HALIDE-ARGININE ION PAIRING IN HALORHODOPSIN.
((D. M. Briercheck, T. J. Walter, and M. S. Braiman)) Department of Biochemistry, University of Virginia Health Sciences Center, Charlottesville, VA 22908.

$Cl^-$, $Br^-$, $I^-$, and $OAc^-$ salts of ethylguanidinium have been prepared. FTIR spectra of these compounds dissolved in a weakly polar solvent (chloroform:methanol, 97:3 by volume) show significant anion dependence for 3 vibrations previously assigned as C–N stretching modes; these vibrations are observed as IR absorption bands near 1675, 1630, and 1170 $cm^{-1}$. The anion dependence of these vibrations can be attributed to ion pairing between ethylguanidinium and its counteranion; this dependence disappears when 100% methanol (a more polar solvent) is used. The different strengths of the ethylguanidinium-halide interactions can be correlated to the differing sizes of the counteranion radii. Similar anion dependence is seen for three infrared bands (near 1695, 1610, and 1170 $cm^{-1}$) of halorhodopsin, the light-driven chloride pump of *H. halobium*. These frequencies are likely due to C–N stretching vibrations of arginine side chains. The magnitude of halide dependent shifts (e.g., a 2.7 $cm^{-1}$ difference for chloride vs. iodide for the highest frequency C–N stretch) is nearly the same in the model compounds and halorhodopsin, although the absolute C–N stretching frequencies are not identical. As a dried film, however, ethylguanidinium acetate has a C–N stretch at 1690 $cm^{-1}$, much closer to the 1695 $cm^{-1}$ C–N stretch seen in halorhodopsin. This increase in frequency is probably due to simultaneous interactions of each guanidino group with more than one carboxylate. We conclude that the side chain of a buried arginine in halorhodopsin is probably involved in multiple ionic interactions, with its counteranions including one or more carboxylate residues as well as a halide.

**M-Pos107**

SYNERGY IN THE SPECTRAL TUNING OF RETINAL PIGMENTS: COMPLETE ACCOUNTING OF THE OPSIN SHIFT IN BACTERIORHODOPSIN ((J. Hu, R.G. Griffin and J. Herzfeld)) Dept. of Chemistry, Brandeis Univ., Waltham, MA 02254-9110 and Dept. of Chemistry and Francis Bitter National Magnet Lab., MIT, Cambridge, MA 02139-4307.

Spectral tuning in retinal pigments is important for color vision. Four mechanisms have been proposed for the bathochromic shift of the spectrum of the retinal protonated Schiff Base (pSB) in various opsins (the opsin shift): a weak counterion for the protonated imine; a negative point charge in the vicinity of the polyene chain; isomerization of the ring-chain linkage from skewed 6-s-*cis* to planar 6-s-*trans*; and a highly polarizable chromophore binding pocket. Here we investigate the possibility of synergy among these mechanisms. Solid-state $^{15}N$ and $^{13}C$ NMR spectra and solid state UV-vis spectra were obtained for the $Cl^-$, $Br^-$, and $I^-$ salts of the 6-s-*trans* pSB of retinal with aniline. As found previously for 6-s-*cis* compounds, there is a progressive red shift with decreasing pSB hydrogen bond strength (from $Cl^-$ to $I^-$). However, the effect is significantly stronger in the 6-s-*trans* compounds. Strong linear correlations are observed between the frequency of maximum UV-vis absorption and the $^{15}N$ and 5-$^{13}C$ isotropic chemical shifts, whether the variations are induced by 6-s-isomerization or by changes in the pSB counterion. It is concluded that the 6-s-conformation and the pSB counterion have synergistic effects on the overall electronic structure of the chromophore. Based on this synergy, the opsin shift and chemical shift tensors of bacteriorhodopsin can be fully explained without the necessity of a negative point charge or polarizability effects in the chromophore binding pocket.

**M-Pos108**

MODELING THE STRUCTURE OF VISUAL PIGMENTS

((L. Tang[1], T. G. Ebrey[1,2,4] and S. Subramaniam[1,3,4])) [1]Center for Biophysics and Computational Biology, [2]Department of Cell and Structural Biology, [3]Computational Group in National Center for Supercomputing Application & [4]Beckman Institute for Advanced Science and Technology, University of Illinois at Urbana-Champaign, IL 61801

Hydropathy plots and previous studies have indicated that there are seven transmembrane segments in the polypeptide of visual pigments. We determined the boundaries of the seven transmembrane segments based on the superimposed hydropathy plot of 23 vertebrate visual pigment sequences. The seven transmembrane segments were assigned an alpha-helical form as predicted by Rao-Argos' algorithm and a composite of earlier topological studies. This "two dimensional" model of visual pigment structure is consistent with previous limited proteolysis, hydrophilic probe labelling, and monoclonal antibody studies.

Although there is no sequence similarity between visual pigments and another membrane protein with seven transmembrane helices, bacteriorhodopsin, we provide concrete evidence that both pigments share a similar, although not identical, topology and three dimensional structure. Thus, a structural model of visual pigments is provided by taking bacteriorhodopsin as a conditional template: the seven helices in the visual pigments are arranged in the same sequential order and similar packing pattern, forming a similar oval circle as those of bacteriorhodopsin. The orientation of each helix in the visual pigment is determined in such a way that (a) the conservation moment of each helix points toward the inside of the protein and (b) the chromophore-interacting residues indicated by the previous studies are facing the inside of the protein.

**M-Pos109**

THREE DIMENSIONAL STRUCTURE OF BOVINE RHODOPSIN AT 9Å RESOLUTION

((V.M. Unger and G.F.X. Schertler)) Laboratory of Molecular Biology, Hills Rd. Cambridge/U.K., CB2 2QH. (Spon. by E.Bäuerlein)

The projection structure (Schertler *et al.*, Nature 1993) of bovine rhodopsin for the first time revealed details of the arrangement of the seven transmembrane helices within this G-protein coupled receptor. Even though the overall topology of rhodopsin is identical to that found in bacteriorhodopsin - the light driven proton pump in Halobacteria - the arrangement of the seven helices in the membrane shows considerable differences suggesting that the three dimensional structures within the superfamily of G-protein coupled receptors might be different from that determined for bacteriorhodopsin. To address this issue images of tilted, frozen hydrated, 2D crystals of bovine rhodopsin were taken and after image processing recombined to give a three dimensional map at a resolution of 9Å. Our interpretation of the density found in the map shows that rhodopsin can be described as an arc shaped group of four rather tilted helices flanked by a pair of helices on its inner side and the remaining helix on the other side. Taking into account that based on sequence constraints alone helix III is expected to be the most buried of the seven transmembrane domains (Baldwin, EMBO J., 1993) it is very likely that in contrast to bacteriorhodopsin the arc shaped feature in rhodopsin is formed by helices I-III and helix V.

**M-Pos110**

NON-EXPONENTIAL DECAY KINETICS OF BATHORHODOPSIN AT LOW TEMPERATURES.

((S.E. Wallace-Williams, T.L. Mah, D. Che, J.W. Lewis, T.E. Thorgeirsson, and D.S. Kliger)) Department of Chemistry and Biochemistry, University of California, Santa Cruz, CA 95064.

The decay of bathorhodopsin was monitored over the temperature range of 145-165 K. The samples consisting of 25% detergent solubilized bovine rhodopsin and 75% glycerol were photolyzed with blue light and monitored with optical multichannel detection as a function of time after photolysis. According to the traditional scheme, bathorhodopsin should decay directly to lumirhodopsin, which is stable at these temperatures. However, the spectral evolution could not be fit to a one-exponential function; three-exponentials are needed to adequately describe the decay. Alternatively, a Gaussian distribution of activation energies and a fractal kinetic model describe the data within the noise. (Supported by NIH grant EY00983)

**M-Pos111**

FORMATION OF METARHODOPSIN II: EXPONENTIAL, FRACTAL OR POWER LAW KINETICS.

((T.E. Thorgeirsson, D. Che, S.E. Wallace-Williams, T.L. Mah, J.W. Lewis, and D.S. Kliger)) Department of Chemistry and Biochemistry, University of California, Santa Cruz, CA 95064.

Results from measurements of absorbance changes following photoexcitation of bovine rhodopsin in sonicated disk suspensions are presented. Measurements are made at 5 temperatures (15-35 °C) using multichannel detection. Three exponentials are required to account for the absorbance changes ($10^{-6}$ - $10^{-1}$s). The results can be explained by discrete kinetic schemes involving the traditional rhodopsin photointermediates (Lumirhodopsin, Metarhodopsin I, and Metarhodopsin II) if an additional intermediate, spectrally similar to Metarhodopsin II, is included. However, analysis of the multiexponential fitting results reveals a rate-amplitude correlation ($a_i = k_i^{-\beta}$) near 380 nm, the absorbance maximum of Metarhodopsin II. As this suggests, the data also fit a power law, as well as a single stretched exponential. Metarhodopsin II formation can thus be modeled in terms of 1-D diffusion or fractal models similar to those that have been advanced to describe the openings and closings of ion channels. (Supported by NIH grant EY00983)

**M-Pos112**

RESONANCE RAMAN STUDIES OF THE C=N CONFORMATION OF OCTOPUS RHODOPSIN

((L. Huang‡, G. Weng‡, H. Deng‡, J. Liang§, Y. Koutalos§, T. Ebrey§, R. Gebhard||, M. Groesbeek||, J. Lugtenburg||, M. Tsuda^, and R. H. Callender‡*)) ‡Dept of Phys, CCNY, NY, NY 10031, §Dept of Physio and Biophys, Univ of Il at U-C, Urbana, IL 61801, ||Dept of Chem. Univ of Leiden, 2300 RA Leiden, The Netherlands, ^Dept of Phys, Sapporo Med Coll, Sapporo 060, Japan.

It has been found that the resonance Raman spectrum of octopus rhodopsin in the fingerprint region is very different from that found in either bovine rhodopsin or free 11-cis retinal Schiff base, and is changed substantially upon Schiff base deuteration, which suggests that the environment of the 11-cis retinal chromophore in octopus rhodopsin is different. In order to study the nature of the chromophore-opsin interaction in more detail, we have obtained the octopus rhodopsin spectrum and its C9-$^{13}$C, C10,C11-$^{13}$C2, C12,C13-$^{13}$C2, C13-$^{13}$C, C14,C15-$^{13}$C2 and ND isotopically labeled derivatives at 120 K using the 'pump-probe' technique. The large spectral change in the finger print region of the retinal protonated Schiff base upon Schiff base deuteration was used to support a C=N syn conformation in the dark adapted bR. Although deuteration of the Schiff base induces large changes in the finger print region of octopus resonance Raman data, our detailed analysis suggest that the retinal Schiff base C=N bond is anti.

**M-Pos113**

LOCATION OF THE SCHIFF BASE COUNTERION IN THE BOVINE RHODOPSIN RETINAL BINDING SITE

((M. Han and S.O. Smith)) Dept. of Molecular Biophysics and Biochemistry, Yale University, New Haven, CT 06520. (Spon. by R.M. Macnab)

Rhodopsin ($\lambda$max =500 nm) is the vertebrate photoreceptor responsible for vision in dim light, and contains an 11-*cis*-retinal chromophore covalently bound to Lys-296 through a protonated Schiff base (PSB) linkage. Glu-113 has been identified as the counterion of the positively charged PSB, but its location and relative orientation are not known. The goals of this study are to decipher the charge interactions in the retinal binding site and determine how these interactions change during the photoreaction. Semiempirical molecular orbital calculations are combined with magic angle spinning NMR measurements to localize the counterion position in the retinal binding site, utilizing the linear relationship between $^{13}$C chemical shift and the charge density of the conjugated carbons. Charge densities along the retinal polyene chain are calculated for various counterion geometries, and correlations with the chemical shift data are evaluated. First, a simple chloride ion is used to roughly map out the location of the negative charge(s). Subsequently, an acetate ion ($CH_3COO^-$) is used to restrain the orientation of the Glu-113 side chain. A unique model is proposed from the calculations where the counterion is located near the middle of the polyene chain, with one oxygen atom of the $CH_3COO^-$ close to $C_{12}$ and the other oxygen pointing away from the chain. Inclusion of a water molecule hydrogen bonded with the Schiff base proton does not alter the fit to the NMR data, although it is consistent with observations obtained from other methods. We also show that the model fits the absorption data of the pigments. Current emphasis is on obtaining $^{13}$C chemical shift data of Meta I and II photointermediates to address the question of proton transfer in the Meta I <—> Meta II transition.

M-Pos114

**FORMATION OF THE SIGNALING STATE S373 FROM SENSORY RHODOPSIN I.** ((A. Xie†, B. Yan§‡, M. R. Chance†, N. Mahoney†, and J. L. Spudich§)) †Albert Einstein Col. of Med., Bronx, NY 10461; §Univ. of Texas Med. Sch., Houston, TX 77030; ‡Sandoz, NJ 07936.

Sensory rhodopsin I (SR-I) is a phototaxis receptor protein in *Halobacterium salinarium*. SR-I with peak absorption at 587 nm (S587) is an attractant receptor. S373, a long-lived photoproduct with peak absorption at 373 nm, is the signaling state of the receptor, responsible for transmitting attractant signal to the SR-I transducer (HtrI). S373 is also photochemically reactive; its photoexcitation generates repellent signals to HtrI. In order to detect conformational motions in the transformation from SR587 to S373, we have measured the kinetics of thermal steps in the SR-I photocycle: SR587 ⇝ S610 → S560 → S373 → SR587, in 20% and 66% glycerol/water (v/v) at 280, 290, 300, and 310 K. Global conformational motions involving solvent-exposed surfaces of SR-I are likely to be slowed down in high solvent viscosity. We found that only the transition from S373 to SR587 is slowed down significantly (20 times) in 66 % gly/water at all temperatures tested, whereas the S373 formation and the S610 to S560 transition are far less sensitive to viscosity. This observation raises the intriguing possibility of a spectroscopically silent transition from S373a to S373b, which involves large conformational motions and could be required for signaling to HtrI. Double flash experiments are being undertaking to test for photochemical differences between early and late S373, which may help to elucidate when the signaling S373 state is formed.

M-Pos115

**SIGNAL TRANSDUCTION DUE TO RHODOPSIN IS MEDIATED BY THE MEMBRANE LIPID COMPOSITION.** ((Michael F. Brown and Nicholas J. Gibson)) Department of Chemistry, University of Arizona, Tucson, Arizona 85721.

A paradigm for visual function is that the MI-MII conformational transition of rhodopsin leads to exposure of recognition sites for the G protein transducin leading to excitation of the retinal rod. We tested the hypothesis[1] that the rod membrane lipids are implicated in visual signal transduction due to their influence on the conformational energetics of photolyzed rhodopsin. Using **flash photolysis** methods we discovered that the membrane lipid composition alters the apparent pK for the MI–MII equilibrium of rhodopsin.[2,3] Substitution experiments with non-native lipids showed that **biophysical properties** of the membrane rather than chemically specific lipid-protein interactions are involved. Relatively small changes due to **lateral and/or curvature stresses** involving the lipid/water interface can explain the free energy shifts for the MI–MII transition among the different recombinants. One possibility is that the **curvature free energy** of the membrane-lipid water interface is important; relief of the curvature frustration can provide a source of work for the uphill MI-MII transition. These findings illustrate vividly that the membrane lipid composition can influence the photochemical activity of rhodopsin, thereby implicating properties of the membrane bilayer in the molecular mechanism of the visual process. [1]T.S. Wiedmann *et al.* (1988) *Biochemistry* **27**, 6469-6474. [3]N.J. Gibson and M.F. Brown (1991) *Photochem. Photobiol.* **54**, 985-992. [3]N.J. Gibson and M.F. Brown (1991) *Biochemistry* **32**, 2438-2454. Supported by NIH Grant EY03754.

M-Pos116

**INFLUENCE OF NONBILAYER-FORMING LIPIDS ON THE CONFORMATIONAL ENERGETICS OF RHODOPSIN.** ((Michael F. Brown, Nicholas J. Gibson, and Robin L. Thurmond)) Department of Chemistry, University of Arizona, Tucson, Arizona 85721.

The visual pigment rhodopsin constitutes an important paradigm for seven α-helix **transmembrane receptors** whose mechanism of action is coupled to G **proteins**. Current knowledge indicates the key triggering event for the visual process is the MI-MII transition of photolyzed rhodopsin. The lipid composition of the native ROS membranes is near a lamellar-reverse hexagonal ($H_{II}$) phase boundary.[1] Hence we tested the hypothesis[2] that nonbilayer-forming lipids govern visual **signal transduction** by influencing the energetics of the MI and MII conformational states of rhodopsin. Using **flash photolysis** techniques we discovered that the membrane lipid composition modulates reversibly the MI-MII acid-base equilibrium.[3] If rhodopsin is recombined with lipids having a native-like head group composition, then docosahexaenoyl (22:6ω3) phospholipids are sufficient for a native like MII/MI ratio. But in the absence of native-like polyunsaturated chains, the presence of non-bilayer forming lipids such as DOPE is also sufficient for native-like behavior. We propose that the signal transducing event in vision is governed by **physicochemical properties** of the membrane bilayer. A major determinant of the conformational energetics of rhodopsin in membranes is the **free energy of curvature** of the membrane lipid/water interface. [1]A.J. Deese et al. (1981) *FEBS Lett.* **124**, 93-99. [2]T.S. Wiedmann et al. (1988) *Biochemistry* **27**, 6469-6474. [3]N.J. Gibson and M.F. Brown (1991) *Biochemistry* **32**, 2438-2454. Supported by NIH Grant EY03754.

M-Pos117

**TRANSDUCIN ACTIVATION BY THE BOVINE OPSIN APOPROTEIN.** ((A.Surya, K.W.Foster and B.E.Knox+)) Syracuse University and SUNY, HSC at Syracuse+. (Spon. by K.W.Foster).

In order to study the signal transduction processes in the light adapted rod photoreceptor cell, we investigated the biochemical properties of bleached rhodopsin. The ability of bovine opsin to activate transducin was compared to that of rhodopsin in urea-stripped rod outer segment membranes (UROS). Opsin was prepared from UROS by bleaching in the presence of 2000 fold molar excess of hydroxylamine, followed by extensive washing to remove retinal completely, as determined by UV-visible absorption spectrum. The ability of the opsin apoprotein to activate transducin was measured using a nucleotide exchange assay with the non-hydrolyzable GTP analog, [$^{35}$S]GTPγS. To determine the total number of transducin molecules activated, the binding reaction was carried out for 2 hours at 22-24°C. For an assay containing 200 nM transducin, the concentration of opsin required to activate 50% of the transducin was 160 nM. This was 10 times more than the amount of light-activated rhodopsin required to activate the same quantity of transducin. The time required to activate half of a 200 nM solution of transducin by excess opsin was found to be 8 minutes. This was 12 times slower than found for excess light-activated rhodopsin. Control experiments demonstrated that the activity was not due to the effect of ROS lipids on transducin. The opsin activity was light independent and insensitive to 20 mM hydroxylamine. At the concentrations of opsin and transducin tested, only about 70% of the transducin could be stimulated in the exchange assay. Light-activated rhodopsin was able to stimulate 100% of the transducin. The effect of retinal isomers on the light-independent opsin activity was studied. Opsin incubated with 5 fold molar excess of 11-*cis* retinal was unable to activate transducin in the dark. Opsin incubated with 5 fold molar excess of all-*trans* retinal showed a greatly enhanced activity in the dark. The ability of opsin to interact and activate transducin could play a role in bleaching adaptation and the inhibitory effect of 11-*cis* retinal in the dark may have a function in minimizing rod cell noise.

M-Pos118

LIGHT CONTROLS THE $PIP_2$ HYDROLYSIS IN ROS MEMBRANES WITH HELP OF βγ-TRANSDUCIN. ((I.D. Volotovski, I.V. Grigorjev, A.N. Griz, I.D. Artamonov*)) Institut of Photobiology, Academy of Sciences of Berlarus, Minsk, 220733 Belarus.; *Institut of Bioorganic Chemistry, Russian Academy of Sciences, Moscow 178235, Russia

It has been previously shown that light and GTP stimulate the hydrolysis of phosphatidylinositol 4,5-bisphosphate ($PIP_2$) in rod outer segment membranes. These effects were demonstrated to be due to transducin because cholera and pertussis toxins inhibited the stimulation. However, only βγ-transducin (not α-transducin) exerted the stimulation effect even without any light illumination of ROS membranes. On the contrary, α-transducin added into the ROS suspension inhibited the light stimulation. It was concluded that retinal rod phospholipase C is activated by light with participation of βγ-transducin which is formed after αβγ-transducin dissociation under the light action. The relation of this finding to light-induced and transducin-dependent phenomena and the role of phosphoinositide metabolism in functioning of visual rods were discussed.

M-Pos119

EQUILIBRIUM AND KINETIC STUDIES ON THE INTERACTIONS OF IRBP WITH RETINOIDS

((Y. Chen and N. Noy))
Division of Nutritional Sciences, Cornell University, Ithaca, NY 14853

Interphotoreceptor retinoid-binding protein (IRBP) is a large retinoid-binding glycoprotein which is found primarily in the interphotoreceptor matrix (IPM) between the retinol pigment epithelium (RPE) and the photoreceptors. The equilibrium constants for binding of several retinoid species to IRBP were measured by fluorescence methods. HPLC was employed in conjunction to confirm the isomeric and structure integrity. The rate constants of the dissociation by retinoids from IRBP were determined by monitoring the transfer of the retinoids between IRBP and synthetic unilamellar vesicles. The results of these studies indicate that of all the retinoids studied, all-trans retinol and 11-cis retinal have the highest affinity for IRBP. These retinoids also show the slowest rate of dissociation from the protein.

M-Pos120

**EXCITATION OF *LIMULUS* PHOTORECEPTORS IN THE ABSENCE OF $Ca^{2+}$ RELEASE.** ((Kyrill Ukhanov and Richard Payne)) Dept. of Zoology, Univ. of Maryland, College Park, MD 20742.

Ventral photoreceptors were pressure injected with 500 $\mu$M of fura-2 so as to measure intracellular $Ca^{2+}$ ($Ca_i$). The light-activated current or receptor potential was recorded using a two-electrode voltage clamp. When bathed in artificial sea water containing 1 mM EGTA and no added $Ca^{2+}$ (0Ca-ASW), 340/380 nm light elicited a saturated electrical response and a rapid increase in $Ca_i$ from 200 nM to >5 $\mu$M. The preparation was then incubated for 30 min with added 50-100 $\mu$M Ca-ionophore 4-Br-A23187 and 1-2% DMSO followed by 5 min in 0Ca-ASW. After treatment, a 5 sec 340/380 nm flash of light still elicited an inward current of several hundred nanoamperes, but $Ca_i$ remained unchanged at 50-200 nM. Ionophore increased the time-to-peak of the response and decreased the sensitivity to dim flashes of light in a manner similar to intracellular injections of Ca-chelators or pharmacological blockade of the phosphoinositide pathway (Faddis and Brown, J. Gen. Physiol. 101, 909). After ionophore treatment, bathing the cells in 10 mM $CaCl_2$ ASW elevated $[Ca^{2+}]_i$ to >5 $\mu$M and reversibly suppressed the photocurrent. Control treatment with 1% DMSO did not affect $Ca^{2+}$ dark level nor light-induced Ca-release in response to saturating 340/380 nm light. We conclude that light-induced elevation of $Ca_i$, as detected by fura-2, is not absolutely necessary for phototransduction.

M-Pos121

**ON THE CALCIUM PERMEABILITY OF LIGHT SENSITIVE CHANNELS IN RHABDOMERIC PHOTORECEPTORS** ((Maria del Pilar Gomez and Enrico Nasi)) Department of Physiology, Boston University School of Medicine and Marine Biological Laboratory, Woods Hole, MA (Spon by B. Kaminer)

Recent observations in *Drosophila* photoreceptors suggest that a component of the light-sensitive conductance is highly selective to Ca ions. The desensitizing action of cytosolic Ca may then implicate light-dependent channels as part of a regulatory loop in visual transduction. We have employed isolated photoreceptors from *Lima* and *Pecten* to investigate the generality of such a proposition. We had previously shown two distinct components of the photocurrent - a situation subsequently confirmed in *Drosophila* - and demonstrated that they reflect the activation of separate light-sensitive conductance systems, rather than the modulation of other channels or the activation of a Na/Ca exchanger. Because these complexities make it difficult to examine shifts in reversal voltage with manipulations of $[Ca]_o$, we studied the fall kinetics of the photocurrent, which - like in *Drosophila* - slows down with depolarization, an effect attributed to changes in Ca influx. Intracellular dialysis with BAPTA failed to abolish the phenomenon. Since this may be due to improper cytosolic perfusion, we directly investigated ion permeation through single light-dependent channels, varying the composition of the patch pipette solution. Normal channel events were recorded with 0-Ca ASW or with NaCl. By contrast, the unitary currents were minute with $BaCl_2$, negligibly small with $Ca^{2+}$ and absent with $Mg^{2+}$. To rule out patch vesiculation, we also performed whole-cell measurements, using a fast local perfusion technique that avoids Ca loading due to prolonged exposure, and response desensitization. In the presence of Ca alone the photocurrent is nearly abolished in a reversible way. These results indicate that, at least in molluscan photoreceptos, Ca influx through the light-sensitive conductance - if existent - may be too small to be detectable by electrical measurements and is unlikely to be a major factor in the down-regulation of the light response. Supported by NIH grant RO1 EY07559.

M-Pos122

MECHANISMS OF INTRACELLULAR CALCIUM REGULATION IN BALANUS PHOTORECEPTOR. ((H. Kohmoto and H. Mack Brown)) Dept. Physiology, Univ. Utah School of Medicine, Salt Lake City, UT 84108.

Blocking $Na^+/Ca^{2+}$ exchange with $Li^+$ in Balanus photoreceptors reduces the plateau phase of the receptor potential and light sensitivity (J. Smolley & H.M. Brown, Biophys. J., 59:530, 1991). Since these effects are also sequelae of light adaptation, intracellular $Ca^{2+}$ regulation may have important functional consequences for light adaptation. The present experiments were addressed to quantitative changes in intracellular $Ca^{2+}$ $[Ca^{2+}]_i$ under conditions that alter $Na^+/Ca^{2+}$ exchange and also sought to identify other potential mechanisms of $[Ca^{2+}]_i$ regulation. The $Ca^{2+}$ indicator Arsenazo III (0.2 M KCl, pH 7.35) was injected into the photoreceptors and absorbance changes at 570, 650 and 720 nm were monitored with an LED microspectrophotometer (B. Rydqvist & H.M. Brown, J. Neurosci. Meth. 48:43, 1993). As expected, diminishing ($K^+$-free) or reversing ($Na^+$-free) the $Na^+$ gradient across the membrane increased $[Ca^{2+}]_i$ (11% and 44%, respectively). Unexpectedly, we observed that raising the bath pH to 9.35 produced as great an effect on $[Ca^{2+}]_i$ as $Na^+$-free solutions. The effect of pH was additive with the $Li^+$ effect, suggesting a different exchange mechanism than $Na^+/Ca^{2+}$ exchange. Removal of $Na^+$ or pH elevation in $Ca^{2+}$-free solutions reduced $[Ca^{2+}]_i$ slightly rather than increasing it, indicating that these exchange mechanisms are located in the limiting cell membrane. We conclude from these experiments that $Na^+/Ca^{2+}$ exchange is an important $Ca^{2+}]_i$ regulatory mechanism in these photoreceptors and suggest than an additional mechanism, $H^+/Ca^{2+}$ exchange, is also a significant participant in intracellular $Ca^{2+}$ homeostasis. (We thank R. Meech for suggesting the pH experiments).

M-Pos123

**CALCIUM DEPENDENCE OF RHODOPSIN PHOSPHORYLATION IN FROG PHOTORECEPTOR OUTER SEGMENTS.** **(V.A.Klenchin, P.D.Calvert* and M.D.Bownds*#) Laboratory of Molecular Biology, *Neuroscience Training Program and #Department of Zoology, University of Wisconsin, Madison, WI 53706.**

**Recent studies indicate that recoverin (S-modulin in the frog) can slow photoresponse recovery in a $Ca^{2+}$-dependent manner, probably via inhibition of rhodopsin phosphorylation by a $Ca^{2+}$-bound form of the protein. We studied $Ca^{2+}$-dependence of rhodopsin phosphorylation in frog rod outer segments (ROS) without recoverin added (0.27 $\mu$M endogenous S-modulin) and in the presence of 10 $\mu$M recoverin. The addition of recoverin had no influence on rhodopsin phosphorylation observed at low (< 1 $\mu$M) free $Ca^{2+}$ levels. It increased $Ca^{2+}$-dependent suppression of phosphorylation in the range of 1-100 $\mu$M $Ca^{2+}$, higher levels than previously reported and above the physiological concentrations in ROS. Finally, in the mM free $Ca^{2+}$ range the inhibition of rhodopsin phosphorylation was maximal and unaffected by exogenous recoverin. The data suggest that recoverin activity may not be a function of membrane binding and/or that other $Ca^{2+}$-dependent control of rhodopsin phosphorylation occurs in ROS. Inhibition of rhodopsin phosphorylation by $Ca^{2+}$ does not depend on the amount of rhodopsin (0.1-100%) bleached, implying $Ca^{2+}$ action on rhodopsin kinase rather the rhodopsin substrate.**

M-Pos124

**EFFECT OF ETHANOL ON RECEPTOR CONFORMATION CHANGE: PHOSPHOLIPID ACYL CHAIN UNSATURATION AUGMENTS ABILITY OF ETHANOL TO ENHANCE BOTH META II FORMATION AND ACYL CHAIN PACKING FREE VOLUME.** ((Drake C. Mitchell & Burton J. Litman*)) Dept. of Biochemistry, Univ. of Virginia H. S. C., Charlottesville, VA, 22908, and *Laboratory of Membrane Biochemistry & Biophysics, N.I.A.A.A., N.I.H., Rockville MD 20852.

We have examined the effects of ethanol on both acyl chain packing free volume and the ability of rhodopsin to undergo its activating conformation change in native disk membranes, POPC, and PDPC. Rhodopsin is a member of the super family of heptahelical G protein-activating receptors, and the meta II photointermediate corresponds to the active conformation of bleached rhodopsin which binds and activates transducin. Modulation of meta II formation by ethanol was assayed by resolving the post-bleaching spectral contributions of meta I and meta II. The effect of ethanol on acyl chain packing free volume was studied independently by deriving the fractional free volume parameter, $f_v$, through analysis of time-resolved fluorescence of the membrane probe DPH. Formation of meta II is enhanced by ethanol in disks, POPC, and PDPC. At ethanol concentrations less than 500mM this enhancement is more pronounced in disks and PDPC, which contain polyunsaturated acyl chains. Under the same conditions $f_v$ was increased in all three bilayers, with a greater increase in the systems with polyunsaturated acyl chains. (Supported by NIH grants EY00548 & 5P01GM47525).

M-Pos125

LONGITUDINAL DIFFUSION COEFFICIENT OF cGMP IN VERTEBRATE ROD OUTER SEGMENTS. ((Y. Koutalos[1], K. Nakatani[2] and K.-W. Yau[1,3])) Dept. of Neuroscience, Johns Hopkins Univ. Sch. Med.[1], Howard Hughes Med. Inst.[3], Baltimore, MD 21205, USA and Inst. of Biological Sciences, Univ. of Tsukuba[2], Tsukuba, Ibaraki 305, JAPAN.

cGMP is the intracellular transmitter that mediates phototransduction in vertebrate rods. Since photoisomerizations of rhodopsin molecules are local events, the longitudinal diffusion of cGMP should be a factor in the cell's sensitivity to light, especially in the case of excitation by a single photon. We have employed the truncated rod outer segment preparation from tiger salamander and bullfrog to measure the cGMP diffusion coefficient. The distal portion of a rod outer segment is drawn into a suction pipette and the rest of the cell is sheared off by a glass probe. In this way the cGMP-gated channels on the outer segment membrane are readily accessible to cGMP supplied through the bath. Under our experimental conditions, the bath application and removal of cGMP can be considered to be step changes in concentration at the cell's open end. When cGMP hydrolysis is inhibited by IBMX, the diffusion equation describing the diffusion of cGMP inside the truncated cell has a simple analytical solution. We have utilized this analytical solution to analyze the rise and decay kinetics of the cGMP-elicited currents. From these measurements we have obtained a diffusion coefficient of $(66\pm9)\times10^{-6}$ $cm^2$ $sec^{-1}$ for bullfrog and $(63\pm5)\times10^{-6}$ $cm^2$ $sec^{-1}$ for tiger salamander, which is 6-7 times less than the value in aqueous solution.

**M-Pos126**

**MODULATION OF CALCIUM CURRENTS IN *HERMISSENDA* PHOTORECEPTORS BY 5-HT AND GABA.** E. Yamoah* and T. Crow. Dept. Neurobiology & Anatomy, Univ. of Texas Medical School, Houston, TX 77225.

5-HT and GABA are two putative neurotransmitters known to mediate $Ca^{2+}$-dependent plasticity in *Hermissenda* photoreceptors. Recently, two voltage-activated $Ca^{2+}$ currents have been characterized in these cells (Yamoah & Crow, 1993). We examined modulatory effects of 5-HT and GABA on two voltage-activated $Ca^{2+}$-currents, (transient and sustained currents) using the whole cell version of the patch-clamp technique. Recordings were made in 10 mM bath $Ca^{2+}$ and under conditions in which $K^+$-currents were suppressed with channel blockers (TEA, EGTA, 4-AP) and $Na^+$ and $Cl^-$ currents were removed by ion substitutions (choline for $Na^+$ and acetate for $Cl^-$). 5-HT (25-50 μM) reduced (> 80%) the sustained current without having any substantial effect on the transient current (Fig. 1a). The action of 5-HT may be mediated through protein kinase C (PKC) because; (1) staurosporine, an inhibitor of PKC partially reversed 5-HT effects (2) activators of PKC (TMA & PDB) reduced the sustained current. GABA, at low concentrations, (10 nM - 20 μM) increased both the transient and sustained currents (Fig. 1b) and at high concentrations (> 50 μM), the sustained current was blocked. c-AMP enhanced the $Ca^{2+}$-currents and this effect together with the enhancement actions of GABA were removed with the PKA inhibitor, PKI(6-22)amide. This suggests that the action of GABA at low concentrations is PKA mediated. However, is unclear which second messenger mediates the action of GABA at high concentrations.

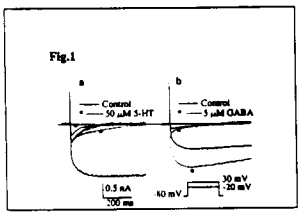


## HORMONE-RECEPTOR COUPLING

**M-Pos127**

**INSULIN BINDING AND ACTIVATION OF THE INSULIN RECEPTOR AS CHARACTERIZED BY FLUORESCENCE SPECTROSCOPY.** ((S. Scarlata[1], J. Lee[2], P. Pilch[2] & S. Shoelson[3]) [1]Dept. of Physiol.& Biophys., SUNY Stony Brook, Stony Brook, NY 11794-8661, [2]Dept. of Biochem., Boston Univ., Boston MA, 02118, [3]Joslin Diab.Cntr., Harvard Med. School, Boston, MA 02215

The insulin receptor is an transmembrane tyrosine kinase that plays a key role in cell differentiation, growth and metabolism. In the absence of insulin, kinase activity is inhibited. The binding of insulin to the extracellular domain of the receptor promotes phosphorylation of intracellular tyrosines and subsequent activation of the intracellular kinase. The conformational pathways that result upon ligand binding and lead to activation are not understood. To this end, we have characterized the time course of conformational changes in the receptor using fluorescence spectroscopy. When monitored at $\lambda_{ex}$=280nm, binding of insulin to a purified detergent solution of receptor results in a time-dependent increase in fluorescence anisotropy that appears to be complete after 40'. This increase is accompanied by a small blue shift in spectral mass and a small decrease in intensity. Alternately, the binding of a fluorescent-insulin (A1-EDANS-insulin) occurs at very short times (< 1'). Thus, these slower process must represent backbone movements of the protein. Activation of the kinase by the addition of ATP and metal also produced a time-dependent increase in intrinsic anisotropy with a midpoint of ~2min indicating that the major conformational changes that produce kinase activation occur within this time. Energy transfer between two probes on a doubly-labelled insulin indicate that the conformation of the ligand remains unchanged upon binding.

**M-Pos128**

**PRELIMINARY SPECTROPHOTOMETRIC ANALYSIS OF NORMAL AND SICKLE ERYTHROCYTES TREATED WITH NX069999 USING FURA2-AM.** ((S.O. Fadulu[1] and D.E. Houston-Hawkins[2])) [1]Texas Southern University, Houston, TX 77004 and [2]Purdue University, West Lafayette, IN 47906.

Peripheral blood erythrocytes from normal persons and sickle cell sufferers were analyzed, using the esterized form of the fluorescent dye Fura2 (Fura2-AM), to measure free calcium ionic concentration after treatment with the antisickling agent NX06999. Baselines were obtained from both washed sickled and washed normal erythrocytes after 45 min treatment with Fura2-AM at 37°C. The treated samples were stimulated with a range of wavelengths between and including 300nm and 450nm of laser generated light using a SLM 8000 fluorimeter. The highest light intensity is emitted from a calcium-bound, Fura2 treated sample when it is excited with 340nm of light, while the lowest light intensity is emitted when stimulated with 380nm of light. A ratio using the intensity values at these two points, 340nm/380nm, can be compared with the same values obtained from calibration buffers of known calcium concentrations. Our preliminary findings suggest that there is a highly significant increase in the internal free calcium ion when samples were measured in a calcium free buffer after the addition of NX06999. *Supported by Howard Hughes Medical Institute.*

**M-Pos129**

**APPEARANCE OF WENCKEBACH-LIKE RHYTHMS, DEVIL'S STAIRCASE, BURSTING, AND CHAOS IN INTRACELLULAR $Ca^{2+}$ SPIKES IN NON-EXCITABLE CELL MODELS**

((Teresa Ree Chay* and Young Seek Lee**)) Department of Biological Sciences, University of Pittsburgh, Pittsburgh, Pennsylvania 15260* and Department of Biochemistry, Hanyang University, Ansan, Kung-gi-do, 425-791, Korea**

We show in this paper that complex patterns of intracellular calcium concentration, $[Ca^{2+}]_i$, arise in non-excitable cell models, when driven repetitively by the application of agonists that activate the phospholinositide-signalling pathway. Such patterns include phase-locked Wenckebach-like rhythms, bursting, and even chaos. These patterns are similar to action potential responses observed in excitable cells when driven periodically by external current stimuli. A model used in this study is based on the receptor-operated model,[1] which is formulated under the assumptions that phospholipase C is a GTPase activating protein and a build-up of the GTP-bound α-subunit is a slow dynamic variable responsible for the refractory period. We have also considered a $Ca^{2+}$-operated calcium channel model,[2] which contains a fast activating d-gate and a slowly inactivating f-gate. In this model, the f-gate is responsible for the refractory period. Unlike the d- and f-gates of the action potential model,[3] these gates depend on $[Ca^{2+}]_i$. With these models we have constructed a Devil's staircase using a two-pulse protocol. We then showed that the rules governing this staircase are indeed universal even in agonist phase-locking systems. This work thus provides a theoretical explanation for the appearance of blocked and delayed responses of $[Ca^{2+}]_i$ spikes in response to pulsed agonists and demonstrates the existence of universality in such phase-locking systems.

1. KRS Cuthbertson and T. Chay, Cell Calcium,12: 97-108 (1991).
2. TR Chay, *In*: Patterns, Information and Chaos in Neuronal Systems, edited by B. J. West. World Scientific Publishing. River Edge, New Jersey. pp 73-122 (1993).
3. TR Chay and YS Lee, J. Theor. Biol. 155, 137-171 (1992).

**M-Pos130**

**KINETICS OF CA RELEASE FROM STORES BY INSP3 IN SINGLE GUINEA PIG HEPATOCYTES.** David Ogden & Thierry Capiod. N.I.M.R., Mill Hill, London NW7 1AA U.K. & INSERM U274, 91405 Orsay, France.

The activation of Ca release channels by InsP3 has kinetic features important in the hormonal regulation of cytosolic free [Ca]. Concentration and timecourse of free [Ca] were monitored with the fluorescent low Ca affinity dye furaptra following a pulse of InsP3 released from 'caged' InsP3 in the cytosol by flash photolysis. Dye and 'caged' InsP3 were introduced during whole cell patch clamp recording of membrane Ca-activated K conductance. Rate of rise of [Ca] was measured to monitor the Ca efflux into the cytosol. InsP3 concentrations of 0.4μM or higher produced an increase of free [Ca], with maximal activation at 5μM. At low InsP3 concentration (0.6μM) there was a delay of 300ms and free [Ca] rose to a peak (averaged over the cell) of 1.2μM with rate of rise 0.8μM/s. At high concentration (>5μM) there was no delay and free [Ca] rose to 14μM at 8μM/s (means, range 5-30μM and 3-19μM/s). Rates of rise of [Ca] of 1-2μM/s observed during the initial phase of Ca mobilisation by norepinephrine indicate that Ca efflux from stores during hormone action is similar to that evoked by 0.5-1μM InsP3.

The onset of InsP3 insensitivity that follows elevation of cytosolic [Ca] was investigated with a two pulse protocol of varied separations >600ms. Inhibition was complete at 600 ms at high submaximal InsP3 concentrations and was partially established within this time at low InsP3 concentrations. Two unusual features were noted: (1) the response to a second pulse (judged by the rate of rise) within 1s of the first was suppressed completely even though a high level of Ca efflux remained from the first pulse; and (2) the integral of free [Ca] was much larger (mainly due to prolongation) following closely spaced twin pulses even though the second pulse of InsP3 had no additional effect on Ca efflux into the cytosol.

**M-Pos131**

REGULATION OF ENDOTHELIAL CELL $Ca^{2+}$ INFLUX BY CYTOCHROME P450 MECHANISMS ((W.F. Graier and M. Sturek)) Vascular Cell Biophysics Laboratory, Dalton Cardiovascular Research Center and Department of Physiology, Univ. of Missouri, Columbia, MO 65211. (Spon.: H.-D. Kim)

Second messenger regulation of $Ca^{2+}$ influx via ligand-gated channels in vascular endothelial cells is unclear. We tested the hypothesis that agonists (histamine, bradykinin) or direct depletion of intracellular $Ca^{2+}$ stores in human umbilical vein and bovine coronary artery cells stimulate $Ca^{2+}$ influx via P450-dependent pathways. $Ca^{2+}$ influx was determined by fura-2 microfluorometry of intracellular free $Ca^{2+}$ ($Ca_i$) and $Mn^{2+}$ quench and whole-cell patch clamp. Inhibition of P450 by 5 $\mu$M econoazole, 1 mM cyanide, 5 $\mu$M miconazole, 50 $\mu$M SKF 525A, or 10 $\mu$M methylene blue inhibited histamine-induced $Ca^{2+}$ influx from 46-95% without affecting intracellular $Ca^{2+}$ release. These P450 inhibitors also inhibited $Ca^{2+}$ influx stimulated by direct depletion of $Ca^{2+}$ stores with 1 $\mu$M thapsigargin (TG), 15 $\mu$M 2,5-di-(tert-butyl)-benzhydroquinone (BHQ), or 10 $\mu$M cyclopiazonic acid (CPA) from 78-97%, while $Ca^{2+}$ release was unchanged. Induction of P450 enzymes by 10 $\mu$M ß-naphtoflavone amplified agonist-induced $Ca^{2+}$ increases 6.7-fold, while 100 $\mu$M methyl-cholanthrene did not affect agonist-induced $Ca^{2+}$ influx. BHQ activated inward current at the $K^+$ equilibrium potential of -80 mV coincident with increased $Ca_i$. Our data support the hypothesis and suggest that ligand-gated channel activation depends on P450 enzymes that are activated by depletion of intracellular $Ca^{2+}$ stores. (WFG is a Max Kade Foundation fellow; supported by Austrian National Bank 4715, NIH HL41033, RCDA HL02872)

**M-Pos132**

REVERSAL OF ATTENUATED ISOPROTERENOL-STIMULATED cAMP LEVELS BUT NOT CONTRACTILITY IN CARDIAC MYOCYTES FROM AN ANIMAL MODEL OF ß-ADRENOCEPTOR DESENSITISATION. ((D.G. Wynne, P. O'Gara and S.E. Harding)) National Heart & Lung Institute, London, UK, SW3 6LY.

The ß-adrenoceptor (ßAR) desensitisation seen in human heart failure is thought to be related to reduced levels of cAMP. An animal model of ßAR desensitisation was produced by a 7 day infusion of norepinephrine (900µg/kg/h) into guinea-pigs using mini-osmotic pumps. Control animals were sham-operated. The contractility of isolated cardiac myocytes was measured using a video-microscopy image-analyzing system. Compared to control myocytes, those isolated from the hearts of the norepinephrine-treated guinea-pigs (NETGP) gave attenuated maximum contractile responses to isoproterenol (ISO), expressed as a % of the maximum $Ca^{2+}$ response (35.4 ± 5.7% n=7 vs 87.7 ±2 .9% n=6 in controls, $p<0.001$). This is indicative of ßAR desensitisation. Radioimmunoassay of myocyte cAMP levels (values expressed as pmol cAMP/mg protein) showed that levels in the NETGP were reduced compared to control either under basal conditions (8.6 ± 0.8 n=8 vs 22.9 ± 4.2 n=8, $p<0.02$) or after stimulation by ISO (13.4 ± 1.5 n=8 vs 31.0 ± 5.0 n=8, $p<0.01$). The depressed ßAR stimulated levels in NETGP were reversed to control levels (27.7 ± 5.3, n=8) by a threshold inotropic concentration (10µM) of the phosphodiesterase inhibitor, IBMX. The same concentration of IBMX did not significantly increase the depressed maximum contractile response to ISO. ßAR desensitisation is a result of both decreased production of cAMP and a post-production effect, since ISO-stimulated contractility remained depressed even after restoration of cAMP levels to normal values.

**M-Pos133**

REGULATION OF ATP-ACTIVATED K CHANNEL BY CYTOSOLIC ATP AND OTHER NUCLEOTIDES IN ATRIAL CELLS ((C. Fu, D. Kim)) Chicago Medical School, North Chicago, IL 60064.

Extracellular ATP, like adenosine, activates the muscarinic-gated K ($K_{ACh}$) channel via G protein in atrial cells. Earlier studies have shown that the $K_{ACh}$ channel activated by ACh or adenosine can be modulated by internal ATP presumably via phosphorylation. We examined whether the ATP-activated K channel kinetics could also be modified by internal ATP in a similar way. With ATP as the agonist, the $K_{ACh}$ channel activity was always low in cell-attached patches compared to that in inside-out patches with 100 $\mu$M GTP in the bath solution. The single channel conductance and mean open time were similar to those obtained using adenosine or ACh as the agonist (30 pS in 140 mM KCl, 0.71 ms). Internal ATP produced an irreversible increase in $K_{ACh}$ channel activity at low levels (<1 mM) and a reversible decrease at higher levels (1-4 mM; $K_{1/2}$=1.3 mM). The increase in channel activity was associated with a prolongation of channel open time duration (0.7 ms to 2.4 ms). AMPPNP (a nonhydrolyzable analogue) had no effect up to 1 mM, but mimicked the effect of ATP at higher concentrations. Other nucleotides such as CTP, ITP or UTP could also inhibit the $K_{ACh}$ channel activity but only after the patch had been exposed to ATP. These effects of nucleotides on the $K_{ACh}$ channel function were different from those observed with adenosine as the agonist. Thus, the membrane components involved in the signal transduction pathways by which the $K_{ACh}$ channels are activated by ATP and adenosine may be different.

**M-Pos134**

CALCIUM-MOBILIZING AGONISTS STIMULATE CHLORIDE CHANNELS IN VASCULAR SMOOTH MUSCLE CELLS. ((C.R. White, T.S. Elton and R.L. Shoemaker)) University of Alabama at Birmingham, Birmingham, AL 35294.

Radioisotope flux measurements and electrophysiological techniques were used to characterize calcium-sensitive chloride currents in rat aortic vascular smooth muscle cells (VSMCs). Transmembrane $^{125}$iodine ($^{125}$I) efflux from cultured VSMCs was used as an indicator of $Cl^-$ movements to study the relationship between intracellular calcium concentration ($[Ca^{2+}]_i$) and $Cl^-$ channel activity. The $Ca^{2+}$-mobilizing agonists, adenosine 5'-triphosphate (ATP/$10^{-4}$ M) and angiotensin II (Ang II/$10^{-7}$ M), and the $Ca^{2+}$ ionophore ionomycin (5 $\mu$M) stimulated rapid, transient increases in $^{125}$I efflux rates. In VSMCs pre-treated with 1,2-bis(o-aminophenoxy)ethane-N,N,N',N'-tetraacetic acid (BAPTA:20 $\mu$M, 20 min), a membrane-permeable $Ca^{2+}$ chelator, Ang II- and ATP-mediated increases in $^{125}$I efflux and fura 2-sensitive $[Ca^{2+}]_i$ were blocked. When external EGTA was used to blunt agonist-stimulated $Ca^{2+}$ influx, $^{125}$I efflux was still increased in response to Ang II and ATP. Using standard patch clamp techniques, single $Cl^-$ channels were characterized in excised patches and intact VSMCs. In inside/out patches, we identified a $Cl^-$ conductance which demonstrated anion selectivity ($P_I > P_{Br} > P_{Cl}$) and $Ca^{2+}$ sensitivity since channel openings occurred more frequently as the bath $Ca^{2+}$ concentration was raised from 0 to 100 nM. In cell-attached patches, Ang II and ATP stimulated outward $Cl^-$ currents which had a similar time of onset as agonist-stimulated $^{125}$I efflux. These data suggest that the activation of $Cl^-$ channels facilitates VSMC membrane depolarization and may therefore play an important role in the regulation of vascular tone.

**M-Pos135**

**ATP-, GTP- AND PHOSPHOLIPID-DEPENDENT MODULATION OF Ca-ACTIVATED CHLORIDE CURRENT ($I_{Cl,Ca}$) IN GIANT MEMBRANE PATCHES FROM XENOPUS OOCYTES.** ((V. Golubev, J.P. Foley and D.W. Hilgemann)) Dept. of Physiology, UTSW Med. Ctr., Dallas, TX, 75235.

Modulation of $I_{Cl,Ca}$ was studied in inside-out giant membrane patches (~10pF) from Xenopus oocytes. The $I_{Cl,Ca}$ was generally recorded as an outward current: 25 mM $Cl_e$, 1 mM $Cl_i$, 0 mV, 2 $\mu$M $Ca_i^{2+}$ with 10 mM EGTA at 31°C. The $K_{1/2}$ for free $Ca_i^{2+}$ ranged from 2 to 10 $\mu$M with a Hill slope of 2 to 7. The following nucleotides all enhanced outward $I_{Cl,Ca}$ by a factor of about 4 with a $t_{1/2}$ of about 30 s (~half-maximal concentration in mM): GTPγS (0.1); UTP (0.1); ATP (0.3); GTP (0.3); and AMP-PNP (0.5). Reversal of the stimulation, after removal of nucleotides, was typically much faster than onset of the effect. ATP increased the Hill slope of the $Ca_i^{2+}$ dependence and increased the maximum current. The reversal of the effect of ATP was slowed by reversing Cl gradients. p-nitrophenol-phosphate (5) and NaF (1.0) mimicked closely the nucleotide effects. ADP(2.0) and ATPγS(0.2) blocked stimulation by ATP when applied before ATP; they also blocked *reversal* of the stimulatory effect when applied *after* ATP. Cytoplasmic application of phosphatidylserine (PS) vesicles stimulated $I_{Cl,Ca}$ to a similar extent as nucleotides over 1 min. The effect of PS was non-additive to that of ATP, and it reversed over ~3 min after PS removal. PC and PE did not stimulate $I_{Cl,Ca}$, while application of 1:1 PI:PC vesicles 'freezes' the nucleotide effects, similar to effects of ADP.

**M-Pos136**

MODULATION OF $CA^{2+}$ CHANNELS BY PTX-SENSITIVE G PROTEINS IS BLOCKED BY N-ETHYLMALEIMIDE IN RAT SYMPATHETIC NEURONS. ((M.S. Shapiro, L.P. Wollmuth and B. Hille)) Dept. Physiol/Biophys., Univ. of Washington, Seattle, WA 98195.

We studied inhibition of N-type $Ca^{2+}$ channels in acutely dissociated rat superior cervical ganglion (SCG) cells using the whole-cell patch clamp. Inhibition of $I_{Ca}$ by G proteins in the SCG uses at least three separable pathways: one pertussis toxin (PTX)-sensitive and voltage-dependent and two PTX-insensitive. N-ethylmaleimide (NEM) treatment (50 µM for 2 min) wholly abolished PTX-sensitive, and slightly reduced PTX-insensitive, inhibition by several transmitters. Suppression of $I_{Ca}$ by 250 nM somatostatin is all PTX-sensitive, and was reduced by NEM from 54 ± 3% to 6 ± 1% (n=11). Inhibition by 10 µM norepinephrine (NE) is *ca.* half PTX-sensitive, and was reduced by NEM from 54 ± 3% to 24 ± 2% (n=11). For cells cultured overnight with 500 ng/ml PTX, NEM did not further reduce NE inhibition. A muscarinic agonist, oxotremorine-M (oxo-M), suppresses $I_{Ca}$ both via a PTX-sensitive, voltage-dependent pathway and a PTX-insensitive, voltage-independent pathway that uses a cytoplasmic second-messenger. For PTX-treated cells, inhibition by 10 µM oxo-M was reduced by NEM from 55 ± 4% (n=8) to 38 ± 4% (n=10) and was still wholly voltage-independent. Inhibition by 500 nM pancreatic polypeptide (PP) is *ca.* one-third PTX-sensitive and was reduced by NEM from 42 ± 4% to 22 ± 2% (n=13). After PTX or NEM treatments, PP inhibition was all voltage-independent. Inhibition by substance P is all PTX-insensitive and was only slightly affected by NEM, from 27 ± 5% to 22 ± 4% (n=24). Thus, NEM inactivates PTX-sensitive G proteins, and partly impedes the second-messenger utilizing, PTX-insensitive pathway in the SCG. *Supported by NS08174, NS07097, and the McKnight and W.M. Keck Foundations.*

**M-Pos137**

ANGIOTENSIN II REGULATES THE SARCOLEMMAL $Na^+$-$K^+$ PUMP IN RABBIT HEART VIA PROTEIN KINASE C.
((Livia C.Hool & Helge H. Rasmussen)) Department of Cardiology, Royal North Shore Hospital, Sydney, Australia.

We have reported that 8 days' treatment of rabbits with an angiotensin converting enzyme inhibitor, captopril (Cap), increases $Na^+$-$K^+$ pump current ($I_p$) of right ventricular myocytes. Since Cap reduces angiotensin II (AII) levels, we hypothesized that its effect on $I_p$ is mediated via AII. To test this we treated rabbits with the AII antagonist Losartan for 8 days. Cells were isolated and $I_p$ measured using patch-pipettes containing 10 mM $Na^+$. $I_p$ (mean±SE,pA/pF) of cells from Losartan treated rabbits was larger than $I_p$ of cells from control animals (0.51±0.04, n=16 v 0.32±0.03, n=9, $p<0.005$), but similar to $I_p$ from Cap treated animals (0.56±0.04, n=10). We also incubated cells from Cap treated animals with 10 nM AII for 60 min. $I_p$ (0.32±0.03, n=7) was similar to $I_p$ of cells from untreated animals (0.32±0.03, n=9). Since AII activates protein kinase C (PKC), we examined if the effect of AII is mediated via PKC. Cells from Cap treated animals were preincubated with 20 nM staurosporine for 20 min before exposure to AII. $I_p$ was similar to the $I_p$ of cells from Cap treated animals not exposed to staurosporine or AII (0.51±0.01, n=6 v 0.56±0.04, n=10, NS). This suggests that AII reduces pump activity by activating PKC. To further support this, we incubated cells from Cap treated animals with 160 nM phorbol,12-myristate,13-acetate (PMA) for 60 min. $I_p$ was reduced compared to the $I_p$ of cells from Cap treated animals not exposed to PMA (0.39±0.03, n=5 v 0.56±0.04, n=10, $p<0.005$). The *in vivo* effect of Cap to increase $I_p$ may be due to a decrease in the "background" AII levels. AII appears to decrease pump activity by activation of PKC.

**M-Pos138**

**INACTIVATION AND REACTIVATION PROPERTIES OF AN ATRIAL G PROTEIN-GATED $K^+$ CHANNEL, KGA, EXPRESSED IN *XENOPUS* OOCYTES.**
**((C. A. Doupnik, N. F. Lim, W. Schreibmayer, N. Dascal, N. Davidson, and H. A. Lester)), Division of Biology, Caltech, Pasadena, CA 91125.**

The voltage- and time-dependent properties of a cloned G protein-activated inward rectifier $K^+$ channel (KGA) from rat atrium were studied in voltage clamped *Xenopus* oocytes co-expressing human muscarinic m2 receptors. Inward $K^+$ currents carried by 98 mM external $K^+$ were recorded at a holding potential of -80 mV. Acetylcholine (ACh)-evoked $K^+$ currents ($I_{K,ACh}$) were obtained by subtracting "resting" currents from currents elicited by 1 μM ACh. $I_{K,ACh}$ amplitudes changed in an instantaneous manner during jumps to voltages (V1) ranging from -120 to +60 mV. $I_{K,ACh}$ exhibited strong inward rectification reversing at the predicted $E_K$ of 0 mV. When the voltage was repolarized to -80 mV (V2), the time course for $I_{K,ACh}$ reactivation consisted of 3 distinct components whose amplitudes, but not rates, depended on V1. $I_{K,ACh}$ reactivation consisted of an instantaneous current ($I_i$), a component with $\tau_f$ = 30-40 ms, and a component with $\tau_s$ = 200-400 ms. Varying V2 from -10 to -120 mV revealed that both $\tau_f$ and $\tau_s$ decreased 2-4 fold at depolarized levels of V2. The fractional instantaneous current ($I_i/I_{K,ACh}$) decreased with depolarizing V1 and was well described by a Boltzmann relation having a $V_{1/2}$ at -21 mV and a limiting charge valence of 1.6 $e^-$. $I_i$ was also dependent on V1 duration, decreasing with longer times at V1. Examination of $I_{K,ACh}$ during V1 at the $V_{1/2}$ for inactivation, revealed a current decay similar to the time dependence of $I_i$. These results suggest that KGA inactivates in a time- and voltage-dependent manner reminiscent of several voltage-gated channels. The molecular mechanisms underlying KGA inactivation are currently being investigated. Support: NIH, NIMH, Israel-US BSF, NRSA, Austrian Res. Found.

**M-Pos139**

THE ATRIAL G PROTEIN-GATED K CHANNEL, KGA, CAN BE ACTIVATED VIA β2AR IN *XENOPUS* OOCYTES.
((N.F. Lim*, N. Dascal#, W. Schreibmayer+, N. Davidson*, & H.A. Lester*)) *Div. of Biol., Caltech, Pasadena, CA, 91125; #School of Med., Tel Aviv U., Ramat Aviv 69978, Israel; +Inst. Med. Phys. & Biophys., U. Graz, A-8010 Graz, Austria.

The inward rectifying K channel of atrial cells, KGA, is activated following acetylcholine (ACh) binding to m2 receptors. A similar K channel in brain is regulated by serotonin (5HT) 1A, opioid, somatostatin, and several other 7-helix receptors. These receptors are thought to couple to the K channel by G proteins of the Gi or Go family, since channel activation is inhibited by pertussis toxin. We have previously shown that KGA can be expressed in *Xenopus* oocytes, and that inward currents (200 nA to 3 μA at -80 mV in 96 mM external $K^+$) can be activated via coexpressed 5HT1A, δ opioid, and m2 receptors. As expected, when KGA and the β2 adrenergic receptor (β2AR, which couples to Gs) were coexpressed in oocytes, addition of 0.02-1 μM isoproterenol (iso) produced only weak activation of KGA (0-90 nA at -80 mV; n = 24). Surprisingly, iso-activated currents were increased 10- to 20-fold when Gαs mRNA was coinjected with KGA and β2AR mRNA. Like the current evoked by ACh, opioids, or 5HT, the iso-activated current in Gαs coexpressing oocytes is inwardly rectifying and blocked by 200 μM $Ba^{+2}$. However, the kinetics of KGA activation and deactivation are 2- to 3-fold slower for iso than for ACh, suggesting differences in mechanism of KGA regulation by the different receptors. Elevation of cAMP or protein kinase A activity does not activate KGA since application of forskolin, IBMX and dibutyryl-cAMP does not mimic the iso response. We are investigating whether βγ subunits also released by β2AR stimulation may be responsible for KGA activation by isoproterenol.
Support: Israel-US BSF, NIH, NIMH, NRSA, Austrian Research Found.

**M-Pos140**

PARTIAL AGONIST-MEDIATED ACTIVATION OF MUSCARINIC $K^+$ CURRENT.
((T.T. Ivanova, L.Y. Hamosh and G.E. Breitwieser)) Johns Hopkins Univ. School of Med., Dept. of Physiology, Baltimore, MD 21205.

The ability of different muscarinic cholinergic agonists to activate the G protein-coupled inwardly rectifying $K^+$ current, IK[ACh], was investigated by whole cell patch clamp techniques applied to atrial myocytes from the bullfrog *Rana catesbeiana*. The full agonists acetylcholine (ACh), carbachol, and oxotremorine-M (oxo-M) induced whole cell currents of comparable magnitudes when applied at concentrations which saturated muscarinic receptors (assessed by displacement of [$^3$H]NMeQNB binding in isolated bullfrog cardiac membranes). In contrast, saturating concentrations of two partial agonists, McN-A-343 and oxotremorine-5 (oxo-5), were unable to activate appreciable IK[ACh] under comparable conditions. McN-A-343 and oxo-5 were, however, able to partially inhibit the stimulatory effect of isoproterenol on $Ca^{2+}$ current in atrial myocytes. The inability of these agonists to activate IK[ACh] is not due to activation of distinct populations of muscarinic receptors, since McN-A-343 was able to prevent activation of maximal IK[ACh] by saturating concentrations of ACh, suggesting competition for a common population of sites. Full agonists increased the GTPγS-mediated rate of IK[ACh] activation as a function of receptor occupancy, while McN-A-343 and oxo-5 at saturating concentrations only increased the activation rate 9 and 20-fold, respectively, suggesting that partial agonists are unable to activate whole cell IK[ACh] in GTP because of decreased "efficiency" or rate of muscarinic receptor-mediated G protein activation. NIH HL41972 and AHA EI.

**M-Pos141**

MODELING AND TESTING TRANSMEMBRANE HELIX CONTACTS IN G-PROTEIN COUPLED RECEPTORS
((J. A. Ballesteros and H. Weinstein)) Dept. Physiol./Biophys., Mt. Sinai Sch. Med., NY, NY 10029 (Spon. M. Glucksman).

A key issue in the process of modeling the structure of G-protein coupled receptors (GPCRs) is the prediction and testing of helix-helix packing interactions. The hypothesis that amino acid (AA) sites whose substitution pattern during evolution is coordinated are in spatial proximity, was proposed and tested for soluble proteins (D. Altschuh et al., J. Mol. Biol. 193: 693, 1987). Coordinated sites were identified by concomitant changes of the AA identity over a sequence alignment of homologous proteins. To use this hypothesis in modeling the structures of GPCRs we have introduced correlation coefficients to identify such sites and to quantify the degree of coordination. The correlation is based on the AA identity (e.g. Ile-to-Tyr) or on AA properties, such as volume, that could be evolutionary conserved in a correlated manner. The proposed residue interactions should define continuous helix-helix interfaces consistent with α-helical periodicity. The methodology is tested on the TMH packing found in the Photosynthetic Reaction Center crystal structure, and applied to modeling the helix packing in GPCRs. To enable experimental tests of the resulting models, we have selected those coordinated AA sites that are putative double revertant mutants, as defined by: (1) AA sites that show a complementary substitution pattern of structural determinants such as volume, charge, etc.; (2) Single mutations must cause a significant alteration of the receptor structure, measurable as functional disruption; and (3) The second (coordinated) mutation rescues receptor function. Two such sites were predicted and successfully tested in the Gonadotropin-Releasing Hormone Receptor (Wei et al., Mol. Pharmacol., in press). *Supported by grants from the NIH: DA-06620 and DA-00060, and by a Fulbright/MEC (Spain) (JAB).*

**M-Pos142**

MODELING G-PROTEIN RECEPTOR RECOGNITION: THE STRUCTURE OF INTRACELLULAR LOOPS.
((K. Haydock and H. Weinstein)) Department of Physiology and Biophysics, Mount Sinai School of Medicine NY, NY 10029 (Spon. W.A. Brodsky)

Signal transduction through G-protein coupled receptors (GPCRs) is thought to entail an interaction with the G-proteins (GPs) through the intracellular loops that link the putative seven transmembrane helices of receptors. To explore these interactions and the mechanisms of signal transduction, we have made a comparative analysis of the intracellular loops of GPCRs that interact with various GPs. A combination of multiple sequence alignment, secondary structure prediction, and homology modeling approaches was used in conjunction with results from site-specific mutagenesis and synthetic peptide construction experiments. For each class of GPCR that binds to a given GP type we have thus identified particular residues and structural elements that may be important in their interaction. Regions that are considered not to be involved in such interactions because they lack homology with other receptors in their class have also been identified. Models of possible loop structures resulting from these studies are being constructed, consistent with the available data. These models suggest specific experiments to verify and refine the structures of the GPCR and to simulate their functions. Supported by an Aaron Diamond Fellowship (KH) and NIH grants DA-06620 and DA-00060.

M-Pos143

**CHARACTERIZATION OF THE AGONIST-INDUCED CALCIUM MOBILIZATION IN TRANSFECTED CHO CELLS EXPRESSING THE RAT NEUROTENSIN RECEPTOR.** ((E. Hermans, Ph. Gailly, J.N. Octave, J.M. Maloteaux and J.M. Gillis)) Catholic University of Louvain, Medical School, Brussels, Belgium.

CHO cells were stably transfected with the cDNA sequence encoding for the rat neurotensin receptor (NTR). The Scatchard analysis of the specific binding of [$^3$H]neurotensin indicated a Kd value of 0.24 nM and a $B_{max}$ of 1570 fmol/mg protein. NTRs were functionally coupled to the activation of phospholipase C through a GTP-binding protein. Stimulation of the receptor by its agonist produced an important increase of the intracellular calcium concentration ($[Ca^{2+}]_i$) followed by a long sustained plateau. Return of $[Ca^{2+}]_i$ to its basal level was rapidly obtained by the addition of an excess of antagonist. In presence of external EGTA or Lanthanum, the sustained phase was abolished, suggesting the involvement of an influx of external calcium following the depletion of the calcium stores. Successive stimulations produced similar calcium responses. This emphasized a lack of rapid desensitization of the receptor. In contrast, after stimulation, receptor-ligand complexes were specifically internalized. Our observations thus indicate that receptor desensitization and internalization might constitute independent processes.

M-Pos144

**MUTATIONAL ANALYSIS SUGGESTS DIRECT INTERACTION OF GnRH ARGININE RESIDUE WITH GLUTAMIC ACID IN THE GnRH RECEPTOR**

((C.A. Flanagan, I.I. Becker, J.S. Davidson, I.K. Wakefield, W. Zhou, S.C. Sealfon and R.P. Millar)) M.R.C. Regulatory Peptides Research Unit, University of Cape Town Medical School, Observatory, 7925 South Africa, Fishberg Research Center in Neurobiology and Department of Neurology, Mount Sinai School of Medicine, New York, NY 10029. (spon. by D. McIntosh)

Gonadotropin releasing hormone (GnRH) is a decapeptide which regulates reproduction. GnRH analogues containing Gln or Glu instead of Arg in position 8 have reduced affinity for the GnRH receptor and higher doses are required to stimulate biological responses. This suggested interaction of $Arg^8$ with an acid residue in the receptor. We mutated acid residues in the transmembrane and extracellular domains of the mouse GnRH receptor to their equivalent amides. One mutant receptor showed reduced affinity for GnRH, but not for [$Gln^8$]-GnRH and did not discriminate position 8-substituted GnRH analogues. It did however discriminate high affinity GnRH analogues with substitutions in positions 5,6,7 and 10. The mutant receptor supported GnRH-stimulated inositol phosphate production with a higher $ED_{50}$ for GnRH commensurate with its reduced affinity.

These data suggest that a specific Glu in the GnRH receptor confers selectivity for analogues of GnRH containing $Arg^8$ and may reflect a direct interaction between the two side chains.

M-Pos145

EXCITATORY RESPONSES INDUCED BY LOW CONCENTRATIONS OF OPIOID AGONISTS IN DRG NEURONS. ((P. Koplas and G.S. Oxford)) Curriculum in Neurobiology, University of North Carolina, Chapel Hill, NC 27599.

Opioid regulation of electrical activity in sensory neurons is quite complex and involves both excitatory and inhibitory effects on neurotransmitter release and ionic currents. Recent studies in the lab have focused on characterization of excitatory opiate responses which have been observed in other labs with lower agonist concentrations (Crain & Shen, *Trends Pharmacol. Sci.* 11:77, 1990; Suarez-Roca et al., *Brain Res.* 579:187, 1992). The patch clamp technique was used to record various opioid responses in cultured neonatal rat dorsal root ganglion (DRG) neurons. In a subset of the population, low concentrations of morphine (30nM) increased neuronal excitability. Specifically, spontaneous action potentials and decreased thresholds for spike initiation were observed in the responsive DRG. Morphine at 30nM also reversibly decreased voltage-activated potassium currents in a subset of the neurons, which suggests one possible mechanism for the excitatory modulation. Experiments utilizing agonists for specific opioid receptor subtypes have also been performed. These experiments should provide additional information regarding the regulation of ionic currents and the specific molecular mechanisms involved. Further characterization of opioid modulation in sensory neurons is critical for increasing the effectiveness of clinical treatments of pain. (Supported by NIH grant NS18788).

M-Pos146

ROTATIONAL DYNAMICS OF RECEPTOR-BOUND EGF MEASURED BY TIME-RESOLVED FLUORESCENCE, PHOSPHORESCENCE AND ST-EPR. ((R.A. Stein, E.J. Hustedt, D.L. Rousseau, Jr., J.V. Staros, J.M. Beechem, and A.H. Beth)) Dept. of Mol. Biol. and Dept. of Mol. Physiol. and Biophys., Vanderbilt University, Nashville, TN 37235.

The rotational dynamics of the EGF receptor in membrane preparations has been previously investigated using time-resolved phosphorescence (Zidovetzki, *et al.*, 1986) and ST-EPR (Rousseau *et al.*, 1993) without agreement in the values of the rotational correlation time for receptor-bound EGF. We have employed both of these techniques and have added the sub-microsecond time domain obtainable with time-resolved fluorescence. All experiments were carried out with spectroscopic probes attached to the N-terminus of EGF. The time-resolved phosphorescence anisotropy of erythrosin-EGF bound to the receptor was essentially flat from 8-500 microseconds indicating that there was no motion of the occupied receptor on this time-scale, in contrast to previous results. The non-zero residual anisotropy does suggest a restriction of motion of the receptor. Previous ST-EPR experiments carried out at 50 kHz with an $^{15}N$,$^2H$ spin-label conjugated to EGF indicated a correlation time in the 1 microsecond time-domain assuming a uniaxial model, which has been confirmed by measuring the ST-EPR at 100 kHz. We have also carried out time-resolved fluorescence anisotropy experiments of pyrene-EGF bound to the receptor. The anisotropy in these experiments indicate a correlation time in the range of 0.5-1 microsecond. Together these data suggest that the correlation time of the receptor-bound EGF is on the order of 1 microsecond. (Supported by grants from the NIH: P01 CA43720, T32 CA09582, T32 DK07186)

M-Pos147

MEASUREMENT OF THE KINETICS OF PDGF RECEPTOR AGGREGATION USING ICS.
((P. W. Wiseman and N. O. Petersen)) Department of Chemistry, U.W.O., London, Ont. Canada, N6A 5B7. ((P. L. Höddelius and K. E. Magnusson)) Department of Medical Microbiology, Faculty of Health Sciences, University of Linköping, Linköping, Sweden. (Spon. A. C. Groom)

Aggregation of receptor proteins in biological membranes has been implicated in signal transduction across the bilayer. Elucidation of the kinetics of receptor aggregation is integral to the understanding of the whole process of signal transduction. Image correlation spectroscopy (ICS) is a new fluorescence scanning confocal microscopy based technique which provides quantitative information on membrane receptor aggregation. Measurements of the underlying distribution of platelet derived growth factor receptors (PDGFR-β2) on AG 1523 human foreskin fibroblasts were carried out using ICS. ICS was also used to characterize the temporal dynamics of the aggregation of PDGF β receptors in these fibroblasts as induced by monoclonal antibodies, and after stimulation with PDGF BB. Preliminary results indicate a factor of two decrease in the number of detected clusters following PDGF stimulation, which could possibly be consistent with a dimerization event.

M-Pos148

**STOICHIOMETRY OF BASIC FIBROBLAST GROWTH FACTOR BINDING TO HEPARIN MEASURED BY S.E.C. WITH LIGHT SCATTERING DETECTION.** ((T. Arakawa, J. Wen and J. S. Philo)) Amgen Inc., Amgen Center, Thousand Oaks, CA 91320

Fibroblast growth factors bind strongly to heparin or heparan sulfate. This binding stabilizes the protein and also appears to be required for receptor activation. We have studied the interactions of basic FGF (bFGF) with heparin using size-exclusion chromatography with on-line light scattering, absorbance, and refractive index detection. Combining data from the three detectors allows us to measure the molecular weight of the protein component of the complex, and therefore to determine the binding stoichiometry. A series of samples were prepared with constant bFGF concentration and varying amounts of low molecular weight (~5000) heparin (LMWH). At bFGF to LMWH molar ratios above 1.5, a mix of complexes containing 3, 2, or 1 bFGF molecules bound to single LMWH molecules is observed, with an average of 2.2 bFGF molecules per complex. Similar experiments with high molecular weight (~15000) heparin show an average of 6.3 bFGFs bound per heparin. Both types of heparin give a heparin mass of ~2300 Da per bFGF binding site, corresponding to an octasaccharide. This indicates that bFGF molecules are so closely packed that the density of binding may only be limited by steric hindrance. The implications of these results for the specificity of bFGF binding and for receptor activation will be discussed.

**M-Pos149**

SIMULTANEOUS DETECTION OF SUPEROXIDE PRODUCTION AND CHANGES IN MEMBRANE POTENTIAL IN HUMAN MONOCYTE-DERIVED MACROPHAGES DURING PHAGOCYTOSIS. K.O. Holevinsky and D.J. Nelson, University of Chicago, Chicago, IL

We report the simultaneous monitoring of respiratory burst activity and changes in membrane potential in human monocytes during phagocytosis in an attempt to correlate these two events at the single cell level. Respiratory burst was monitored photometrically through detection of superoxide ($O_2^-$) using $F_c$-Oxyburst, an immune complex coupled to dichlorodihydro-fluorescein (DCFH). Whole-cell voltage clamp experiments were carried out in physiological solutions during phagocytosis of the labelled immune complexes. An increase in fluorescence, which represented an increase in $O_2^-$ production, was observed concommitantly with a membrane depolarization of approximately 60 mV and the generation of a large non-selective current. The lag time preceding the onset of the response appeared to be correlated with the length of time cells were maintained in culture, with older cells displaying a slower response time. In the absence of stimulus, cells exhibited stable whole-cell currents and no change in fluorescence. A decrease in the fluorescence response was seen in cells pre-incubated in 5μM cytochalasin B, an inhibitor of phagosome formation. In the absence of phagocytosis, the exposure of macrophages to $O_2^-$ generated by a xanthine-xanthine oxidase reaction activated a non-selective current similar to that seen after stimulation with $F_c$-Oxyburst. This current was blockable by 1mM $LaCl_3$ and therefore does not appear to be due to membrane destruction mediated by reactive oxygen products. These results suggest that the current generated during respiratory burst may be activated by $O_2^-$. Supported by RO1 GM36823.

**M-Pos150**

A CHEMILUMINESCENT SUPEROXIDE PROBE, 2-METHYL-6-[p-METHOXYPHENYL]-3,7-DIHYDROIMIDAZO-[1,2a]PYRAZIN-3-ONE (MCLA), REVEALS THE TIME COURSE OF SUPEROXIDE PRODUCTION AT FERTILIZATION IN SEA URCHIN EGGS. ((C. A. O'Grady and E. B. Ridgway)) Department of Physiology, Medical College of Virginia, VCU, Richmond, VA 23298.

De-jellied sea urchin (*S. purpuratus*) eggs incubated in sea water at 14°C show a slow, weak, natural luminescence (detected by photon counting) following fertilization with diluted sperm. In the presence of 0.3 μg/ml extracellular MCLA (a superoxide probe based on a modified *Cypridina* luciferin; courtesy of O. Shimomura, Woods Hole) fertilization leads to a much larger chemiluminescent signal with a more rapid time course (peaking 3-4 minutes post fertilization). The MCLA signal presumably reflects superoxide production. Inhibition of the endogenous ovoperoxidase by 1 mM extracellular 3-amino-1, 2, 4-triazole (ATA) heightens baseline luminescence and markedly broadens the MCLA-dependent luminescence peak. Cleavage proceeds normally in the presence of these concentrations of MCLA and ATA for at least 3 hours. We tested the limits of MCLA toxicity on cleavage in *Phialidium gregarium*. The upper limit of tolerated extracellular MCLA was 1.2 μg/ml; the upper limit for microinjected intracellular MCLA was 0.03 μg/ml cytoplasm. This suggests the egg membrane is rather impermeable to MCLA. Supported in part by NSF grant IBN-9207470.

**M-Pos151**

MAG-INDO REPORTS CYCLIC CA DECREASES IN INTRACELLULAR STORES DURING CA OSCILLATIONS OF PITUITARY GONADOTROPES. ((F.W. Tse, A. Tse and B. Hille)) Dept. Physiol. & Biophys., U. Washington, SJ-40, Seattle, WA 98195.

Gonadotropin-releasing hormone (GnRH) induces oscillations of $[Ca^{2+}]_i$ and $I_{K(Ca)}$ in gonadotropes. We could load mag-indo into intracellular Ca stores by the AM-method followed by unloading and quenching of cytosolic dye with a whole-cell pipette containing 1 mM $Mn^{2+}$. Simultaneous with voltage-clamped $I_{K(Ca)}$, the $Ca^{2+}$ concentration in intracellular stores ($[Ca^{2+}]_s$) was measured ratiometrically. Fluorescence was calibrated in gonadotropes pipette-loaded with 100 or 200 μM mag-indo and known $[Ca^{2+}]$. Assuming that the environment of intracellular stores is similar to the cytosol, $[Ca^{2+}]_s$ was typically 50-200 μM, which is 1000-fold higher than cytosolic $[Ca^{2+}]$. During GnRH application, as cytosolic $[Ca^{2+}]$ rose cyclically and activated $I_{K(Ca)}$, cyclic decreases in $[Ca^{2+}]_s$ could be observed, usually after the first few cycles. In each typical cycle, $[Ca^{2+}]_s$ decreased by 5 to 20 μM as $I_{K(Ca)}$ was activated; during the rest of the cycle (~10 s) $[Ca^{2+}]_s$ recovered almost completely. Similar cyclic changes in $[Ca^{2+}]_s$ were also observed when GnRH-induced oscillations persisted in the absence of extracellular $Ca^{2+}$. Our data suggest that the release and refilling of intracellular stores are nearly balanced in each cycle even without entry of extracellular $Ca^{2+}$. We estimate that the total $Ca^{2+}$ stored in each cell may be 10 times the amount released in one cycle of oscillation. (Supported by HD 12629, AR 17803 and the A.W. Mellon and W.M. Keck Foundations.)

**M-Pos152**

DETECTION OF EXPRESSION OF RAB3 PROTEINS IN PERITONEAL MAST CELLS. ((A.F. Oberhauser, V. Balan, C.L. Badilla-Fernandez, and J.M. Fernandez)) Mayo Clinic, Rochester MN 55905.

Rab proteins are ras-like low molecular mass GTP-binding proteins, which are postulated to act as specific regulators of membrane trafficking in exocytosis and endocytosis. We have previously shown that synthetic peptides, corresponding to the effector domain of rab3 proteins, stimulate a complete exocytotic response in mast cells (Oberhauser, et al (1992) Nature 360, 270). We have used a PCR-cloning strategy to investigate the presence of rab3 mRNA transcripts in mast cells. cDNA was generated from total cellular RNA (~$10^6$ mast cells) by RNA-PCR. PCR was then performed on this cDNA using degenerate oligonucleotides primers based on two conserved sequences among rab3 proteins. However, no PCR products were obtained, even for proteins known to be expressed in high copy numbers in mast cells (βActin and FcεRI receptor). We have found that the problem resides in the presence of mast cell secretory granule-derived heparin, that copurifies with the RNA and acts as an inhibitory factor of RNA-PCR. After treating the RNA (obtained from ~500 mast cells) with heparinase, several PCR products of varying size were obtained using primers specific for rab3 proteins. These products were cloned and sequenced. We have found clones containing sequences that had a 100% homology at the deduced amino acid level to a portion of rab3B and rab3D (amino acids 16 to 83). However, this region is highly conserved within rab3 isotypes. We are currently working on the full identification of these transcripts by sequencing the hypervariable regions at the N terminus, which are distinct to each rab3 isoform.

**M-Pos153**

RECRUITMENT OF THE INSULIN REGULATED GLUCOSE CARRIER (GLUT4) BY MICROMOLAR $CA^{2+}$ AND GTPγS IN PERMEABILIZED NEONATAL CARDIOMYOCYTES.
S. Lehmann-Klose, J. Cuppoletti, J.C. Rüegg, and G. Pfitzer, II. Physiologisches Institut, Universität Heidelberg, Germany, and Dept. Physiology and Biophysics, University of Cincinnati, USA

Insulin dependent facilitated glucose transport depends on the recruitment of GLUT4 from intracellular vesicles to the plasma membrane. In cardiomyocytes, the recruitment is also triggered by contractile activity whereby the signal may well be $Ca^{2+}$. We tested this hyothesis in α-toxin permeabilized cultured neonatal cardiomyocytes. A novel immunoprecipitation technique was developed to monitor the recruitment of GLUT4 using a peptide antibody directed against the exofacial loop of GLUT4. Neonatal cardiomyocytes were cultured until confluency (about 8 days) and were kept in serum free medium for 24 hours before use α-toxin permeabilized cardiomyocytes were still responsive to insulin which at pCa 8 increased immunoreactivity in the precipitate 1.7 fold. A similar increase was observed after increasing $Ca^{2+}$ to 10 μM in the absence of insulin. GTPγS (200 μM) had the largest effect on immunoreactivity (2.7 fold increase) which was further stimulated by $Ca^{2+}$ (3.8 fold increase, total) suggesting that GTPγS and $Ca^{2+}$ may be additive. In conclusion, we have shown that micromolar concentrations of $Ca^{2+}$ are sufficient to induce reruitment of GLUT4 to the plasma membrane in cardiomyocytes suggesting that $Ca^{2+}$ may be the common signal which stimulates contraction and increases glucose transport capacity.
Supported by DFG and NIH DK 43816 and DK 43377 (J.C.)

**M-Pos154**

P.A.C.A.P. STIMULATES CALCIUM AND POTASSIUM CURRENTS IN RAT PITUITARY GONADOTROPHS. ((S.R. Rawlings, N. Demaurex and W. Schlegel)) Fondation pour Recherches Médicales, University of Geneva, Switzerland. (Spon. by D. Bertrand)

The hypothalamic factor pituitary adenylate cyclase-activating polypeptide (PACAP) binds to specific cell surface receptors and can modulate the release of a variety of pituitary hormones including luteinising hormone from gonadotrophs. However, the molecular mechanisms of PACAP action are still poorly understood. The present study used whole-cell patch clamp recordings with microfluorimetry to concurrently measure ionic currents and $[Ca^{2+}]_i$ in PACAP-stimulated gonadotrophs. In identified gonadotrophs voltage-clamped at -50 mV, PACAP stimulated repetitive high amplitude (> 1 μM) oscillations in $[Ca^{2+}]_i$, which were due to $Ins(1,4,5)P_3$-stimulated mobilisation of an intracellular $Ca^{2+}$ store. In addition PACAP stimulated two cell membrane currents. The first was a $Ca^{2+}$-dependent outward $K^+$ current of 40-100 pA which parallelled the oscillations in $[Ca^{2+}]_i$. This current had an activation threshold of around 350 nM $[Ca^{2+}]_i$, and was blocked by d-tubocurarine and apamin. The second current was a small (5-10 pA), non-inactivating, inward $Ca^{2+}$ current that was blocked by $NiCl_2$. Intracellular perfusion of $Ins(1,4,5)P_3$ stimulated repetitive $Ca^{2+}$ oscillations, the $Ca^{2+}$-dependent outward $K^+$ current, but not the small inward current. Ongoing studies on the modulation of these ionic currents by PACAP will reveal further information on the action of this peptide at the single cell level.

**M-Pos155**

ASSOCIATION OF RAT BRAIN OMEGA-CONOTOXIN GVIA RECEPTOR WITH SPECIFIC ISOFORMS OF Na/K-ATPASE.

((M.Takahashi@, A.M. Snowman#, A. Omori@, T. Ito@, C.M. Begg*,T.D. Copeland+, and M.W. McEnery*))
@Mitsubishi-Kasei Inst. of Life Sciences, Tokyo, Japan, #Dept. of Neurosci., J.H.U. Sch.of Med., Baltimore, MD 21205, *Dept. of Physiol. and Biophys., Case Western Res. Univ. Sch. of Med., Cleveland, OH 44106,+ABL-Basic Res. Prog., NCI-Frederick Cancer R& D Center, Frederick, MD 21702,

The omega-conotoxin GVIA sensitive N-type voltage-dependent calcium channel (CTXR) is purified using [$^{125}$I]w-conotoxin GVIA ([$^{125}$I]CTX) as the diagnostic radioligand (McEnery, M.W., Snowman, A.M., Sharp, A.H., Adams, M.E., and Snyder, S.H. Proc. Natl. Acad. Sci. (USA) 88: 10095-10099). CTXR evidences five major proteins of 230 kDa, 140 kDa, 110 kDa, 70 kDa and 58/60 kDa. All proteins cofractionate following extensive chromatographic procedures and sucrose gradient sedimentation. While purification of the 110 kDa protein parallels recovery of the CTXR, the 110 kDa protein can be selectively depleted, without a substantial loss in the binding of [$^{125}$I]CTX. A monoclonal antibody (mAb9A7) immunoprecipitates [$^{125}$I]CTX binding from detergent extracts and, upon Western blot analysis, identifies a 110 kDa protein enriched in crude brain membranes and purified CTXR preparations. Partial sequences of the 110 kDa protein indicate it is identical to the alpha subunit of the Na/K-ATPase. Using Na/K-ATPase isoform specific antibodies, two isoforms of alpha subunit (alpha2>>alpha3) are demonstrated to copurify with CTXR. This report suggests a complex formed between CTXR and a fraction of Na/K- ATPase which persists through detergent solubilization, immunoprecipitation, column chromatography and sucrose gradients.

**M-Pos156**

**SINGLE VESICLE RELEASE IS COUPLED TO ACTION POTENTIALS IN RAT ADRENAL CHROMAFFIN CELLS.** Z. Zhou and S. Misler Washington University Medical Center, St. Louis, MO. 63110

Adrenal chromaffin cells respond to depolarization with increased action potential activity and catecholamine release. We have examined the relationship of action potential (AP) activity to quantal secretion from rat chromaffin cells by combining current clamp recording in the perforated patch mode with carbon fiber amperometry (Wightman et al.,1991; Chow et al., 1992). Brief depolarizations which trigger single APs, result in single amperometric spikes often with delays of <100ms. More prolonged depolarizations which trigger trains of APs, produce more frequent amperometric spikes. Repeated trains of APs often exhaust secretion; the recovery time can be several minutes.

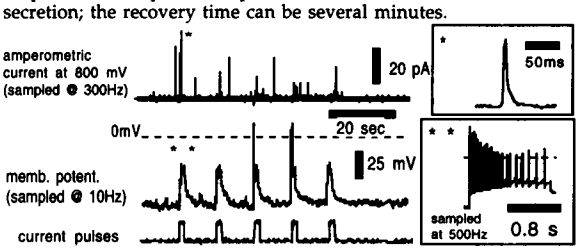


**M-Pos157**

VOLTAGE DEPENDENCE OF EXOCYTOSIS IN VERTEBRATE CONE PHOTORECEPTORS. ((F. Rieke and E. A. Schwartz)) Dept. of Pharmacological and Physiological Science, The University of Chicago, 947 E. 58th St., Chicago, IL 60637.

Cone photoreceptors from the tiger salamander (*Ambystoma tigrinum*) retina have small synaptic vesicles which are released at presynaptic endings formed at the base of the cell body. In solitary cones, the voltage at the release site can be controlled by a whole-cell voltage clamp through a perforated patch. Capacitance changes induced by exposure to extracellular calcium were measured using a digital phase-sensitive detector. When the membrane voltage was between -30 mV and -10 mV, a voltage operated calcium current (VOC) was apparent and the capacitance increased 100-300 fF. When the membrane voltage was between -70 mV and -50 mV, the VOC was not apparent (< 2 pA) and the capacitance increased 20-60 fF. A capacitance increase required 4-5 seconds to reach a maximum. After removal of extracellular calcium, the capacitance decreased over the course of 10-20 seconds and returned approximately to its original level. Capacitance changes at -50 mV were blocked by 100 μM $Cd^{+2}$, but not by 5 μM nimodipine, an efficient blocker of the VOC. Under physiological conditions cone photoreceptors operate between -35 and -70 mV. Our data suggest that cones possess two mechanisms which control exocytosis at physiological voltages: One mechanism depends on the VOC and overlaps only slightly with the physiological range; a second mechanism does not depend on the VOC and overlaps broadly with the physiological range.

**M-Pos158**

$Ca^{2+}$ influx through nicotine-gated channels triggers exocytosis from bovine chromaffin cells.((P.E. Mollard, E.P. Seward and M.C. Nowycky)) Dept. Anatomy & Neurobiology, Med. Coll. Penn., Philadelphia PA 19129.

In chromaffin cells, ACh induced opening of nicotinic receptors (nAChR) depolarizes the cells causing $Ca^{2+}$ influx through voltage-gated $Ca^{2+}$ channels which triggers exocytosis of catecholamine containing vesicles. We examined whether the $Ca^{2+}$ influx through nAChR is sufficient to stimulate exocytosis. Standard whole cell patch clamp recording techniques were used to measure nicotine induced inward currents and changes in membrane capacitance ($\Delta C_m$) resulting from fusion of chromaffin vesicles with the plasma membrane. The internal solution contained 0.3mM BAPTA which does not prevent $C_m$ increases resulting from $Ca^{2+}$ influx during depolarizing steps. Under near physiological conditions (external $Na^+$ 130mM, $Ca^{2+}$ 2mM, holding potential -60mV), pressure application of nicotine (200ms, 50μM) produced a sustained increase in $C_m$ (up to340fF) providing the nicotinic current was >1nA. Increasing the holding potential to -90mV, and therefore the driving force for $Ca^{2+}$ influx, enhanced both the inward current amplitude and the size of $\Delta C_m$. Addition of the nicotinic antagonist, d-tubocurarine (1μM) markedly attenuated the inward current and prevented any change in $\Delta C_m$. In 0 $[Ca]_o$ or with 10mM $[BAPTA]_i$ nicotine-induced currents failed to trigger exocytosis. These results suggest that $Ca^{2+}$ influx through the nicotine-activated cation selective channels is sufficient to trigger exocytosis. Experiments in which the pipette contained the fluorescent $Ca^{2+}$ probe fluo-3 confirmed that nicotinic currents were associated with increases in both $[Ca^{2+}]_i$ and $C_m$. Thus, secretion of catecholamines in response to cholinergic stimulation may be induced by $Ca^{2+}$ influx through not only voltage gated $Ca^{2+}$ channels but also through the nicotinic channels themselves.

**M-Pos159**

DHP-INSENSITIVE CALCIUM CHANNELS IN INSULIN SECRETING CELLS. ((V. Magnelli, A. Pollo, M. Lovallo, E., Carbone)) Univ. of Turin, 10125 Turin, ITALY.

We have investigated the kinetic properties of high-voltage-activated (HVA) dihydropyridine (DHP)-insensitive Ca channels in insulin secreting RINm5F cells with the whole-cell and single-channel patch-clamp technique. Beside the typical DHP-sensitive L-type channel (contributing 50-55% to the total current), whole-cell experiments revealed at least two DHP-insensitive Ca channel subtypes: a ω-conotoxin (ω-CgTx)-sensitive channel (10-15%) and a DHP- and ω-CgTx-insensitive one (15-20%). The DHP- and ω-CgTx-insensitive component was reversibly depressed by ω-agatoxin fraction IVA (ω-Aga). While DHP-sensitive current activated around -30mV, DHP-insensitive currents activated at more positive potentials. This was proved by the different blocking potency of nifedipine (5μM) and a mixture of ω-Aga (200nM) plus ω-CgTx (3μM) at various potentials. At +10mV the two toxins blocked about 41% of the current while nifedipine blocked 34%. On the contrary, at -20mV nifedipine and the two toxins reduced the current by 61% and 27% respectively. In 12 out of 15 ω-CgTx chronically treated cells simultaneous perfusion of 5μM nifedipine and 250nM ω-Aga spared 10 to 25% of the current at +10mV suggesting the existence of a DHP-, ω-CgTx and ω-Aga-insensitive component. In cell-attached and outside-out patches the L-type channel was characterized by long openings in the presence of Bay-K (22pS in 100mM $Ba^{2+}$) and absence of activity with nifedipine. The ω-CgTx-sensitive channel was better identified in outside-out patches. The channel exibited long-lasting activities with multiple conductance levels (0.6-0.9pA) and brief openings ($\tau_o$=0.8ms). The DHP- and ω-CgTx-insensitive Ca channels were recorded in both configurations. They activated above 0mV and exibited multiple conductance levels (10, 16, 18pS) with fast openings ($\tau_o$=0.6ms) and a long-lasting flickering behaviour over 700ms depolarization.

**M-Pos160**

**$Ca^{2+}$ PERMEABILITY OF RAT PAROTID GLAND BASOLATERAL MEMBRANE.**

*((Tim Lockwich, Irene Hong, and Indu Ambudkar))*
NIDR, NIH, Bethesda, Md. 20892.

The enhanced ability of $Ca^{2+}$ to enter agonist-stimulated parotid gland acinar cells was investigated using $Mn^{2+}$ entry into internally $Ca^{2+}$-depleted cells (depl-acini) loaded with fura2 or by measuring $^{45}Ca^{2+}$ flux into isolated basolateral plasma membrane vesicles (BLMV). Our data reveal that $Ca^{2+}$ permeability across this membrane is inhibited by carbodiimide type carboxyl group reagents and that the critical carboxyl residue(s) is localized on the cytoplasmic side of the membrane. Low temperature also inhibited $Ca^{2+}$ permeability in depl-acini but in a non-linear fashion as revealed by an Arrhenius plot, suggesting a more complex $Ca^{2+}$ permeability across the membrane than a simple pore. Kinetic studies of $^{45}Ca^{2+}$ entering the BLMV revealed two distinct pathways with low temperature eliminating a high-affinity, saturable $Ca^{2+}$ permeability pathway. Interestingly, this same $Ca^{2+}$ permeability pathway is also eliminated by 50 μM miconazole, an anti-fungal agent.

**M-Pos161**

CYTOPLASMIC CALCIUM BUFFER CAPACITY DETERMINED WITH NITR-5 AND DM-NITROPHEN. ((N.F. Al-Baldawi and R.F. Abercrombie)) Department of Physiology, Emory University, Atlanta, GA 30322.

We determined intracellular calcium buffer capacity of isolated cytoplasm from the giant axon of the marine invertebrate *Myxicola infundibulum* by photolytically releasing calcium from "caged" compounds (NITR-5 and DM-Nitrophen), while monitoring free calcium with Ca-sensing electrodes. Two phases of the pCa response were observed upon light exposure: an initial rapid drop from basal pCa, followed by a (nearly linear) slow rise. Buffer capacity ($\Delta$bound Ca/$\Delta$free Ca) was calculated based on the initial pCa change (from basal) at light exposure, the change 10 min after light exposure, and an intermediate change determined by extrapolating the linear phase of the pCa record to the start of the photolysis. The apparent buffer capacities at pH 7.0 and 7.5 were the same; however, raising basal free calcium from below 1 $\mu$M to above 3 $\mu$M significantly reduced the buffer capacity. Removal of MgATP reduced the initial pCa drop upon light exposure but increased the change (from basal) ten min later. The buffer capacity calculated based on the extrapolated change in pCa varied widely from one giant axon to another but averaged ~ 50 in the absence of ATP and ~100 in the presence of 1 mM ATP for $[Ca^{2+}]$ below 3 $\mu$M. For $[Ca^{2+}]$ above 3 $\mu$M, the buffer capacity dropped to ~10. Supported by NIH NS-19194.

**M-Pos162**

CAPACITANCE MEASUREMENTS FOLLOWING FLASH PHOTOLYSIS OF CAGED-$CA^{2+}$. ((C. Heinemann[1,2], R. H. Chow[1], J. Klingauf[1], R. S. Zucker[2], and E. Neher[1])) [1]MPI for Biophysical Chemistry, Am Faßberg, D-37077 Göttingen, Germany. [2]UC Berkeley, Mol.&Cell. Biology, LSA111, Berkeley CA. (Spon. by C. Heinemann)

The kinetics of the secretory response in bovine chromaffin cells following flash photolysis of caged-$Ca^{2+}$ (DM-nitrophen) were studied by capacitance measurements with millisecond time resolution. After Ca elevation, capacitance rises rapidly with one or more exponentials. When only one component is present, it falls in the same class as the slow component when two exponentials are present. When fitted with an exponential, the inverse rate of the fast component increases with Ca (range 3-600 $\mu$M) from <1 $s^{-1}$ up to 1000 $s^{-1}$ (or up to about 100,000 fF/s). The slow component is also Ca-dependent, is about an order of magnitude slower than the fast component, and reaches about 50 $s^{-1}$ at high Ca. At $[Ca^{2+}]$ >30 uM, clear indications of endocytosis are seen in some cases. There is a Ca-dependent delay before capacitance rises, which may reflect the kinetics of multiple Ca ions binding to the secretory apparatus. The time course was fitted by the model of Heinemann et al. (*Pflüg Arch*, 1993, 424:105) with the following extensions: a) a second reserve pool with slow rates of exchange, b) the secretion reaction is split into 3 Ca-binding steps followed by a secretion step with finite rate. With this model, the $K_D$ of the elementary $Ca^{2+}$ binding step is in the range of 10 to 20 $\mu$M.

**M-Pos163**

SUBMEMBRANE CA TIME COURSE AT SECRETORY SITES UPON DEPOLARIZATION ((R.H. Chow[1], J. Klingauf[1], C. Heinemann[1,2], E. Neher[1])) [1]MPI für biophysik. Chemie, Am Faßberg, D-37077 Göttingen, Germany and [2]UC Berkeley, Molec. & Cell. Biology, LSA111, Berkeley, CA (Spon. R.H. Chow)

In chromaffin cells, amperometric latency histograms of single vesicle events provide the secretion rate as a function of time relative to a secretion stimulus (Chow et al, 1992, *Nature* 356:60). Such information can be used to report the submembrane calcium concentration ([Ca]) if one has a "Ca dose response relationship" for secretion (from caged-Ca experiments, see abstract of Heinemann et al., this meeting). This approach leads to estimates of peak submembrane [Ca] of less than 10 $\mu$M during a 20-ms depolarization. In an alternative approach, we found that the average capacitance change for repeated 20-ms depolarizations was about 15 fF (about 6 vesicles), equivalent to a rate of 750 fF/s. Using the Ca dose-response relationship, one finds that a [Ca] of about 5 to 10 $\mu$M gives the measured rate of secretion. Previously many models of single Ca-channel domains showed [Ca] reaching 100's of $\mu$M to a millimolar for millisecond channel openings. Our findings of significantly lower [Ca] at the secretion sites suggest that in chromaffin cells, unlike in squid giant synapse, Ca channels and vesicles are not strictly co-localized. This is further supported by the finding that in chromaffin cells, but not in squid giant synapse (Adler et al, 1991, *J.Neurosci.* 11:1496), 1 to 5 mM EGTA can block secretion.

**M-Pos164**

SOURCES OF SECRETORY DELAY. ((J. Klingauf[1], R.H. Chow[1], C. Heinemann[1,2], R.S. Zucker[2], E. Neher[1])) [1]MPI für biophysik. Chemie, Am Faßberg, D-37077 Göttingen, Germany and [2]UC Berkeley, Molec. & Cell. Biology, LSA111, Berkeley, CA (Spon. E. Neher)

In bovine chromaffin cells, single vesicles fuse after some latency in response to step depolarizations (Chow et al, 1992, *Nature* 356:60), and secretion continues for 10's of milliseconds after the end of the pulse. This is surprising, as the calcium concentration ([Ca]) is expected to rise and collapse in 10's of $\mu$sec's in the immediate vicinity of single Ca channels, where vesicles are presumed to be localized. Possible sources of the delay are i) retardation of the Ca time course due to buffering, ii) Ca binding and unbinding kinetics at the secretory machinery, iii) an intrinsic delay in fusion pore formation, iv) a delay in transmitter release and detection after vesicle fusion. The contribution of Ca binding/unbinding kinetics to the secretory delay is addressed in another poster (Heinemann, C. et al.). Cross-correlation of capacitance and amperometric events shows that the capacitance "step" precedes the amperometric "foot" signal by an average of 5 ms; that is, vesicle fusion and content release are distinct processes. Furthermore, changes in the amount of exogenous calcium buffers (EGTA or FURA-2) alter the decay in secretion rate after a pulse ends. This suggests that the channels and vesicles are not necessarily colocalized (unlike the case of synapses). Thus, multiple factors contribute to the observed secretory delay in neuroendocrine cells.

**M-Pos165**

PROBING THE KINETICS OF EXOCYTOSIS IN ADRENAL CHROMAFFIN CELLS WITH BRIEF DEPOLARIZATIONS ((Frank T. Horrigan & Richard J. Bookman)) Dept. of Molecular & Cellular Pharmacology, Box 016189, University of Miami, Miami, FL, 33101

The early time course of exocytosis was examined in whole-cell patch clamped rat adrenal chromaffin cells by measuring the capacitance response to brief depolarizations under conditions designed to enhance the rise in $[Ca^{2+}]_i$ (10 mM $Ca^{2+}_o$, 100 $\mu$M $BAPTA_i$). 'Jump' increases in membrane capacitance were measured immediately following randomly ordered depolarizations (to +20 mV) of 5 to 100 ms duration. Records were corrected for non-exocytotic changes in capacitance due to Na channel gating charge movement by subtracting the response to a 5 ms pulse (Biophys. J., 64:2, A101, 1993). A small exocytotic response was observed with 10 ms pulses (3.5 fF$\pm$ 2.2) attributable to ~2 vesicle fusions. The responses to longer pulses indicated a progressive decline in the rate of exocytosis. Pooled data from 24 cells exhibit an average time course that is well fit by a single exponential with a time constant of 76ms and an asymptote of 31fF. These kinetics could be accounted for by a first order process as though this initial phase of exocytosis occurs with almost no delay from a small pool of 15-30 releasable vesicles for which the probability of release is constant during the pulse. The results of this study contrast with those obtained by other methods of elevating $[Ca^{2+}]_i$ and could have important implications toward understanding the response of chromaffin cells to physiological stimuli. (Supported by NSF & AHA/FL)

M-Pos166

**THERMODYNAMIC STUDIES OF ALCOHOL-LIPID INTERACTIONS: LIPID SPECIFICITY**

**((Tina Wu Leung, Fengli Zhang, and Elizabeth S. Rowe.)) Department of Biochemistry and Molecular Biology, University of Kansas Medical School, and VA Medical Center, Kansas City, MO 64128.**

**In animal models of alcoholism, the lipid composition of the synaptic membranes has been found to change as a result of chronic exposure to alcohol, suggesting that the membrane interactions of alcohol may vary with membrane lipid composition. In the present investigation, the thermodynamics of the interactions of alcohols with model membrane vesicles having various compositions have been investigated by titration calorimetry. Alcohols with chain lengths from butanol to nonanol were studied. The lipids studied included DPPC, DLPE, DOPC, DOPG and mixed compositions including cholesterol and gangliosides. The enthalpies, partition coefficients, entropies and the heat capacity changes associated with these interactions were measured. The results of these studies suggest that there is very little specificity in the partitioning of alcohols into the various phospholipids. In the mixtures it was found that cholesterol significantly reduces the partitioning of alcohols into the model membranes. (Supported by the Department of Veterans Affairs.)**

M-Pos167

**ETHANOL DISRUPTS SLOW MOTIONS OF THE PROTEIN-ASSOCIATED LIPID NEAR THE SURFACE OF ACETYLCHOLINE RECEPTORS.**

**((Lauraine A. Dalton, Douglas E. Raines and Keith W. Miller)) Department of Biological Chemistry and Molecular Pharmacology, Harvard Medical School and Department of Anesthesia, Massachusetts General Hospital, Boston, MA 02114.**

The motion of lipid acyl chain segments in the boundary region adjacent to the nicotinic acetylcholine receptor was studied by electron paramagnetic resonance (EPR) saturation. The motion of n-doxylstearic acid (n-SASL; n=5,6,9,12,14,16) spin probes was compared for the receptor, reconstituted into dioleoylphosphatidylcholine (DOPC) vesicles, by measuring a saturation parameter (Sigma), in the presence and absence of ethanol. Sigma, the ratio of the integrated intensity of the EPR signal at subsaturating microwave power to the intensity at partially saturating power [Squier and Thomas, Biophys. J. 49, 921 (1986)] is more sensitive to slow motion of the probes in the lipid-protein boundary domain than to the faster motion of probes in the bulk lipid. Ethanol facilitated a marked increase in motion of the 5- and 6-SASL probes, while leaving the deeper probes largely unaffected. On the other hand, deconvolution of EPR spectra into bilayer and receptor-associated components showed ethanol's effects on the latter to be minimal. These studies indicate that ethanol affects slow protein-associated lipid motions only proximal to the headgroup (n=5 and 6) whereas it does not alter faster motions at any depth. Supported by NIAAA 07040.

M-Pos168

FLUORESCENCE STUDIES OF SHORT-CHAIN PHOSPHOLIPID EXCHANGE IN MICELLES.

C. E. Soltys & M. F. Roberts, Department of Chemistry, Boston College, Chestnut Hill, MA 02167

Two fluorescent micellar phospholipid probes (1-hexanoyl-2-(1-pyrenebutyroyl)-PC and 1-octanoyl-2-(1-pyrenebutyroyl)-PC) have been synthesized, characterized, and used to monitor the dynamics of lipid / amphiphile exchange in a variety of detergents and phospholipid micelles using both steady-state and stopped flow fluorescence techniques. The ratio of monomer to excimer band is a good indicator of the extent of lipid mixing at equilibrium. Following the time dependence of increase in the monomer band with stopped-flow methodology provides a rate constant for this process (most systems were well fit with a single exponential).Short-chain pyrene-labeled PC mixing with Triton X-100 micelles is extremely fast and follows a concentration dependence indicative of the importance of micelle collisions for the exchange process. Submicellar amounts of Triton have no effect on the fluorescent dynamics of the probe molecule. Other detergents such as β-octylglucoside and deoxycholate are also effective at high concentrations, although significant differences exist in the extent of probe mixing. Symmetric short-chain PC and lyso-PC mixing rates are moderately fast with mixing times that decrease as the hydrophobicity / chain length of the diluent matrix increases. The rate constants for lipid exchange can be compared to turnover rates of several phospholipases in these assay systems. Anomalous mixing behavior of unusual micelle forming lipids (bolaforms, ω-carboxylate, and polymerizable PC's) is particularly helpful in understanding kinetics of water-soluble phospholipases on these systems. [Supported by GM26762]

M-Pos169

TIME-RESOLVED FLUORESCENCE ANISOTROPY AND DIFFERENTIAL SCANNING CALORIMETRY OF A SERIES OF MIXED-ACID PHOSPHATIDYLCHOLINE BILAYERS: EFFECT OF SN-2 ACYL CHAIN LENGTH AND DEGREE OF UNSATURATION.

((Charles D. Niebylski and Norman Salem, Jr.)) Section of Fluorescence Studies, Laboratory of Membrane Biochemistry and Biophysics, DICBR, NIAAA, National Institutes of Health, Rockville, MD 20852.

Biological systems are capable of discriminating between various polyunsaturated lipids with respect to their function. However, there is little data which compare the biophysical properties of naturally occurring (e.g. mixed-acid) phospholipid species with varying degrees of polyunsaturation. Therefore, a large series of mixed-chain phosphatidylcholines were prepared containing 18:0 at the sn-1 position and one of the following unsaturated species at the sn-2 position: 18:1n9, 18:2n6, 18:3n6, 18:3n3, 20:2n6, 20:3n6, 20:4n6, 20:5n3, 22:4n6, 22:5n3, 22:5n6 or 22:6n3. As unsaturation increased, the time-resolved fluorescence anisotropy (of DPH and TMA-DPH) correlation times decreased. This trend was observed most clearly at 5°C for all species. DPH limiting anisotropies, at 5°C, reached a minimum with the introduction of 2 double bonds (0.070 for 18:2n6) and subsequent unsaturation gradually increased $r_\infty$ to where the 22:6n3 species reported the highest value (0.105) among the polyunsaturates measured. Likewise, two double bond species had the lowest ΔH (as measured by differential scanning calorimetry (DSC)) (1.7 kcal/mole for 18:2n6) while subsequent increases in unsaturation resulted in graded increases in ΔH (i.e. 3.5, 4.3, 4.6 and 6.1 kcal/mole for 18:3n3, 20:3n6, 20:4n6 and 22:6n3, respectively). The effect of sn-2 acyl chain length, degree of unsaturation and location of double bonds on mixed-chain phospholipid bilayer structure is significant and follows complex yet predictable patterns. It was of particular interest, at low temperatures, that the 22:6n3-containing bilayer displayed the fastest local acyl chain motions while exhibiting a relatively high degree of long range lipid packing.

M-Pos170

THERMODYNAMICS OF TRANS-MEMBRANE PHENOMENON: ENTHALPY CHANGES IN THE FORMATION OF MEMBRANE POTENTIAL.

((Ying Wang and Chang-Hwei Chen)) Wadsworth Center for Laboratories and Research, New York State Dept. of Health and Dept. of Biomedical Sciences, University at Albany, State University of New York, Albany, NY 12201-0509 (Spon. by Y. Myer)

Thermochemical investigations of trans-membrane proton electrochemical potential ($\Delta\bar{\mu}_H+$) were carried out using membrane vesicles from cytochrome d - deficient mutant E. coli GR19N. In the presence of D-lactate as the electron donor, ΔpH (proton gradient) and $\Delta\psi$ (electrical potential) generated across the membranes were found to be 57 and 70 mV, respectively, as measured by flow dialysis experiments, which gave a value of 127 mV for $\Delta\bar{\mu}_H+$. The corresponding enthalpy changes ($\Delta H_m$, $\Delta H_{pH}$ and $\Delta H_\psi$) in the formation of $\Delta\bar{\mu}_H+$, ΔpH and $\Delta\psi$, as determined by microcalorimetric measurements, were 9, 2 and 5 kcal/mole, respectively. When the electron donor was NADH, the membranes exhibited 77 mV for $\Delta\bar{\mu}_H+$ and 11 kcal/mole for $\Delta H_m$, indicating a relatively higher $\Delta H_m$ in conjunction with a lower $\Delta\bar{\mu}_H+$. The present results with D-lactate were also compared with those previously reported for membrane vesicles from E. coli 308-225 which exhibited 14 kcal/mole for $\Delta H_m$ and 130 mV for $\Delta\bar{\mu}_H+$. These findings were examined to evaluate components' contribution to $\Delta H_m$, and to relate the energetics of $\Delta H_m$ to membrane coupling site and oxidase activity.

M-Pos171

**EFFECTS OF ANESTHETICS ON THE MEMBRANE DIPOLE POTENTIAL.**

((ZHIHAI QIN AND DAVID S. CAFISO)) DEPARTMENT OF CHEMISTRY, UNIVERSITY OF VIRGINIA, CHARLOTTESVILLE, VA 22901.

Membranes have a large internal dipole potential that is approximately 300 mV hydrocarbon positive. Oppositely charged hydrophobic ion spin-labels were utilized to investigate the effect of anesthetics on this internal potential. Electron Paramagnetic Resonance spectroscopy was used to determine the binding of the ion spin-labels in the absence and presence of anesthetics to egg phosphatidylcholine vesicles, formed by extrusion. Clinically important anesthetics halothane, enflurane and isoflurane were studied, and their membrane concentration was determined by quantitative gas chromatography. These anesthetics decrease the binding of negatively charged spin-labels and increase the binding of positively charged spin-labels. Although translocation rates of hydrophobic ion probes all increase in the presence of the anesthetics, the positively charged spin-labels were affected the most. These effects on ion transport rates and binding are consistent with a decrease in membrane dipole potential. The changes in potential are small at clinically important concentrations, but could modulate voltage-dependent events in membrane proteins.

**M-Pos172**

INTERACTION OF THE AROMATIC HORMONE MELATONIN WITH LIPID MEMBRANES. ((C.S. Shida, E.X. Costa, A.S. Ito and M.T. Lamy-Freund)) Inst. Física, Universidade de São Paulo, CP 20516, CEP 01452-990, SP, Brasil. (Spon. by A.G. Szabo).

The pineal hormone melatonin (5-methoxy-N-acetyl-tryptamine) has been found to interact with different cells, playing a number of distinct physiological functions, although its mechanism of action is not clear, including its proposed ability of crossing the cell membrane and interact at the nucleus. The present work focuses on the role of the lipid phase on the membrane-hormone interaction. Alterations on lipid membrane structure, due to the presence of melatonin, were monitored via the ESR signal of spin labels incorporated in liposomes. Melatonin was found to interact near the membrane head groups, as labels placed deep into the hydrocarbon chain region could not detect any change on lipid organization or mobility. Analysis of the ESR signal of probes placed at the lipid head group or near the 5th position of the hydrocarbon chain showed that both above and bellow the lipid transition temperature, the hormone increases the lipid rotational correlation times and the effective order parameter, therefore, turning the bilayer less "fluid". On the basis of the effect of the hormone on the membrane structure, a partition coefficient was calculated and shown to be dependent on the lipid head group. Changes on the melatonin steady state fluorescence parameters were also used to follow the hormone-membrane interaction. (Financial support: FAPESP and CNPq).

**M-Pos173**

MEMBRANE INTERACTIONS OF A PEPTIDE DESIGNED TO SPONTANEOUSLY INSERT INTO LIPID BILAYERS. ((Laura A. Chung and Thomas E. Thompson.)) University of Virginia, Department of Biochemistry, Charlottesville, Virginia, 22908.

Some proteins can insert into and translocate across lipid bilayers without the assistance of a proteinaceous translocation complex. Examples of this type of insertion include M13 procoat protein, apocytochrome C, melittin, colicin E1, diphtheria toxin and cholera toxin. In order to define the basic requirements necessary for the spontaneous insertion of proteins into bilayers, a previously reported model peptide composed of a 20-mer polyalanine cross-linked to a carrier protein was synthesized (T.S. Moll & T.E. Thompson, *Biophys. J.* 64, A61). This report extends this work using polyalanine peptides from 23 to 30 residues in length, and tests their ability to bind to and insert into lipid bilayers. The physical state of the membrane bilayers is manipulated by changing the lipid composition, and the binding of the peptide to these vesicles is measured by a centrifugation assay. The effect of the vesicle curvature is studied by testing the competition between small (≈ 300-400 Å diameter) and large (≥ 1000 Å diameter) vesicles for peptide binding. The conformation of the peptide in lipid membranes is also under investigation. (This work is funded by NIH grant GM-14628 and NSF grant BIR-92 16996.)

**M-Pos174**

$K_2(LA)_{12}K_2$-AMIDE: A NEW PEPTIDE MODEL OF HELICAL HYDROPHOBIC TRANSMEMBRANE SEGMENTS OF MEMBRANE PROTEINS. ((Y-P. Zhang, R.N.A.H. Lewis, G.D. Henry, R.S. Hodges and R.N. McElhaney)), Dept. of Biochemistry, University of Alberta, Edmonton, Canada T6G 2H7.

$K_2(LA)_{12}K_2$-Amide [$(LA)_{12}$] was synthesized and studied as a peptide model of the α-helical, hydrophobic, transmembrane segments of integral membrane proteins. CD and NMR studies indicate that this peptide adopts predominantly helical conformations in water, organic solvents or phospholipid dispersions. However, FTIR spectroscopic studies indicate that significant populations of non-α-helical structures are also present, the relative proportions of which are affected by the medium in which this peptide is dispersed. FTIR and NMR studies suggest that amide protons located near to the N- and C-termini of the peptide exchange fairly rapidly with the bulk solvent phase whereas those in the central regions of the peptide exchange very slowly. Moreover, the amide protons in the central regions of the peptide are virtually unexchangeable when dispersed in hydrated lipid bilayers. This observation is consistent with the incorporation of the peptide into lipid bilayers with the long axis of its helix oriented along the bilayer normal. DSC studies of lipid/peptide mixtures also indicate that this peptide penetrates lipid bilayers and interacts predominantly with the lipid hydrocarbon chains. We find that $(LA)_{12}$ is more perturbing of the thermodynamic properties of the host lipid bilayer than is the polyleucine analogue $K_2L_{24}K_2$-amide ($L_{24}$) (see adjacent poster). We believe that such differences can be attributed to differences between the roughness of the hydrophobic surfaces of these peptides and to the fact that $(LA)_{12}$ forms more a deformable helical structure in the host lipid bilayer.

**M-Pos175**

COMPARATIVE STUDY OF THE INTERACTION OF TWO TRANSMEMBRANE α-HELICAL PEPTIDES WITH PHOSPHATIDYLCHOLINE BILAYERS. ((Y-P. Zhang, R.N.A.H. Lewis and R.N. McElhaney)), Dept. of Biochemistry, University of Alberta, Edmonton, Canada T6G 2H7.

The interaction of the synthetic α-helical, transmembrane model peptides $K_2(A)_{24}K$-amide ($A_{24}$), $K_2(LA)_{12}K$-amide ($LA_{12}$) and $K_2(L_{24})K_2$-amide ($L_{24}$) with a homologous series of *n*-saturated phosphatidylcholine (PC) bilayers was studied by DSC and FTIR spectroscopy. $A_{24}$ has very little effect on the thermotropic phase behavior of PC bilayers, suggesting that this peptide does not assume a predominantly transbilayer disposition in our reconstitution systems. In contrast, $LA_{12}$ and $L_{24}$ have profound and characteristic effects on PC thermotropic phase behavior, indicating that these peptides do assume a transbilayer arrangement. Both $LA_{12}$ and $L_{24}$ at lower concentrations produce two-component DSC endotherms due to the simultaneous presence at peptide-associated and peptide-nonassociated lipid domains. Both peptides progressively reduce the enthalpy and cooperativity of the PC gel to liquid-crystalline phase transition, although an appreciable chain-melting enthalpy persists even at high peptide concentrations. Moreover, the temperature at which the peptide-associated lipid melts is shifted in a characteristic way according to the predictions of the hydrophobic mismatch theory when the hydrocarbon chain length of the host PC bilayer is altered. As well, both peptides show evidence of gel phase immiscibility in very short chain or long chain PC bilayers. However, $(LA)_{12}$ is intrinsically more perturbing of PC hydrocarbon chain packing in both the gel and liquid-crystalline states compared to $(L)_{24}$, probably because $(LA)_{12}$ forms a more flexible helix with greater surface roughness.

**M-Pos176**

INTERACTION OF ENKEPHALIN PEPTIDES WITH PHOSPHOLIPID BILAYERS. ((Marek Romanowski, Xiaoyun Zhu, Andrzej W. Lipkowski, Aleksandra Misicka, Ronald C. Haaseth, Victor J. Hruby and David F. O'Brien)) Department of Chemistry, University of Arizona, Tucson, AZ 85721.

Traditionally, increased permeability of small peptides across phospholipid bilayers has been pursued by hydrophobic amino acid substitutions. However, as successes of this approach are often limited, it is necessary to explore more intricate modes of interactions between the bilayer and such peptides. To elucidate this concept we compared interactions of two groups of enkephalin analogs with phospholipid membranes. These potential analgesic agents represent different approaches in the design of biologically active peptides. Biphalin is a flexible dimeric peptide, whereas DPDPE is a conformationally constrained peptide that possesses a 14-member ring. Higher permeation coefficients of biphalin, as compared to DPDPE, correlate well with observed values of the free energy of transfer from aqueous to lipid phase. However, calorimetric analysis reveals that modes of the interaction of these peptides with bilayers differ significantly. The transfer of DPDPE is driven by entropy changes, while the transfer of biphalin is a result of favorable enthalpy differences. We propose that the interaction of the flexible biphalin with the bilayer involves conformational changes that allow formation of intramolecular hydrogen bonds. On the other hand, transfer of DPDPE is controlled mostly by the hydrophobicity of its amino acid constituents, as well as specific interactions at the water-lipid interface. It appears that the hydrophobicity of the amino acid composition does not necessarily determine the permeability properties of a peptide, while purposefully designed peptide conformation may be of crucial importance for the efficient membrane transport. (Supported by NIDA Grant POI DA 06284)

**M-Pos177**

BINDING OF ISOPRENYLATED PEPTIDES TO PHOSPHOLIPID BILAYERS. (J.R. Silvius and F. l'Heureux) Department of Biochemistry, McGill University, Montréal, Québec, Canada H3G 1Y6

We have measured the binding of bimane-labeled tri- and tetrapeptides, terminating in a C-terminal isoprenylated cysteine or O-methylcysteine residue, to phospholipid vesicles. The peptides examined represent the carboxyl termini of the proteins Ki-ras, ralA, rhoC and rac2. At low peptide/lipid ratios, the association of the isoprenylated peptides with lipid vesicles behaves as a simple partitioning equilibrium, with rapid (≤ sec.) exchange of vesicle-bound and free peptides. At 37°C, peptides terminating in geranylgeranylcysteine bind to neutral egg PC/egg PE (9:1) vesicles with partition coefficients $K_p$ (= $X_{bilayer}/X_{aqueous}$) of the order of $10^7$; binding is enhanced 10- to 25-fold upon methylation of the cysteine residue. Binding of analogous farnesylated peptides to vesicles is on average 45-fold weaker. Peptide binding to vesicles incorporating 20 mol% anionic lipid (PG or PS) is enhanced by up to 60-fold upon O-methylation of the isoprenylated cysteine. Incorporation of 45 mol% cholesterol into the vesicles, or replacement of most of the vesicle PC by PE, only modestly alters the $K_p$ values for various isoprenylated peptides. A C-terminal farnesylcysteine appears to be similar to an N-terminal myristoylglycine in 'bilayer-anchoring' ability, while a farnesylated O-methylcysteine or a geranylgeranylated (O-methyl-) cysteine is considerably more potent than myristoylglycine in this regard. (Supported by the MRC of Canada).

**M-Pos178**

**SYNERGY BETWEEN THE ANTIMICROBIAL PEPTIDES, MAGAININ 2 AMIDE AND PGLa.** ((Jessica Blazyk, Janet Hammer, Jin Hua and Jack Blazyk)) Chemistry Department, Molecular and Cellular Biology Program, and College of Osteopathic Medicine, Ohio University, Athens, Ohio 45701.

Magainin 2 amide (mag2a) and PGLa are small cationic peptides, isolated from the skin of the African clawed frog, which can kill a wide variety of bacteria and enveloped viruses, but are not toxic to mammalian cells at antimicrobial concentrations. The bactericidal activity of these peptides arises from their ability to permeabilize the plasma membrane of target organisms. While each of these peptides possesses considerable antimicrobial activity in its own right, a mixture of the two peptides at a 1:1 molar ratio exhibits a strong synergistic effect in its bactericidal activity (Dr. Michael Zasloff, personal communication). In order to study the molecular basis of this synergism, we examined the effects of the two peptides individually and in combination in the presence of lipid bilayers containing DPPC and/or DPPG using FT-IR spectroscopy. At a lipid-to-peptide ratio of 10:1, all of the peptide binds to acidic DPPG bilayers, while <10% binds to neutral DPPC bilayers. For a 1:1 mixture of DPPC and DPPG, 90% of mag2a and 82% of PGLa binds; however, only 68% of the peptide mixture is bound under the same conditions. The effects of peptide binding on lipid fluidity was determined by monitoring the position and width of the symmetric methylene C–H stretching band of the lipid acyl chains as a function of temperature. Mag2a and PGLa each lower the $T_m$ of DPPG by ~2-5°, but have little effect on the DPPC/DPPG mixture. For the mag2a/PGLa mixture, however, the $T_m$ of both pure DPPG and DPPC/DPPG bilayers is reduced by 5°, and the bandwidth in the lipid mixture is increased far greater than with either peptide alone. Analysis of amide I bands permits an estimation of peptide conformation. Significant differences in conformation are evident in the peptide mixture compared to the individual peptides, particularly when bound to DPPC/DPPG bilayers. These data suggest that the synergistic antimicrobial activity of mag2a and PGLa may arise from intermolecular interactions which result in unique conformers which alter membrane structure and permeability.

**M-Pos179**

THEORETICAL MODELS OF POLYPEPTIDE ASSOCATION AND TRANSMEMBRANE CHANNEL FORMATION. ((Z. Zhang+, O. G. Mouritsen* and M. J. Zuckermann*,+)) Dept. of Physics, McGill University, Montréal, Québec, Canada H3A 2T8 and *Dept. of Physical Chemistry, Technical University of Denmark, DK-2800 Lyngby, Denmark.

We present two theoretical models for polypeptide association for different physical chemical situations. The first describes dimer formation of gramicidin A in lipid bilayers. We represent the lipid bilayer by two weakly interacting monolayers each modelled by an extended Pink multistate model. Each monolayer contains a distribution of Gramicidin A monomers which can associate with monomers in the opposing monolayer by a direct hydrogen bonding interaction thereby forming ionic channels. Numerical simulation methods are used to obtain momomer-dimer equilibrium with the lipid-dimer interactions described by the matress model of Bloom and Mouritsen. The second model describes transbilayer formation via aggregation of protein components in a bilayer due to a combination of lateral diffusion and anisotropic inter-component interactions. Numerical simulations are used to examine optimal conditions for the formation of channel aggregates. Application to experiment is discussed.

**M-Pos180**

EFFECTS OF PEPTIDES ON SUBMICROSECOND LIPID DYNAMICS USING LONG-LIVED FLUORESCENCE PROBES. ((Bo Shen, Piotr Targowski, John Lobo and Lesley Davenport)) Dept. of Chem., Brooklyn College of CUNY, New York 11210.

The effects of the peptide melittin on *submicrosecond* lipid dynamics have been investigated using coronene and a coronene-phospholipid conjugate (Cor-PC) where the fluorophore is attached to the Sn2' position of the glycerol backbone and is in a fixed location within the bilayer. Previously we have shown (Biophys. J., Targowski et al., 61:A503) that polarized fluorescence emissions from coronene ($\tau_{av}$=200ns) are sensitive to lipid disordering events occurring on the submicrosecond timescale and can be interpreted using a 'gated' fluctuation model which invokes a *distribution* of lipid 'melt' rates. Like the parent fluorophore, Cor-PC also exhibits a long mean fluorescence lifetime ($\tau_{av}$=120ns) with rotational sensitivity to submicrosecond lipid disordering events. Steady-state emission anisotropy values, <r>, (as a function of increasing temperature) were recorded for DMPC/melittin SUVs (1:50 peptide to phospholipid mole ratio) labeled with either coronene, Cor-PC or DPH. Below the lipid melt temperature ($T_c$=23°C) significant (~30%) *decreases* in <r> were detected for coronene labeled SUVs in the presence of peptide, suggesting a disordering of the lipid packing, whereas the relatively short-lived DPH probe ($\tau_{av}$=8ns), reported little change. In contrast, Cor-PC labeled SUVs showed an *increase* (~45%) in <r> values below $T_c$ on incorporation of melittin into the bilayer; measurement of time resolved anisotropy at 14°C revealed that the longer of the two observed rotational correlation times ($\phi_1$=2ns, $\phi_2$=240ns) increased to 520ns, suggesting an increase in lipid order. Fluorescence lifetimes for coronene and Cor-PC were insensitive to the presence of peptide. Preliminary data suggests that melittin has a significant effect on *submicrosecond* lipid dynamics. Discrepancies in the emission anisotropy data reported by the two probes may reflect their different locations in the bilayer matrix. The application of our 'gated' fluctuation model to fluorescence decay data from long-lived probes in lipid-peptide systems and the effect of peptide on altered fluctuation rates will be discussed. (Supported in part by the AHA-NYC affiliate and NSF DMB-9006044).

**M-Pos181**

**ANALYSING THE BINDING OF PERIPHERAL PROTEINS TO CHARGED LIPID MEMBRANES** **((T.Heimburg and D.Marsh)), Abt.01, Max-Planck Institut für biophysikalische Chemie, 37077 Göttingen, Germany**

We derived an expression for the binding isotherm of ligands to charged surfaces using a statistical thermodynamic model that describes binding in terms of both the electrostatic free energy of the ligand/surface complexes and the free energy of the ligand distribution on the surface. This model has been used to describe the binding of native and denatured cytochrome c to dioleoyl phosphatidyl glycerol membranes over a wide range of the ionic strength. An apparent degree of saturation (highly dependent on salt concentration) has been observed in the experimental binding isotherms at a degree of binding far below the complete filling of the surface which could consistently be described by the model. An effective charge of the protein far below the expected net charge of the protein was obtained. The fits to the data provided a lipid/protein stoichiometry in a binding site that is consistent with the dimensions of both, lipid and protein. At low ionic strength the lipid/protein stoichiometry is no longer constant, indicating binding of more than one layer of protein. The bound denatured protein maintains a similar lipid/protein stoichiometry and effective charge per protein to the native protein. However, the intrinsic binding constant increases significantly. This indicates that denatured cyt.c remains mainly globular on the lipid surface but integrates into the hydrophobic core of the lipid membrane.

**M-Pos182**

STRUCTURE AND FLEXIBILITY OF CALMODULIN IN SOLUTION AND IN ITS COMPLEXES WITH TARGET PROTEINS ((P.B. O'Hara, Z. Grabarek, Y. Mabuchi, V.J. Macek, G.A. Pianka, G.E. Hallert)) Amherst College, Amherst, MA 01002 and Boston Biomedical Research Institute 02114

Two sets of double cysteine mutants of calmodulin (CaM) have been designed and produced by site specific mutagenesis in order to elucidate the details of the processes by which CaM binds and activates its diverse target proteins. In one set, the two cysteines are predicted to move closer together when the target peptide M13 binds. In the other set, the two residues should move further apart. Derivatization of these cysteines with fluorescent donors and acceptors, allows energy transfer to be used to measure the distance. Results show that in the presence of M13, CaM undergoes a dramatic compaction. This is not seen with other intact proteins, suggesting that CaM's structure depends on what it is binding to. Lifetime distributions also show that the intrinsic flexibility in CaM is reduced upon target protein binding.

**M-Pos183**

INTERFACIAL ACTIVATION OF $PLA_2$ ON ZWITTERIONIC VESICLES: GLOBAL CHANGES IN VESICLE STRUCTURE MAY TRIGGER HIGH ACTIVITY. ((W.R. Burack, A. Dibble, M. Allieta, T. Hønger and R.L. Biltonen)) Dept. of Pharmacology and Pathology, Univ. of Virginia, Charlottesville, VA 22908

Hydrolysis of large unilamellar vesicles by phospholipase $A_2$ proceeds in a complex manner: a period of slow product accumulation (the lag) ends with a sudden increase in rate (the burst). The burst, which occurs when a critical mole fraction of the reaction products (1-mono-palmitoyl-phosphatidylcholine and palmitic acid) has accumulated in the bilayer, is associated with lateral phase separation of reaction products and the substrate, DPPC. To better understand the consequences of lateral phase separation, we characterized vesicles made from ternary codispersions of reaction products and substrate. Above the critical mole fraction required for phase separation, the dispersions spontaneously form 50 nm disk-like structures as determined by freeze-fracture electron microscopy. $^{31}$P-NMR spectra are similar to those expected of small unilamellar vesicles. No micellar structures are apparent. The thermotropic phase behavior was studied by differential scanning calorimetry, fluorescence probes, and light scattering. All techniques show a pronounced hysteresis consistent with non-ideal mixing. Simultaneous recordings of $PLA_2$ activity and light scatter show that a profound change in vesicle structure is concomitant with the burst. These data imply that reaction products in the amount necessary to induce lateral phase separation and the burst, may also induce a change in the morphology of the entire vesicle. $PLA_2$'s increased activity may not be due to lateral phase separation *per se*, but rather to the vesicle's disk-like morphology. (Supported by grants from NIH)

**M-Pos184**

**REFOLDING, BILAYER INCORPORATION AND RECONSTITUTION OF BACTERIO-OPSIN.**

((Anthony W. Scotto, Helen Seow and Nahla Khalek)) Dept. of Medicine, Cornell University Medical College, New York, NY 10021.

The incorporation of bacteriorhodopsin (BR) from the purple membrane into preformed vesicles results in the inclusion of phytolipids into the nascent proteoliposome (PRL). These endogenous lipids affect the interaction of this membrane protein with the phospholipids of the preformed vesicle and enhance its stability. Furthermore, these lipids affect the behavior of the nascent PRL with protein-free vesicles. In order to prepare a PRL containing bacterio-opsin (BO) or BR without endogenous lipids, we have explored several approaches to reassembling this protein in a vesicle. Using BO purified in SDS, we prepared PRLs by refolding the protein into mixed micelles followed by detergent dialysis. In an alternative approach, micelles of SDS and phospholipids were mixed with unfolded BO and vesicles were formed containing incorporated and reconstituted BR upon removal of the detergent and the addition of retinal. Use of unfolded BO as starting material does not result in all of the protein being inserted into the bilayer. In fact, of the protein that does insert, only a portion reconstitutes with retinal to form the holoprotein. Reconstitution of the chromophore after vesicle formation and stability of the retinal binding is dependent upon phospholipid composition. PRLs formed from either delipidated BR or unfolded-refolded BO in phospholipids demonstrate increased sensitivity to proteases as compared to native BR. These results suggest that reconstitution or stability of the chromophore is insufficient evidence for a proper fit or reassembly of BO/BR into a model bilayer or vesicle. (Supported by NIH grant GM-44749).

**M-Pos185**

LONG-RANGE BACTERIORHODOPSIN/PHOSPHATIDYLCHOLINE INTERACTIONS IN VESICULAR AND PLANAR MULTIBILAYERS.

((J.F. Tocanne, E. Perochon, B. Piknova, V. Schram and A. Lopez)) LPTF, CNRS, F-31062, Toulouse, France

Consequences of hydrophobic matching between bacteriorhodopsin (BR) and dilauroyl- (DLPC), dimyristoyl- (DMPC), dipalmitoyl- (DPPC), distearoyl- (DSPC) and egg yolk- (egg-PC) phosphatidylcholine have been studied. Fluorescence investigation of the phase behaviour of the lipids indicates that BR produces positive or negative shifts ($\Delta T$) in the phase transition temperature Tm of the host lipids depending on the strength and sign of the mismatch between the lipid and protein hydrophobic thicknesses. $\Delta T$ was positive for DLPC and DMPC, nil for DPPC and negative for DSPC. Phase diagram, in temperature versus BR concentration, were constructed for DLPC. On account of current threoretical models, a value of 1.2 nm was found for the coherence length $\xi$ which characterizes the distance over which the hydrophobic thickness of the lipid bilayer is perturbed by the protein. Through fluorescence recovery experiments, the lateral diffusion coefficients D of lipids were measured in BR/egg-PC recombinants. On the ground of computer simulations of lipid D in the presence of obstacles, the data suggests that as an obstacle, BR is to be seen, not naked but surrounded by about two layers (corresponding to a distance of ~ 1.7 nm) of partially immobilized lipids, a result which is consistent with the above conclusion and current theoretical predictions.

**M-Pos186**

THE GECKO PHOTORECEPTOR MEMBRANE MAY HAVE A POSITIVE SURFACE CHARGE DENSITY

((Jie Liang and Thomas G. Ebrey)) Center for Biophysics & Computational Biology, and Dept. of Cell & Structural Biology, University of Illinois at Urbana-Champaign,Urbana, IL 61801

Most biological membranes are known to be negatively charged. However, gecko photoreceptor membranes behave as if they have a positive surface charge density. During spectral titrations of the Schiff base of the gecko visual pigment P521 in membranes, we found that as the salt concentration increases from 50 mM to 3.0 M, the measured $pK_a$ of the spectral change increased from 9.9 to 10.6. If the membrane of the photoreceptor carried a net negative charge, the $pK_a$ would be expected to decrease as the salt concentration increases, *e.g.*, as observed in the case of octopus photoreceptor microvilli (Koutalos, Y., *et al.*. 1990, *Bioph. J.*, 58, 493-501). The increase in $pK_a$ with salt concentration indicates that gecko photoreceptors may have a positively charged membrane. Examination on the amino acid sequence of the putative loop regions of gecko P521 (Kojima, D. *et al.*, 1992, *PNAS.*, 89, 6841-6845) indeed shows a positive net charge compared to the net negative charge of bovine rhodopsin. Assuming the gecko photoreceptor membrane has the same number of negatively charged lipids as bovine, then a net positive charge density would be expected.

**M-Pos187**

PROTON BUFFERING POWER OF CLATHRIN COATED AND UNCOATED ENDOSOMES

((J.A. Watkins, C-Y. Li, J.D. Altazan, J. Barton and J. Glass)) Hematology-Oncology Section, Center for Excellence in Cancer Research, Treatment, and Education, LSUMC-S, Shreveport, LA, 71130.

Proton fluxes and the resulting acidification of endosomes is thought to be important to vesicular targeting and function. Proton buffering power ($\beta$; $\Delta H^+/\Delta pH$), is important for accurate estimates of proton fluxes and electrochemical coupling of anion and cation fluxes to the vacuolar $H^+$-ATPase. We have measured the internal and external buffering power of rabbit reticulocyte endosomes over a pH range from 5.0 to 8.0 using additions of 3 to 200 nanomoles of HCl or NaOH to approximately 1 mg of vesicle protein in 1 ml of 50 mM NaCl, 50 mM KCl, 1mM HEPES buffer at 37°C. The apparent $pK_a$ and effective concentration of the buffering groups were observed to be 7.186±0.026 and 7.02±0.17 mM/mg for the intravesicular surface and 7.428±0.010 13.75±0.18 mM/mg for the extravesicular surface of both coated and uncoated vesicles. The lipid composition of these endocytic vesicles is similar although the protein composition is quite different. Using fluorescence measurements, incomplete pH gradient dissipation was observed for both coated and uncoated vesicles. Dissipation of the pH gradient (or leak) was very dependent on $\Delta pH$ and vesicle protein composition. These observations suggest that the buffering power arises from the lipid composition which gives rise to an apparent surface phospholipid "head group" concentration. Dissipation of the proton gradient is likely to arise from a non-electrogenic proton pore or channel. It is proposed that the $\Delta pH$ achieved by endosomes is due to flux balences between the $H^+$-ATPase, $Na^+/H^+$ antiport and to a lesser extent on the $Na^+/K^+$-ATPase. Supported by NIH DK-37866.

**M-Pos188**

**USE OF AN ORIENTED TRANSMEMBRANE PROTEIN TO PROBE THE ASSEMBLY OF A SUPPORTED PHOSPHOLIPID BILAYER**

((P.B. Contino, C.A. Hasselbacher, J.B.A. Ross and Y. Nemerson)) Departments of Medicine and Biochemistry, Mount Sinai School Medicine of the City University of New York, New York, NY 10029.

Planar supported phospholipid bilayers formed by adsorption of vesicles on glass are used increasingly in the investigation of lipid-dependent reactions. We have studied the way in which these bilayers are formed with phospholipid vesicles containing the transmembrane protein tissue factor (TF). TF complexed with the serine protease, factor VIIa, is the primary initiator of blood coagulation by way of activation of the zymogen factor X. TF has been shown to orient randomly on the inner and outer leaflets of vesicles. We have used proteolytic digestion to produce vesicles in which the extracellular domain of TF is located only on the inner leaflet. These vesicles show no cofactor activity for factor VIIa due to the inability of the extracellular domain of TF to bind VIIa. After freeze/thaw, 50% of the cofactor activity is regained, indicating reorientation of the sequestered, inner-leaflet TF. Adsorption of these vesicles to the inner surface of glass microcapillaries results in a continuous phospholipid bilayer. The microcapillaries were perfused with a solution of factors VIIa and X and the effluent monitored for factor Xa production, a sensitive measure of the activity of the TF-VIIa complex. For coatings produced with the digested vesicles, minimal TF-VIIa activity was observed, showing that the supported bilayer preserves the orientation of the leaflets in the vesicles; i.e., the outer leaflet of the vesicles forms the outer leaflet of the supported bilayer.

Supported by Grant HL-29019 from the National Institutes of Health.

**M-Pos189**

INFLUENCE OF A LIPID-BINDING PROTEIN ON THE CONFORMATION AND ORIENTATION OF PHOSPHOLIPID MONOLAYERS STUDIED BY POLARIZED ATTENUATED TOTAL INTERNAL REFLECTANCE INFRARED SPECTROSCOPY.

((M. Subirade and M. Pézolet)) CERSIM, Département de chimie, Université Laval, Québec, Canada ((D. Marion)) Laboratoire de Biochimie et Technologie des protéines, INRA, Nantes, France.

Recently, a lipid transfer protein (LTP) that is able to catalyse the transfer of a large variety of phospholipids has been purified from wheat seedlings. Although its physiological role is not yet well established, its capacity to interact with micelles and lipid vesicles has been clearly demonstrated *in vitro*. However, the mechanism by which the LTP transfers lipids is not yet understood and little is known on the effect of LTP on lipid bilayers. In this study, the monolayer technique was used to study the interaction of LTP with phospholipids. The conformation and orientation of both the protein and the phospholipid at the air/water interface for different surface pressure have been monitored by polarized attenuated total internal reflectance infrared spectroscopy. The results show that the conformation of the protein at the interface is more helical than in solution. At low surface pressure, the protein decreases the conformational order of the lipid acyl chain while at high pressure LTP is squeezed out of the monolayer. From the dichroism of the infrared spectra, the orientation of each component has been determined. A mechanism for the action of LTP will be proposed.

**M-Pos190**

COLLAGEN-INDUCED CHANGES IN PLATELET MEMBRANE LIPID ASYMMETRY. ((K. Boesze-Battaglia and R. J. Schimmel)) Department of Cell Biology, UMDNJ-School of Osteopathic Medicine, Stratford, N.J. 08084. (Spon. by G. Willsky)

Phospholipids are distributed asymmetrically in many plasma membrane bilayers. This lipid asymmetry is prominent in platelets whose outer membrane monolayer contains virtually no phosphatidylserine and very little phosphatidylethanolamine (PE). When platelets aggregate the phospholipid asymmetry is postulated to be disrupted by the translocation of the amine containing phospholipids from the inner to the outer monolayer. Since model membrane studies have suggested that PE rich membranes provide a thermodynamically unfavorable environment for cholesterol, studies were undertaken to determine if the distribution of cholesterol within the membrane bilayers also changed when platelets aggregate. To measure membrane cholesterol, the fluorescent probe 7-nitro-2,1,3-benzoxadiazol-4-yl (NBD)-cholesterol was incorporated by incubation with phosphatidylcholine vesicles containing NBD-cholesterol. The amount of NBD-lipid in the outer monolayer was calculated from a decrease in fluorescence upon addition of sodium dithionate (Biochemistry, 30: 11819, 1991). A 10-20 % decrease in the amount of cholesterol in the outer monolayer was found upon stimulation with collagen. This decrease in outer monolayer cholesterol occurred to a lesser extent when thrombin was the stimulus and not at all with ionomycin or ADP. The translocation of cholesterol was time and calcium dependent. Treatment of platelets with the chaotropic agents urea or guanidine HCL, blocked collagen-induced translocation of cholesterol from the outer monolayer. Collagen also caused a 15-20 % increase in the amount of NBD labeled PE on surface of platelet membranes. This finding confirms the exposure of amine containing phospholipids at the surface of collagen stimulated platelets. This heretofore unrecognized redistribution of cholesterol in platelet membranes may reflect a physiological important event associated with platelet aggregation and may be linked to the concomitant redistribution of amine containing phospholipids.

**M-Pos191**

ACTIVATION OF $PLA_2$ DURING FREEZE-DRYING ((E. Fisk, L.M. Crowe, and J.H. Crowe)) University of California, Davis 95616

Phospholipase $A_2$ ($PLA_2$) is a small (14 kDa), membrane-associated enzyme which attacks the acyl ester bond at the *sn*-2 position of phospholipids. Recently, it has been found that many organisms unable to survive long periods of dehydration accumulate high levels of free fatty acids (FFAs). One possible explanation for the increased FFA production is that $PLA_2$ is becoming activated during dehydration. Our experiments show that liposomes lyophilized in the presence of $PLA_2$ and rehydrated to 8% water content show an increased leakage compared to controls dried without $PLA_2$. Liposomes not lyophilized show the same leakage with or without $PLA_2$. The increase in leakage seen when liposomes are lyophilized with $PLA_2$ is specifically caused by the enzyme because liposomes dried with BSA show the same low level leakage seen with liposomes lyophilized with no protein present. The activation of $PLA_2$ is not due to the freezing event during lyophilization because liposomes frozen and thawed in the presence of $PLA_2$ show only a minimal increase in leakage compared to liposomes frozen and thawed without $PLA_2$. Liposomes lyphilized with $PLA_2$ show no increase in leakage 24h after rehydration when rehydrated at 0% or 15% RH. Samples rehydrated between 20% and 95% RH had increasing leakage with increasing water availability. The increase in leakage seen with liposomes lyophilized with $PLA_2$ is not due to fusion of the liposomes. It is possible to inhibit $PLA_2$ activation with dehydrin and arbutin, compounds found at high levels in desiccation tolerant organisms. We conclude that $PLA_2$ is activated during rehydration in freeze-dried model systems. Future experiments will determine whether this activation is also found in organisms undergoing dehydration. (Supported by NSF grant # IBN93-08581).

**M-Pos192**

STOPPED-FLOW FLUORESCENCE STUDIES OF THE INTERACTION OF A MUTANT FORM OF CYTOCHROME B5 WITH LIPID VESICLES ((Peter W. Holloway, N. Krishnamachary, Frances A. Stephenson, and A. W. Steggles*)) Dept. of Biochemistry, Univ. of Virginia Sch. Med., Charlottesville, VA. *Dept. of Biochemistry, Northeastern Ohio Univ. Coll. Med., Rootstown, OH.

Cytochrome $b_5$ binds spontaneously to lipid vesicles and also self-associates in aqueous solution. Two forms of the protein have been generated with mutations in the membrane-binding domain, one form has a self-association constant which is less than that of the native protein, while the other has a larger self-association constant. All three proteins have Trp in the membrane-binding domain but as aqueous solutions of these proteins contain differing amounts of monomeric protein, the kinetics of fluorescence enhancement when the proteins are mixed with lipid vesicles are complex. Similar complex kinetics are seen when the Trp are quenched by addition of bromolipid vesicles. One of these mutants, where Trp 108 and 112 are replaced by Leu, does not self-associate appreciably and its stopped-flow fluorescence kinetics are mono-exponential. Identical rate constants are seen with this mutant for fluorescence enhancement by POPC and fluorescence quenching by three bromolipids with bromines at the 6,7-, 9,10-, and 11,12-positions of the sn-2 acyl chain. This rate constant is only 1% of the calculated collisional rate constant and it is suggested that the reduced rate is caused by a reduction in the number of productive collisions rather than by a slow rate of penetration of the membrane-binding domain into the bilayer. Supported by a Grant-in-Aid from the American Heart Association, Virginia Affiliate, Inc.

**M-Pos193**

ELECTRON TRANSFER DYNAMICS AND STRUCTURE OF SELF-ASSEMBLED MYOGLOBIN-SURFACTANT FILMS. ((James F. Rusling,* Alaa-Eldin F. Nassar,* Zhe Zhang,* and Thomas F. Kumosinski#)) *Department of Chemistry, Box U-60, University of Connecticut, Storrs, CT 06269-3060, and #Eastern Regional Research Center, U.S. Department of Agriculture, Wydmoor, PA 19118

Multilayer films of surfactant didodecyldimethylammonium bromide (DDAB) incorporated myoglobin from solutions at pH 5.5-7.5 to give stable, liquid crystal Mb-DDAB films. Electron transfer involving the heme Fe(III)/Fe(II) couple in Mb-DDAB films on electrodes was >1000-fold faster than for Mb in water. Similar results were found in films of lecithin and other surfactants. Supramolecular structure of Mb-surfactant films was examined by linear dichroism, reflectance FT-IR, and phase transition studies. Molecular dynamics of Mb-surfactant models was used to examine interactions between Mb and surfactant. Results suggest that Mb-DDAB films feature lamellar liquid crystal DDAB in bilayers with tilted hydrocarbon tails as in biomembranes. Mb in DDAB films retains its native secondary structure, is preferentially oriented, and has high spin Fe(III)heme. Fast electron transfer may be related to interfacial surfactant adsorption and/or Mb orientation.

**M-Pos194**

A DIAGONAL PROTON WIRE AS A CONDUCTOR OF PROTONS ACROSS STRAIGHT-CHAINED PHOSPHOLIPID BILAYERS. ((Thomas H. Haines))Dept. of Chem.& CUNY Med. School, City College, NY 10031.

Water, and molecules its size, diffuse rapidly across biological membranes and phospholipid bilayers above the $T_m$. It was earlier shown by a random walk calculation (Haines, T.H. & Liebovitch, L.S., Biophys. J. 64, A184 (1993)) that, using the lateral diffusion of phospholipids, **in the plane of a bilayer**, one may calculate the water permeability **through the bilayer**. This calculation, is based on a model using Trauble's mechanism of water transport between kinks that move along the chains, suggests that every headgroup jump in the plane of the bilayer is associated with a water molecule traversing the bilayer. Diffusing kinks are thus used to explain both the water movement and the lateral movement of the lipid chains. Assuming headgroup lateral interactions are the most powerful interactions between phospholipid molecules, the water transport model also explains the order parameter profile obtained by deuterium quadrupole coupling nmr. The water transport model implies a "proton wire" like that proposed by D.W. Deamer and also by J.F. Nagle emerges. Here each water molecule is isolated during its transport. The volume of water in the bilayer implies a diagonal "proton wire". The frequency of "proton wire" formation is calculable from measurements of water vs. proton diffusion. Water diffusion rates are independent of bilayer thickness, in published measurements and in the model. In contrast, the diagonal "proton wire" is dependent on bilayer thickness. It depends on wire formation frequency which increases with bilayer thickness. Perturbants, e.g., cholesterol, that inhibit water transport inhibit proton transport.

**M-Pos195**

MEMBRANE BINDING OF MYRISTOYLATED PEPTIDES CORRESPONDING TO THE $NH_2$-TERMINAL REGION OF $pp60^{v\text{-}src}$. (C. A. Buser[†], C. Sigal[§], M. Strzelczyk[†], L. Mooney[†], M. D. Resh[§], S. McLaughlin[†]) [†]SUNY Stony Brook, Stony Brook, NY 11794, [§]Memorial Sloan-Kettering Cancer Center, NY, NY 10021.

Cell transformation by $pp60^{v\text{-}src}$ requires association with the plasma membrane. We are studying how two factors contribute to membrane association of $pp60^{v\text{-}src}$: (i) the hydrophobic insertion of the N-terminal myristate into the membrane and (ii) the electrostatic interaction between basic residues and acidic phospholipids. We have measured the membrane binding of peptides corresponding to the N-terminal region of $pp60^{v\text{-}src}$ (myr-GSSKSKPKDPS and myr-GSSKSKPKDPSQRRRSL). Both myristoylated peptides bind to electrostatically-neutral PC vesicles with a partition coefficient $K_i = 10^4\ M^{-1}$; $1/K_i = 10^{-4}$ M may be regarded as an apparent dissociation constant that is equal to the accessible lipid concentration at which half of the peptide is bound. These results imply that the myristoyl chain provides barely enough energy to bind $pp60^{v\text{-}src}$ to the plasma membrane and explain why myristate is necessary but not sufficient for membrane association. Incorporating 33% acidic lipids into the vesicles increases membrane association of the myristoylated-src peptides > 10-fold, indicating an electrostatic interaction between basic residues and acidic phospholipids. This percent of acidic lipids also increases the binding of $pp60^{v\text{-}src}$ about 10-fold, suggesting that N-terminal basic residues are important for membrane association of $pp60^{v\text{-}src}$. C.A.B. is supported by the Cancer Research Fund of the Damon Runyon-Walter Winchell Foundation Fellowship, DRG-1267.

**M-Pos196**

CALCULATING ELECTROSTATIC POTENTIALS ADJACENT TO PHOSPHOLIPID MEMBRANES USING THE NONLINEAR POISSON-BOLTZMANN EQUATION ((R.M. Peitzsch[†], M. Eisenberg[†], K. Sharp[‡], S. McLaughlin[†])) [†]SUNY Stony Brook, Stony Brook, N.Y. 11794, [‡]Univ. of Pennsylvania, Philadelphia, PA. 19104-6059

We used the nonlinear Poisson-Boltzmann (PB) equation to calculate the electrostatic potential in the aqueous phase (0.1M monovalent salt) adjacent to a molecular model of a bilayer comprised of 400 phospholipids. The bilayers were formed from mixtures of zwitterionic (PC) and acidic (PG,PS) lipids arranged in a hexagonal array (68Å$^2$ per lipid) with the polar head-group parallel to the surface and partial charges assigned to atoms in the head-group. For a bilayer with 100% acidic lipid, the -25, -50, and -100mV equipotential profiles are essentially flat and agree well with the predictions of Gouy-Chapman theory, which assumes a uniformly smeared surface charge. Even for a bilayer with 30% acidic lipid, the -25mV equipotential profile is surprisingly flat. Two factors in our model diminish discreteness-of-charge effects and flatten the equipotential profiles: the assignment of partial atomic charges and the inclusion of a 2Å ion-exclusion layer adjacent to the bilayer. Of course when the membrane contains $<10\%$ acidic lipid and the distance between charges ($>30$Å) is larger than $1/\kappa$ (10Å), the -25mV equipotential surface around each acidic lipid is approximately a hemisphere. The potential predicted by the nonlinear PB equation is significantly smaller than that predicted by the linear PB equation, even for a single charge at the membrane-solution interface.

**M-Pos197**

ELECTROFUSION AND DIELECTROPHORESIS OF CELL-SIZE LIPOSOMES. ((N.G. Stoicheva and S.W. Hui))Biophysics Department, Roswell Park Cancer Institute, Buffalo, NY 14263.

Cell size liposomes of egg phosphatidylcholine (PC), transacylated egg phosphatidylethanolamine (PE), bovine brain phosphatidylserine (PS) and egg phosphatidylglycerol (PG), suspended in 5% of polyethylene glycol (m.w.8,000), Ficoll (m.w. 400,000) or Dextran (m.w.71,200) were used as models to study the effects of lipid composition or forces between lipid bilayers in electrofusion. The dielectrophoresis thresholds for charged and uncharged liposomes were measured at frequencies between 100 kHz and 3 MHz. The lower threshold for charged vesicles could be explained if surface conductivity were taken into account. Cell size liposomes were aligned by dielectrophoresis and fused by applying a 1.7 kV/cm pulse of varying durations. The fusion yields (FY) at different pulse lengths were measured by microscopy. The minimal required pulse length of 19 $\mu$sec was limited by the minimum rise time for the smallest vesicles capable of reaching the bilayer breakdown voltage induced by the pulse. The FY curves were sigmoidal and shifted to longer pulse length with increasing external media conductivity or vesicle surface charge. The shifting of FY curves were quantitatively accounted for by the balance of pulse-induced dipole-dipole attraction and electrostatic repulsion.

**M-Pos198**

ANOMALOUS DIFFUSION DUE TO BINDING: A MONTE CARLO STUDY.

((Michael J. Saxton)) Institute of Theoretical Dynamics, University of California, Davis, California 95616, and Laboratory of Chemical Biodynamics, Lawrence Berkeley Laboratory, Berkeley, California 94720.

In classical diffusion, the mean-square displacement increases linearly with time. But in the presence of obstacles or binding sites, anomalous diffusion may occur, in which the mean-square displacement is proportional to a nonintegral power of time for at least some range of times. Models of binding are presented, including an obstruction-binding model in which immobile membrane proteins are represented by obstacles that can bind diffusing particles in nearest-neighbor sites. The models suggest that anomalous diffusion is sensitive to the range of the binding forces, and to the initial conditions. Specifically, diffusion may be anomalous if the diffusing particles start at random positions in the lattice, but normal if the particles start at thermal equilibrium positions. This result may be relevant to fluorescence photobleaching recovery experiments if photobleaching changes the obstacle-tracer interaction energy significantly. (Supported by NIH grant GM38133.)

**M-Pos199**

APPROACHES TO QUANTIFICATION OF ADIPOCYTE GROWTH AND BODY CONTENT ((R.P. Spencer)) University of Connecticut Health Center, Farmington, CT 06030.

One hypothesis concerning hyperphagia in the Zucker obese male rat is that it arises from adipocyte rapid filling (see: Vasselli at al, Am. J. Physiol. 31:R33, 1992). In order to quantify this, an expression is needed for adipocyte lipid content versus time. From Vasselli's Table 2, we can calculate a relationship between ug lipid/cell (L) and age in weeks (T), at 10, 20, 30 weeks. For homozygous lean and obese rats:

Lean rats log L = 0.23 T - 1.12 (corr. coeff. = 1)
Obese rats log L = 0.22 T - 0.53 (corr. coeff. = 1)

Slopes of the lines are nearly identical, but the intercepts are quite different. An interpretation is that the starting points are distinct (volume or characteristics), but the rate of gain is similar. Mean body weights of both groups of rats appear to approach an asymptote. Thus an expression such as the Michaelis-Menten equation can be used. Both the maximum expected weight and time to half-maximum can be estimated for each group of rats. In a related area, Rozman et al (Exp. Hematol. 17:34,1989) had shown that, for human bone marrow, the size of individual adipocytes was described by a Gaussian distribution. The same function also appears to be descriptive of replicative capacity versus log of colony size for perirenal adipocytes in 3 months old rats (Table 4 of Kirtland et al, Am.J.Physiol. 258:C296, 1990). Hence, there are emerging quantitative expressions for adipocyte size/growth which may allow further comparisons.

## PROTEIN STRUCTURE PREDICTION

**M-Pos200**

THE EFFECT OF A GLY -> ALA MUTATION ON COLLAGEN TRIPLE HELIX STABILITY. ((J.A. Weinstein, G. Paterlini, G. Némethy and H.A. Scheraga)) Dept. of Biomathematical Sciences, Mount Sinai School of Medicine, New York, NY 10029. (Spon. by T.A. Krulwich)

Collagen is a fibrous protein which exists in a triple helical structure. Normally, the sequence consists of strictly repeating $(Gly\text{-}X\text{-}Y)_n$ tripeptides, in which every third residue must be Gly, but X and Y can be almost any residue. A mutation in a Gly position causes various diseases such as osteogenesis imperfecta. A triple helix with n=4 was constructed with a Gly to Ala mutation in one of the three strands. The other two strands were $(Gly\text{-}Pro\text{-}Pro)_4$. Energy minimization calculations were performed and six of the 35 conformations were analyzed in detail, based on changes in residue geometry as well as nonbonded interaction energies. After minimization, the conformations of the Ala residue resulted in a change in structure relative to the unperturbed triple helix. The mutual distances of the strands increases, but repulsive atomic overlaps are eliminated. With this single mutation, the triple helix can be maintained with moderate distortion.

**M-Pos201**

NONLINEAR EXTENSION OF THE THERMODYNAMIC THEORY OF THE DENATURATION OF PROTEINS ((A. Hirsh, L. Tsonev, P. Mehl, and S. Litvinovich)) Transplantation Laboratory, American Red Cross, 15601 Rockville, MD 20855

In the standard model of the thermodynamic description of protein unfolding the denaturational increment of heat capacity is taken to be a positive constant. In contrast, this study is predicated on the assumption that the coefficients up to fourth order of the Taylor expansions of the actual (unknown) denaturational heat capacity increment functions of proteins, taken about the temperature of heat denaturation, make significant contributions to predicting the physical chemistry of protein unfolding. This approach leads to equations for heat capacity, enthalpy and Gibbs free energy which predict a rich array of novel behaviors, including: (1) some proteins probably do not cold denature at all when cooled in the absence of strong denaturants; (2) the $\Delta C_p$ of cold denaturation can become negative at some temperature below the threshold of cold denaturation; (3) $\Delta C_p$ may sometimes fall below zero over a narrow temperature range ten to twenty degrees below the heat denaturation temperature; (4) at temperatures below the temperature at which the $\Delta C_p$ reverses sign the denaturational enthalpy can reverse sign and become endothermic, as it is at high temperature; and, (5) at still lower temperatures, in the case of proteins which do cold denature, $\Delta G_{den}$ may reverse sign to become positive again thus causing an ultra-low temperature restabilization of the native state.

Supported in part by a grant from the G.harold and Leila Y. Mathers Charitable Foundation and NIH BSRG 2 507RR05737

M-Pos202

## COMPUTATION OF MOLECULAR TOPOLOGY OF PROTEINS

((B. Mao )) Upjohn Research Labs, Kalamazoo, MI 49001.

Topological stereochemistry of proteins was first discussed for the structure of a mammalian active scorpion neurotoxin (variant 3) from *Centruroides sculpturatus* EWING and related proteins in other scorpion species; the light chain of methylamine hydrogenase was shown recently to be only the second topologically chiral protein molecule. These two molecules share many topological stereochemical properties; for example, both structures are topologically simple. Such topologically simple structures are represented by Kuratowski's graph. The conversion of the three-dimensional polypeptide conformation into the graph representation is usually accomplished through manually re-arranging and re-drawing the chain structure of the protein molecule. A procedure has been designed to replace this manual process and compute the topological chirality directly from the Cα tracing of a protein structure. Applications of this procedure for engineering topologically interesting proteins will be discussed.

M-Pos203

## CLASSIFICATION AND ANALYSIS OF TURNS IN PROTEINS.

((Ronald N. Cole and Shankar Subramaniam)) Beckman Institute, Center for Biophysics and Computational Biology, National Center for Supercomputing Applications, University of Illinois, Urbana, IL 61801

We have performed an extensive analysis of turns in proteins whose high resolution structures (< 2.5Å) are available. Following Efimov's scheme, we have delineated the phi-psi (Ramachandran) map into well-defined structural regions and have tabulated all the turns based on this regional definition. This serves the context for direct comparison of turns based on the backbone structure. Turns connecting alpha-alpha, alpha-beta, beta-alpha and beta-beta regions are extensively analyzed based on the correlations in sequence, structure, size, solvent exposure, hydrogen bonding patterns and the positional pairwise correlations of residues in turns. In addition to providing useful homology modeling tools, the analysis of turns sheds light on specific sequence and motif requirements. The relative importance of sequence similarity and context similarity in homology modeling of turns has also been analyzed. (Supported partially by funding from the NIH via a graduate-training grant and by the ONR.)

M-Pos204

## 3-D, SEQUENCE-ORDER-INDEPENDENT COMPARISONS OF PROTEIN STRUCTURES

((D. Fischer[1], C.-J. Tsai[2], S.-L. Lin[2], H. Wolfson[2] and R. Nussinov[2,3])) [1]Tel Aviv Univ., Computer Sci. Dept., Tel Aviv 69978, [2]NIH, NCI, Lab. of Mathematical Biol., P.O. Box B, Frederick, MD 21702, [3]PRI/Dyncorp, NCI/FCRDC, Frederick, MD 21702

We have recently developed a fast approach to comparisons of three-dimensional structures. Our method is unique, treating protein structures as collections of unconnected points (atoms) in space. It is completely independent of the amino acid sequence order. It is unconstrained by insertions, deletions and chain directionality. It matches single, isolated amino acids between two different structures strictly by their spatial positioning regardless of their relative sequential position in the amino acid chain. It automatically detects a recurring 3-D motif in protein molecules. No predefinition of the motif is required. The motif can be either in the interior of the proteins or on their surfaces. A typical pair-wise comparison of two protein molecules requires less than 3 seconds on a workstation. We have scanned the structural database with dozens of probes, successfully detecting structures which are similar to the probe in a matter of minutes. To illustrate the power of the method we compare the structure of a trypsin-like serine protease, against the structural database. Besides detecting homologous trypsin-like proteases, we automatically obtain 3-D, sequence order-independent, active site similarities with subtilisin-like and sulfhydryl proteases. These similarities equivalence isolated residues, not conserving the linear order of the amino acids in the chains. Using this methodology, a 3-D, non-redundant structural dataset has been created.

M-Pos205

## PREDICTING $Ca^{++}$ BINDING SITES IN PROTEINS

Murad Nayal and Enrico Di Cera
Department of Biochemistry & Molecular Biophysics, Washington University School of Medicine, Box 8231, St. Louis, MO 63110.

The coordination shell of $Ca^{++}$ ions in proteins contains almost exclusively oxygen atoms supported by an outer shell of carbon atoms. The bond strength contribution of each ligating oxygen in the inner shell can be evaluated using an empirical expression successfully applied in the analysis of crystals of metal oxides. The sum of such contributions closely approximates the valence of the bound cation. When a protein is embedded in a very fine grid of points and an algorithm is used to calculate the valence of each point representing a potential $Ca^{++}$ binding site, a typical distribution of valence values peaked around 0.4 is obtained. In 32 documented $Ca^{++}$ binding proteins, containing a total of 62 $Ca^{++}$ binding sites, a very small fraction of points in the distribution has a valence close to that of $Ca^{++}$. Only 0.06% of the points have a valence $\geq 1.4$. These points share the remarkable tendency to cluster around documented $Ca^{++}$ ions. A high enough value of the valence is both necessary (58 out 62 $Ca^{++}$ binding sites have a valence $\geq 1.4$) and sufficient (87% of the grid points with a valence $\geq 1.4$ are within 1.0 Å from a documented $Ca^{++}$ ion) to predict the location of bound $Ca^{++}$ ions. The algorithm can also be used for the analysis of other cations and predicts the location of $Mg^{++}$ and $Na^{+}$ binding sites in a number of proteins. The valence is therefore a tool of pinpoint accuracy for locating cation binding sites, which can be exploited in engineering high affinity binding sites and characterizing the linkage between structure and functional energetics for molecular recognition of cations by proteins.

M-Pos206

## MIF PROTEINS ARE GLUTATHIONE S-TRANSFERASE HOMOLOGS AND CONTAIN A GLUATHIONE BINDING SITE.

((F.A. Blocki, L.B.M. Ellis, and L.P. Wackett)) University of Minnesota, St Paul, MN 55108.

MIF proteins are mammalian polypeptides of approximately 13,000 MW. These proteins act as macrophage migration inhibition factors (MIFs), transcription factors, and lens crystallins. MIF proteins were previously linked to glutathione S-transferases (GSTs) by demonstrating transferase activity and observing N-terminal sequence homology with a mu class GST (F.A. Blocki, P. Schlievert & L.P.Wackett 1992, *Nature* 360, 269-270). Here, MIF proteins are shown to be structurally related to the theta class of GSTs and to contain a GST glutathione-binding G-site. This was established in several ways. First, polyclonal antibodies raised against recombinant human MIF cross-reacted on Western blots with rat theta GST but not with alpha and mu GSTs. Second, primary sequence patterns spanning the GST G-site were developed for each of the GST gene classes. These patterns identified MIF proteins as theta-like transferase homologs in the G-site region. Third, homology modeling indicates that theta class GSTs contain a serine residue in place of the N-terminal tyrosine that is implicated in glutathione deprotonation and activation in other classes of GSTs. The MIF proteins contain a threonine at this position. That MIF proteins have a glutathione binding site may provide a common structural key towards understanding the varied functions of this widely distributed emerging gene family. Since theta is thought to be the most ancient evolutionary GST class, MIF proteins may have diverged early in evolution but retained a glutathione binding domain.

M-Pos207

## SURFACE DESCRIPTION AND BIOMOLECULAR RECOGNITION (DOCKING).

((S.-L. Lin[1], D. Fischer[2], H. Wolfson[2] and R. Nussinov[2,3])) [1]NIH, NCI, Lab. of Mathematical Biol., P.O. Box B, Frederick, MD 21702, [2]Tel Aviv Univ., Computer Sci. Dept., Tel Aviv 69978, [3]PRI/Dyncorp, NCI/FCRDC, Frederick, MD 21702

We have defined a molecular surface representation that describes precisely and concisely the complete molecular surface. The representation consists of a limited number of critical points disposed at key locations over the surface. These points adequately represent the shape and the important characteristics of the surface, despite the fact that they are modest in number. Using this representation, we are able to achieve accurate and efficient protein-protein and protein-small molecule docking. The docking algorithm is unique in fulfilling the following criteria: (i) There is no predefinition of the receptor or the ligand binding sites. The sole requirements are the atomic coordinates of the docked molecules. (ii) Successful docking is achieved with small (drug) and large (protein) ligands and protein receptors. (iii) Docking is performed in high speed, completing all docking calculations in minutes of CPU time on a workstation. (iv) The quality of the docked conformations is very high, with small RMS deviations from the crystallographic complexes. (v) The number of potential solutions generated is relatively small. (vi) A fast geometry-based surface-contact scoring routine ranks the predicted "correct" solutions at the top. (vii) An efficient energy evaluation function verifies that for all complexes examined, the predicted solutions closest to the crystallographic conformations, top the list. This methodology allows quick scanning of large databases of drugs/inhibitors, essential for rational molecular design.

**M-Pos208**

MODELING OF 3-D STRUCTURES OF G-PROTEIN COUPLED RECEPTORS FROM SEQUENCE DIVERGENCE ANALYSIS.
((P. Du)), Molecular Research Institute, 845 Page Mill Road, Palo Alto, CA 94304.

Sequence divergence analysis is a newly developed method for protein three dimensional structure prediction. This method identified solvent and lipid accessible residues from the variability of amino acids among a family of homologous sequences and use the variabilities for the prediction of transmembrane regions, secondary structures, and a 3-D model. Its novelty is that is does not require a template with known structure. Results of bacteriorhodopsin has been successfully validated by its structure. In this study, 3-D models of the transmembrane domain of human rhodopsin, D1 dopamine receptor, and δ opiates receptor were predicted. Ligand binding sites were proposed for agonists and antagonists in these receptors.

**M-Pos209**

PREDICTION OF TRANSMEMBRANE DOMAINS OF PROTEINS WITH NEURAL NETWORKS.
((R.CASADIO, P.FARISELLI, C.TARONI and M.COMPIANI)) Lab.of Biophysics, Dept. of Biology, University of Bologna, Bologna, Italy.

Back-propagation feed-forward neural networks are used to predict transmembrane domains of proteins whose membrane-buried α-helices are known at atomic resolution. Training sets comprise the reaction center subunits of *Rhodobacter sphaeroides* and *R.viridis*, bacteriorhodopsin, melittin and other anphiphilic peptides. Nets are tested on the same membrane proteins with a jackknife procedure. Transmembrane assignment scores as high as 0.92 and 0.87 of correct predictions on the learning and testing sets, respectively. In spite of the existing homology between the L and M subunits of the reaction center protein, the seven membrane spanning stretches of bacteriorhodopsin are predicted with an accuracy of 0.71 and 0.87, depending on the presence or not of the protein on the training set. These scores are similar or even higher than those obtained with other predictive methods based on the frequency distribution of residues in known membrane spanning segments and/or the potential of average hydrophobicity per residue of the protein sequence.

**M-Pos210**

MODELLING TRANSMEMBRANE HELICES IN MEMBRANE PROTEINS.
((S.R. Durell and H. R. Guy)) Lab of Mathematical Biology, NCI, NIH, Bethesda, MD 20892.

Computer methods are being developed to predict the packing of transmembrane helices in integral membrane proteins. The methods utilize amino acid contact potentials, analysis of sequence conservation, and helix-packing theory. Although the existing contact-potential energy scales were developed from water soluble proteins only, procedures are developed to account for the hydrophobic environment due to the membrane. The pattern of sequence conservation is important to predicting the structure because conserved residues tend to cluster at structurally and functionally important sites, and the hypervariable hydrophobic residues tend to be exposed to the surrounding lipids. The methods will be tested on bacteriorhodopsin, for which a medium resolution structure of the 7 transmembrane helices has been determined (1). The goal is to automate the procedure of assigning sequence segments to the helices, and determining their relative orientations. If successful, the methods will be applied to rhodopsin, for which a projection density map has been recently determined (2), and to other types of G-protein coupled receptors.

1. Henderson, R. *et al.* (1990) *J. Mol. Biol. 213*, 899-929.
2. Schertler, G *et al.* (1993) Nature 362, 770-772.

**M-Pos211**

MOLECULAR MODELING OF A CHANNEL-BLOCKING PEPTIDE FROM *TRIMERESURUS WAGLERI*.
((M. Hyvönen[1], K. Mattila[1], T.T. Rantala[2] and L.C. Sellin[1])). Depts. of Biophysics[1] and Physics[2], University of Oulu, 90570 Oulu, Finland.

The 22-amino acid peptide (WTX1) from a SE Asian snake has recently been purified, sequenced (GGKPDLRPCHPPCHYIPRPKPR) and tested for mouse lethality (0.368 mg/kg i.p.). WTX1, which has a single disulfide bond, blocks a number of voltage and ligand-gated ion channels. The multiple effects of WTX1 can be due to a common binding site or the ability of the peptide to assume various conformational states. Therefore, we analyzed its 3-D structure using computer-based molecular modeling. Simulations were done using CHARMm software and an empirical potential function. The search for conformations was done by several stepwise annealing processes in microcanonical ensemble from between 700°K and 1000°K to 310°K, resulting in a family of folded conformations. To study the dynamics of conformation, several 30 ps vacuum and a few 10 ps water simulations were performed. The latter was done by simulating WTX1 and about 1000 water molecules in a box with periodic boundry conditions. The main features of both conformations were the bending implied by the disulfide, a helical tail at the C-terminus and a slightly vibrating "knot" in the N-terminus region. The active site of WTX1 may contain the His-10 residue, which is located at the flexible backbone region restricted by the disulfide bridge.

## PEPTIDES

**M-Pos212**

MAGAININ 2 AMIDE INDUCED LEAKAGE OF PURE PHOSPHOLIPID VESICLES
((Steven R. Jones, Patrick J. Devine, and Barry S. Selinsky)) Department of Chemistry, Villanova University, Villanova, PA 19085 (Spon. by A. Shinnar)

Magainins are a class of antimicrobial peptides isolated from the African clawed frog, *Xenopus laevis*. The antimicrobial activity is due to the ability of these peptides to selectively permeabilize microbial membranes. To elucidate the mechanism of action of Magainin 2 Amide (Mgn2a), we have conducted studies on the Mgn2a induced release of carboxyfluorescein (CF) from small and large unilamellar vesicles. Vesicles were prepared using phosphatidylserine (PS; bovine brain), phosphatidylglycerol (PG; egg), phosphatidylcholine (PC; egg), and cardiolipin (CL; bovine heart). The leakage of CF from pure lipid vesicles was monitored at 1 and 2 minutes after Mgn2a. For all systems, the dose response curve can be divided into two segments. At low peptide to lipid ratios, an exponential increase in the leakage rate is seen with increasing peptide concentrations. At higher peptide to lipid ratios, the curve changes to an apparent hyperbolic shape. The contributions of the exponential and hyperbolic segments to the dose response curve differ with the different lipid systems. We attribute the difference in the dose response curves to multiple mechanisms of peptide action upon the vesicles. Different lipid systems have different relative contributions of each mode of dye release. (Supported by Magainin Pharmaceuticals Inc.)

**M-Pos213**

COOPERATIVE MEMBRANE INSERTION OF MAGAININ.
((S.J. Ludtke, K. He, Y. Wu, and H.W. Huang)) Rice University, Houston, TX 77251-1892.

The magainins are 23-residue antibiotic peptides discovered in the skin of xenopus laevis. These peptides exert their cytolytic activity directly on the lipid bilayer rather than interacting with protein targets in the cellular membrane. Using oriented circular dichroism, we have found that magainin 1 adopts an α-helical conformation with two distinct orientations when interacting with a lipid bilayer. At low concentrations, magainin is adsorbed parallel to the membrane surface. However, at high concentrations, magainin is inserted into the membrane. This transition occurs at roughly the same critical concentration required for cytolytic activity (~30:1), implying that the membrane insertion is responsible for magainin's cell-lysing activity. We have also observed this behavior in other amphipathic helical peptides, indicating that it may be an important new mechanism of protein-membrane interaction.

**M-Pos214**

X-RAY DIFFRACTION STUDY OF AMPHIPATHIC HELICAL PEPTIDES INTERACTING WITH MEMBRANES.

((H.W. Huang, Y. Wu, K. He and S.J. Ludtke)) Rice Univ., Houston TX 77251

We have shown that a variety of natural and synthetic amphipathic helical peptides have common characteristics as well as important differences in their interactions with lipid bilayers (Huang and Wu, 1991, Biophys. J. 60, 1097; Ludtke et al., to be published). The common characteristics are that the peptides associate with a membrane in two ways. At low concentrations the majority of them adsorbs parallel to the membrane surface; occasionally, by thermal fluctuations, some insert into the bilayer forming ion channels. At high concentrations they insert perpendicularly in the bilayer; in cells this would cause cytolysis and that is the biological function of these peptides. The transition between these two states occurs over a small range of concentration, indicating that it is a cooperative phenomenon. To understand the structure of peptide-lipid interactions, we performed x-ray lamellar diffraction and in-plane scattering of alamethicin in lipid multilayers. When the peptides are adsorbed on the interface, the bilayer thickness decreases and concurrently the chain cross section increases with the increasing peptide concentration, indicating a constant area occupied by each peptide. The transition occurs when the above condition can no longer holds (not because the peptide saturates the membrane surface). We believe that when the peptide inserts into the bilayer, membrane mediated interactions cause the cooperative transition.

**M-Pos215**

A SIMPLE AND GENERAL METHOD FOR QUANTITATIVE AND HOMOGENEOUS INCORPORATION OF HYDROPHOBIC PEPTIDES INTO SDS MICELLES

((J. Antoinette Killian[a,b], Theodore P. Trouard[b], Denise V. Greathouse[c], Roger E. Koeppe[c] and Goran Lindblom[b])) [a]Dept. of Biochem. of Membranes, Univ. of Utrecht, The Netherlands; [b]Dept. Phys. Chem., University of Umeå, Sweden; [c]Dept. Chem. Biochem., Univ. of Arkansas, Fayetteville, AR 72701.

A new method is presented for incorporation of hydrophobic peptides into detergent micelles. Qualitatively the method can be described as two important observations: (1) Addition of hydrophobic peptides from a diluted solution in trifluoroethanol (TFE) to an equal volume of a concentrated solution of SDS micelles in water yields a clear solution that stays clear upon addition of water. In this way micelles are obtained in which the peptide is quantitatively and homogeneously incorporated. Depending on the SDS concentration and the ratio of peptide to detergent the initial TFE content can be reduced, making it possible to obtain concentrated micellar solutions with only a small final volume of TFE. (2) Lyophilization of these micellar solutions and subsequent rehydration yields again clear and stable solutions, in which the peptide is homogeneously and quantitatively incorporated into the micelles. These solutions can be highly concentrated and contain no organic solvent. The only variable appears to be the ratio of peptide to detergent: sufficient SDS must be present to incorporate all peptide. For most peptides a ratio of about 1/100 was found to be sufficient.

**M-Pos216**

SUBSTANCE P AND ANALOGUES: INTERACTION WITH LIPID MONO- AND BILAYERS

(( M. Dathe, A. Seelig*, M. Schmidt, E. Krause, M.Bienert))
FMP, Berlin, Germany, * Biozentrum, Basel, Switzerland

The molecular characteristics of Substance P (SP) , D-Arg$^1$-SP, D-Pro$^2$-SP and all-D-SP were investigated at the air/water interface and in interaction with lipid monolayers and liposomes. The peptides show no differences with respect to surface activity and surface area, however, a quite different behaviour in the interaction with neutral phosphatidycholin (PC), negatively charged phosphatidylglycerol (PG) and mixed (PC/PG) model membranes. The degree of binding was evaluated from the area increase of lipid monolayers upon peptide interaction and found to be different for the individual peptides also. Their conformational properties in the presence of liposomes and under structure inducing solvent conditions were proved by CD-spectroscopy. Differences in the binding constants can neither be interpreted by changes in the conformational flexibility of the peptides nor correlated with their effective charge in the membrane environment. The results let rather assume that there is a stereospecific interaction of the L-and D-peptide analogues with the chiral and nonchiral lipid headgroup.

**M-Pos217**

FUNCTIONAL AND CONFORMATIONAL STUDIES OF VASOACTIVE INTESTINAL PEPTIDE.

((Wujing Xian, W.H.Braunlin)) University of Nebraska-Lincoln, Department of Chemistry, Lincoln, NE 68588-0304. ((Sudir Paul)) University of Nebraska Medical Center, Department of Anesthesiology, Omaha, NE 68198-4455

Vasoactive Intestinal Peptide(VIP) is a 28-amino acid peptide that is synthesized in neurons and displays properties of a neurotransmitter and a neuromodulator. The peptide displays autolytic behavior at low concentration (nM range), but not at higher concentrations or in the presence of SDS. VIP was also found to display membrane binding activity. In our CD studies, it was found that the helicity of the peptide increased as the concentration increased or when SDS was present. The results of these experiments will be presented. We will also report CD studies of the effect of lipids on the conformation of VIP and the results of preliminary NMR studies.

**M-Pos218**

MOLECULAR CONFORMATIONS OF MESO-VALINOMYCIN AND ITS [L-Val$^1$,D-Val$^7$] ANALOG ($C_{60}H_{102}N_6O_{18}$) IN NEW CRYSTAL FORMS.

((W.L. Duax[1], D.A. Langs[1], and V. Pletnev[2], )). [1]Medical Foundation. of Buffalo, Inc., Buffalo, NY and [2]Shemyakin Institute of Bioorganic Chemistry, Moscow, Russia.

Analogues of valinomycin differing in ring composition and size are being studied to identify structural features responsible for ion selectivity, capture, and transport. A new crystal form of meso-valinomycin cyclo [-(D-Val-L-Hyi-L-Val-D-Hyi)3] (I) with two independent molecules in the cell has been obtained from octane solution (triclinic P1, a=14.075, b=14.475, c=22.632Å, $\alpha$=95.483, $\beta$=68.323, $\gamma$=119.061°) and the analog Cyclo (L-Val-L-Hyi-L-Val-D-Hyi-D-Val-L-Hyi-D-Val-D-Hyi-D-Val-L-Hyi-L-Val-D-Hyi) (II) has been crystallized from octane/$CH_2Cl_2$ (orthorhombic Pbca, a=11.458, b=25.612, c=23.691Å). Both crystal structures were determined by direct methods. The two crystallographically independent molecules of structure I adopt distinctively different conformations stabilized by six intramolecular 4→1 type H-bonds. One is a bracelet type conformer having a spherical cavity lined with six ester carbonyl oxygens. The second conformation has a similar bracelet, but is noticeably elongated and has two well-ordered water molecules in the negatively charged ellipsoidal central cavity. In contrast, compound II has a highly symmetric, very elongated form with only two intramolecular 4→1 type H-bonds in type II $\beta$-bends. Research supported by NIH Grant GM32812.

**M-Pos219**

**STRUCTURAL STUDIES OF TRANSMEMBRANE VII (RESIDUES 378-403) OF THE DOPAMINE $D_2$ RECEPTOR USING TRYPTOPHAN FLUORESCENCE**

((V.L. Williams, S.H. Courtney, D.I. Schuster and R.B. Murphy)) Dept. of Chemistry, New York University, NY, NY 10003

We have developed a well-defined synthetic model of the dopamine $D_2$ receptor using the seventh transmembrane sequence of the dopamine receptor incorporated into small unilamellar vesicles. Purification of this highly hydrophobic peptide sequence required the development of a novel alcohol-based reversed-phase HPLC solvent system. Small unilamellar vesicles were prepared using the synthetic lipid, dimyristoylphosphatidylcholine (DMPC), and characterized using electron microscopy. The fluorescence properties of the single tryptophan residue in this sequence was used as an intrinsic probe of the microenvironment of the peptide within the DMPC bilayer. In order to distinguish the fluorescence properties which were unique to the peptide, L-tryptophan, tryptophan octyl ester and N-acetyltryptophanamide were used as controls. In 6M urea, the peptide fluorescence emission maxima was 350 nm and the Stern-Volmer constant, derived from acrylamide quenching data, was 9.6. These values are similar to literature values for the quenching of a fully exposed tryptophan residue in a randomly coiled peptide. The expected blue shift of the tryptophan fluorescence emission maxima in vesicles was observed, indicating the incorporation of the tryptophan residue into a nonpolar environment. Values derived from acrylamide quenching data also support this conclusion. Time-correlated single photon counting was used to measure the fluorescence decay and fluorescence anisotropy. The peptide exhibited multiexponential decays in both 6M urea and vesicle solutions. A temperature dependence of the average lifetime was not observed above and below the phase transition temperature of DMPC. Anisotropy measurements of the peptide yielded biexponential decay in 6M urea and single exponential decay in the vesicle solutions.

M-Pos220

## Site Specific Isotopically Labeled $^{13}C$ Vibrational Difference Spectroscopy Gives Insight into Amide I' Band Frequency Assignments in Helical Peptides

((Gary V. Martínez, Wayne R. Fiori, Glenn L. Millhauser)) Department of Chemistry and Biochemistry, University of California, Santa Cruz, CA 95064

Recently, short helical alanine rich peptides have been shown to contain more than one kind of secondary structure along the helix backbone (Fiori et al., *Biochemistry* 1993). Amide I' frequency assignments of these helical domains cannot be characterized in a position dependent fashion by FTIR alone. However, isotopic labeling can give site-specific vibrational information (Tadesse et al., *JACS* 1991 113, 7036-7037). Denoting the position of $^{13}C$ isotopic amide carbonyls with an underline, the labeled peptide analogs used in this study are

| | |
|---|---|
| Ac-AAAA<u>A</u>K<u>AA</u>AAKAAAAKA-$NH_2$ | 3KA |
| Ac-AAAAKAAA<u>A</u>K<u>AA</u>AAKA-$NH_2$ | 3KB |

When correlated with the results of Doubly Labeled Electron Spin Resonance studies of 16 & 21 residue peptides, we expect that Site Specific Isotopically Labeled Vibrational Difference Spectroscopy may determine the local amide I' vibrational characteristics of these peptide helices.

M-Pos221

## HYDRATION OF CHARGED ATOMIC GROUPS OF BIOLOGICAL MOLECULES.

((T.V. Chalikian, A. Sarvazyan*, V.S. Gindikin, and K.J. Breslauer)) Department of Chemistry, Rutgers, The State University of New Jersey, New Brunswick, NJ 08903. *permanent address: Institute of Theoretical and Experimental Biophysics, Russian Academy of Sciences, Pushchino, Russia.

We have used high precision ultrasonic and densimetric measurements to determine changes in the partial molar volume, V, and the partial molar adiabatic compressibility, $K_S$, associated with the neutralization of the charged termini in a family of GLY-GLY-X and X-GLY-GLY tripeptides, where the oppositely charged amino and carboxy termini are known to be hydrated independently. In triglycine, the neutralization of the amino group leads to an increase in V and $K_S$ by 10.8 $cm^3mol^{-1}$ and $7.6 \cdot 10^{-4}$ $cm^3mol^{-1}bar^{-1}$, respectively, while the neutralization of the carboxyl group leads to an increase in V and $K_S$ by 5.3 $cm^3mol^{-1}$ and $27.0 \cdot 10^{-4}$ $cm^3mol^{-1}bar^{-1}$, respectively. The presence of aliphatic side chains in the vicinity of the $-NH_3^+$ group (in ALA-GLY-GLY, VAL-GLY-GLY, AND LEU-GLY-GLY) leads to a diminution in the changes in both the volume (on average by 1 $cm^3mol^{-1}$) and compressibility (on average by $6 \cdot 10^{-4}$ $cm^3mol^{-1}bar^{-1}$) upon neutralization of the amino group. By contrast, the presence of an aliphatic side chain in the vicinity of the $-COO^-$ group (in GLY-GLY-ALA, GLY-GLY-VAL, and GLY-GLY-LEU) results in an increase in the changes in both the volume (by 1-2 $cm^3mol^{-1}$) and compressibility (by $3\text{-}8 \cdot 10^{-4}$ $cm^3mol^{-1}bar^{-1}$) upon neutralization of the carboxyl group. We will discuss the V and $K_S$ data in terms of the hydration of the charged termini and how this hydration is modulated by the nature of neighboring chemical groups.

M-Pos222

## CD, REFTIR, AND NMR SPECTROSCOPY OF $3_{10}$ -HELICAL, AIB-RICH PEPTIDES: IMPLICATIONS FOR THE ELUCIDATION OF PEPTIDE SECONDARY STRUCTURE.

((Adrienne Pettijohn and Atsuo Kuki)) Cornell University, Ithaca, NY 14853

Peptides composed of greater than 70% α-aminoisobutyric acid (Aib) are known to form extremely stable $3_{10}$-helical structures in solution (Basu, G. and Kuki, A., Biopolymers (1993) 33 995-1000, and references therein). We have exploited this $3_{10}$-helix-forming property in order to investigate the effectiveness of CD and REFTIR (resolution-enhanced FTIR) in distinguishing between $3_{10}$- and α-helices in solution. A chiral, Aib-rich peptide (BGLC) has been synthesized to determine the CD spectrum of a short, rigid $3_{10}$-helical peptide:

δ-($^t$Boc-Glu-O$^t$Bu)-Aib-Aib-Leu-Aib-Aib-Ala-Aib-Aib-Aib-$NHCH_2CH_2OCH_3$.

The $3_{10}$-helical conformation is strongly supported by NMR measurements. This peptide is one of a family of similar peptides designed for the investigation of peptide insertion into lipid membranes. Deprotection of the N-terminal δ-Glu amino acid renders the peptide water-soluble, allowing for comparisons between organic and aqueous phases. Preliminary results indicate that while the short $3_{10}$-helix appears to have a CD spectrum which is distinct from that of an α-helix, the CD spectra of the $3_{10}$-helix, α-helix, random coil and β-sheet may not be linearly independent. In contrast to CD, examination of a homo-Aib series of differing lengths reveals that REFTIR is quite sensitive to small differences in conformation, and that α- and $3_{10}$-helices can be readily distinguished by this method. Implications for the reliability of CD spectral analysis and determination of peptide conformation in solution will be discussed.

M-Pos223

## MEASUREMENT OF N-TERMINAL ELECTRIC FIELDS IN A SERIES OF SHORT HIGHLY HELICAL PEPTIDES.

((Matthew Kubasik and Atsuo Kuki)) Department of Chemistry, Cornell University, Ithaca, NY 14853

The magnitude and functional significance of electric fields arising from protein secondary structure continue to be the subject of much theoretical and experimental interest. Electric fields associated with helical peptide structures can be measured by an "internal Stark effect", which quantifies the interaction of the peptide electric field with a photon-induced change in the permanent dipole moment of a chromophore (D.J. Lockhart and P.S. Kim, Science, 257, 947 (1992)) We have implemented this technique using the N-terminal chromophore 2,3-naphthalimide to measure the field of the helical macrodipole in a length-dependent series of short peptides composed exclusively of α-aminoisobutyric acid (Aib) residues. NMR, infrared, and x-ray data have demonstrated that oligopeptides composed of Aib residues adopt 3-10 helical structures. We have measured helix-field induced spectral shifts in a series of organic solvents spanning a wide range of dielectric constants to separate the roles of internal (protein-like) vs solvent dielectric constants in controlling the magnitude of the field from the helix macrodipole. We also observe an increasing red-shift in absorption of this chromophore with peptide length, and our results indicate that theoretical models which predict that the magnitude of the field at the N-terminus saturates after about two turns (~6-7 residues) are likely to be correct.

M-Pos224

## EFFECT OF OPTICAL DISPERSION ON ATR-FTIR MEASUREMENTS OF PEPTIDE ORIENTATION AT THE LIPID-WATER INTERFACE

((W. David Braddock[a], Paul H. Axelsen[b]))
[a]Mayo Foundation, Rochester MN, [b]University of Pennsylvania, Philadelphia PA

**The amide I region of the IR spectrum may be used to examine the conformation and orientation of various peptides in lipid membranes. For mathematical simplicity, several approximations are routinely employed during analysis of this spectral data. We have examined the effects of neglecting the optical dispersion of water, and the weak evanescent field approximation. When spectral data are analyzed using an exact model based on Maxwell's Equations which rigorously includes the elliptical nature of the light and the optical dispersion of water, we find that intense dispersion near 1650cm$^{-1}$ markedly affects the strength of the evanescent fields probing the lipid-water interface. We have applied our results to the study of melittin and the fusogenic peptide of influenza A hemagglutinin on supported POPC monolayers. The calculated order parameters for presumed α-helices in these peptides indicate that the effects of optical dispersion are large, and must not be neglected when ATR-FTIR is used to determine the orientation of α-helical peptides relative to lipid membranes.**

WDB supported by The Keck-Mayo Training Program in Molecular Biophysics.
PHA supported by a Biomedical Scholar Award from the L. P. Markey Charitable Trust.

M-Pos225

## THE KINETICS OF AMYLOID FIBRIL FORMATION CAN BE FOLLOWED WITH ELECTRON SPIN RESONANCE SPECTROSCOPY

((Karen M. Casteel and Glenn L. Millhauser)) University of California, Department of Chemistry and Biochemistry, Santa Cruz, CA 95064

Diagnostic of the prion neurologic diseases in addition to Alzheimer's disease is the presence of amyloid fibril tangles in the brain. The primary component of these plaques in each case is a single peptide which differs in sequence depending upon the disease and associated precursor protein. The various fibril-forming peptides do share a trait of being helical in the protein and forming β-sheets when clipped out. Not understood is the process by which peptides hydrogen-bond in β-sheet conformation to organize and form fibrils that are a few nanometers in width and microns long.

We have shown with transmission electron microscopy that introduction of a nitroxide spin label to appropriate prion and β-amyloid peptides does not disrupt the formation of fibrils. Electron spin resonance (ESR) is thereby used to monitor the free peptide in solution (which yields a fast motional spectrum) as its concentration diminishes during incorporation into the fibrils (which yield a very different ESR spectrum due to the slower rotational diffusion). In this way, amyloid fibril kinetics can be characterized.

**M-Pos226**

EFFECT OF HORMONE FRAGMENTS ON THE MEASUREMENT OF PARATHYROID HORMONE BY RADIOIMMUNOASSAY. ((Alafuele Mbuyi-Kalala and Gerald Ehrenstein)) Biophysics Section, Clinical Neuroscience Branch, NINDS, NIH, Bethesda, MD 20892)

One of the basic assumptions underlying the use of radioimmunoassay and other competitive protein-binding assays is the homogeneity of the antigen or ligand. The existence of circulating parathyroid hormone fragments violates this assumption and hence has the potential for causing errors and high variability in the radioimmunoassay of parathyroid hormone (PTH). Even though region-specific radioimmunological and immunoradiometric assays for PTH measurement have been successful in recognizing limited regions of the hormone, (non-immunological) heteromolecular interactions between the hormone and its fragments (or other co-secreted protein) may still cause significant measurement errors. We therefore undertook to carefully examine experimentally and by modelling the impact of fragments on the estimation of a highly purified intact bovine PTH by radioimmunoassay. Our experimental results show that the impact of fragments could not be attributed only to the simple binding of fragments to the antibody. Indeed we found that the mere presence of the fragments can result in a pronounced underestimation of the amount of the intact hormone. We account for this "fragment's screen effect" by interactions between the hormone and its fragments.

**M-Pos227**

ANALYSIS OF X-RAY IN-PLANE SCATTERING: DISTRIBUTIONS OF PROTEINS IN MEMBRANES.
((Ke He, S.J.Ludtke, Y.Wu and H.W.Huang)) Physics Department, Rice University,Houston, TX 77251.

We have developed a technique for measuring X-ray (or neutron) scattering with the momentum transfer parallel to the plane of the membrane to study the lateral organization of proteins and peptides in membranes (He et al. Biophys. J. 64 (1993), He et al. J. Phys. (Paris) to be publ., He et al. Biophys Chem. to be publ.). Since there is no analytical solution for X-ray scattering in a two dimensional system, we used Monte-Carlo methods to simulate the scattering pattern of protein particles freely diffusing in the membrane. We found that:
1). The scattering peak position is mainly determined by the size of protein, relatively independent of the concentration of protein.
2). The peak intensity is mainly determined by the area ratio of the protein to the lipid.
We will show three examples of in-plane scattering: distribution of gramicidin in a membrane, distribution of gramicidin monomers in a membrane and distribution of inserted alamethicin in a membrane.

**M-Pos228**

IMPLICATIONS OF SEQUENCE ANALYSIS FOR THE P5C DEHYDROGENASE ACTIVITY OF PUTA, A MULTIFUNCTIONAL *ESCHERICHIA COLI* PROTEIN
((Mingfu Ling and Janet M. Wood)) Department of Microbiology, University of Guelph, Guelph, Ontario, Canada N1G 2W1)

Membrane-associated *E. coli* PutA has two enzymatic activities: proline dehydrogenase (DH) and δ'-pyrroline-5-carboxylate (P5C) DH. This protein also represses expression of its corresponding gene *putA*. Previous studies of PutA from *E. coli* and *Salmonella typhimurium* have demonstrated correlations among reduction of the PutA flavin by proline, PutA conformation and association of PutA with membranes (Brown and Wood (1993), J. Biol. Chem. 268, 8972) or with *put* intergenic DNA (Ostrovsky de Spicer and Maloy (1993) Proc. Natl. Acad. Sci. USA, 90, 4295). We would like to correlate structure with function for PutA. The objectives of this study were to sequence *E. coli putA*, to survey the deduced PutA amino acid sequence for DNA, membrane, proline, P5C, FAD and NAD binding sites and to enhance the expression of *E. coli putA*. The 4 kb *E. coli putA* sequence revealed both similarities to and differences from the *S. typhimurium putA* sequence reported by Allen *et al.*, (1993) Nucleic Acids Res. 21, 1676. A region of sequence similarity with several aldehyde DHs from both prokaryotes and eukaryotes and with *Saccharomyces cerevisiae* P5C DH extends from residue 700 through residue 1100 of *E. coli* PutA. These sequence analyses suggest that γ-glutamic semialdehyde, which is believed to equilibrate spontaneously with P5C, is the substrate for P5C DHs. We can test this hypothesis by using aldehyde analogs and affinity-labelling techniques. Limited and intriguing similarities were also found between a portion of the PutA sequence and a sequence near a consensus FAD-binding region shared by succinate DH and fumarate reductase from several organisms. As well, partly for supplying sufficient amounts of protein for X-ray crystallographic structural studies, we have achieved overexpression of the *putA* gene under the promoter of phage T7 RNA polymerase.
(Supported by the Natural Sciences and Engineering Research Council of Canada)

**M-Pos229**

**FLUORESCENCE PREDICTS LOCAL SECONDARY STRUCTURE: Time-Resolved Fluorescence and Circular Dichroism Studies of Highly Purified Neurotoxins**
((T.E.S. Dahms[1,2] and A.G. Szabo[1,2])) [1]Institute for Biological Sciences, National Research Council, Ottawa, Ont., Canada, K1A 0R6. [2]University of Ottawa.

The relationship between ß-sheet secondary structure and intrinsic tryptophan fluorescence parameters of Erabutoxin b, α-cobratoxin and α-bungarotoxin were examined. NMR and X-ray crystallography have shown that these neurotoxins have comparable ß-sheet, ß-turn and random coil secondary structure. Each toxin contains a single tryptophan (Trp) residue (on ß-sheet) and no more than two tyrosine (Tyr) residues. The identity and purity of the HPLC purified toxins and toxin-derivatives were verified by electro-spray ionization mass spectrometry. The time-resolved fluorescence properties of native erabutoxin b and α-cobratoxin are best described by triple exponential decay kinetics, whereas native α-bungarotoxin exhibits a distribution of lifetimes.

Each neurotoxin, treated with 2M, 4M and 6M GuHCl, was studied both by circular dichroism (CD) and time-resolved fluorescence spectroscopy (TRFS). Disappearance of the ß-sheet secondary structural features with increasing concentrations of GuHCl was accompanied by a shift in the relative contribution ('c' value) of each fluorescence decay time (TRFS). At 6M GuHCl the native toxins were completely denatured as evidenced by CD (random coil) and the 'c' values of the three fluorescence decay times (TRFS) were identical to those found for single Trp α-helical peptides in 6M GuHCl (random coil) and were dramatically different than those of the native toxins.

The disulphide bonds of each toxin were reduced to facilitate carboxymethylation and amidocarboxymethylation. The two different toxin derivatives displayed triple exponential decay kinetics for all three neurotoxins. The relative contributions of the fluorescence decay times (TRFS) were similar to those observed for the native toxin in 6M GuHCl. The data suggests that the 'c' values observed for the native toxins are indicative of ß-sheet secondary structure.

## MOLECULAR RECOGNITION I: PROTEINS

**M-Pos230**

A THEORETICAL MODEL OF ANTIGEN RECOGNITION BY A T CELL RECEPTOR AND ITS POSSIBLE IMPLICATIONS FOR SIGNAL TRANSDUCTION. ((A.E. Kister,*† J. Malinsky,‡ A. Smolyar‡ and E.L. Reinherz*§)) *Laboratory of Immunobiology, Dana-Farber Cancer Institute, Departments of †Pathology and §Medicine, Harvard Medical School, Boston, MA 02115 and ‡Mt. Sinai School of Medicine, New York, NY 10029.

A computer model of the trimolecular complex of the murine B10 T cell receptor (TCR), its peptide antigen derived from the C-terminal fragment of pigeon cytochrome c and the α1 and β1 domains of the MHC class II I-Ek molecule was created. This model takes into consideration the effect of hydrophobic interactions during the long distance attraction of molecules and short range specific recognition mediated by hydrogen bond formation between molecules. Ab initio quantum mechanical calculations of putative binding residues predict the effect of electronic redistribution. The model suggests that electrostatic interactions are crucial for receptor binding to antigen. They may also trigger an initial step of signal transduction via charge transfer. Possible mechanisms for this process are proposed based on recent work on conductivity in disordered systems. Phase transitions which may occur in the trimolecular complex and drastically change its electronic properties are considered.

**M-Pos231**

CRYSTALLOGRAPHIC AND SPECTROSCOPIC SOLUTION STUDIES OF THE INTERACTION OF RAT ANNEXIN V WITH LIGANDS. ((M.A. Swairjo*, N.O. Concha*, J.F. Head*, M.-B. Campos**, J.R. Dedman**, M.F. Roberts***, B.A. Seaton*)) *Department of Physiology, Boston University School of Medicine, Boston, MA 02118. **Department of Physiology and Biophysics, University of Cincinnati, College of Medicine, Cincinnati, OH 45267. *** Department of Chemistry, Boston College, Chestnut Hill, MA 02167.

Annexins are a family of twelve homologous calcium-binding proteins, distinct from the "E-F hand" calcium-binding proteins, that bind to acidic-phospholipid (PL) membranes in a calcium-dependent manner. Despite their unknown physiological functions, they are implicated in membrane processes in cells, such as exocytosis and membrane trafficking. Their primary structures exhibits a highly conserved four/eight-domain core, consisting of approximately 70 amino acids and a highly variable $NH_2$-terminal region.

In an attempt to understand the effect of annexin binding on the membrane we conducted $^{31}P$- and $^{1}H$-NMR spectroscopic experiments on the interaction of annexin V (35 kDa) with small unilamellar vesicles containing phosphatidylcholine (PC) and phosphatidic acid (PA). The $^{1}H$-NMR data show no significant insertion of annexin V into the bilayer hydrophobic core. Instead, a peripheral interaction, in which the PA headgroups on the outer vesicular surface are prefered, is indicated from the $^{31}P$-NMR data. CD data, together with the crystal structure of annexin V are consistent with an insertion-free mechanism of interaction. Further, the NMR data reveal that annexin binding to the vesicle outer-leaflet PL affects inner-leaflet phospohlipids as well. The effects ovserved are consistent with a protein-induced reduction in membrane curvature. In parallel, we investigated the effect of ligand binding on the structure of rat annexin V, both in the presence and absence of phospholipids, using X-ray crystallographic and solution methods. In light of the observed ligand-induced conformational changes and the NMR results, a model of the calcium-mediated annexin-membrane interaction is presented.